ISSN 1173-5996

AN ANALYTICAL MODEL FOR VERTICAL FLAME SPREAD ON SOLIDS: An initial investigation

BY

Gregory Allen North

Supervised by

Dr Björn Karlsson, Sweden
and
Dr Andrew H Buchanan, New Zealand

Fire Engineering Research Report 99/12
March 1999

This report was presented as a project report
as part of the M.E. (Fire) degree at the University of Canterbury

School of Engineering
University of Canterbury
Private Bag 4800
Christchurch, New Zealand

Phone 643 364-2250
Fax 643 364-2758

Abstract

Fire statistics have shown that, during the period 1986-1997, approximately 75% of fires occurred within structures. One of the factors that determines the overall effect (severity) that these fires have, is the growth phase. This growth occurs by a process known as "surface flame spread".

Surface flame spread research is presented in this report and can be divided into two individual parts, namely,

1. The development of a simple expression that links the time to ignition of a material to its exposed heat flux level.
2. The incorporation of this simple time to ignition expression into a model that can analyse the upward flame spread characteristics for various different combustible materials.

Thirty one different materials were investigated in the flame spread model and the results are described in this report. Twenty-four of the materials come from the European Standard Room/Corner test and the rest are from Finnish research using a Vertical Wall test method

An equation that could satisfactorily represent the time to ignition of a given material was obtained and the research into the analytical flame spread model has produced very satisfactory comparisons between the calculated values and those obtained from the experimental studies undertaken by three different Scandinavian research programs.

Acknowledgements

I would like to sincerely thank and show my deepest appreciation to the following people and organisations. Their support and understanding was crucial for me during the production of this work and the completion of my Masters Degree in Fire Engineering.

* Dr. Björn Karlsson, my research supervisor in Sweden, who always seemed to find time to give me the necessary guidance. Without his invaluable contribution, this research would not have possible.
* Dr Andy Buchanan, for his dedicated work in the Fire Engineering course at Canterbury University and for his organisation of my studies in Sweden.
* Dr Charley Fleischmann, for all his help and guidance during the Fire Engineering course and in the initial stages of my research.
* Students and Staff of the Fire Safety Engineering program at Lund University, Sweden, who made me feel at home during this research. Their help, from translating Swedish to showing me the Swedish way of life, has been most appreciated.
* University of Canterbury's Engineering Library Staff, who were always available to help gather any resource material that I needed during my studies in New Zealand.
* My family, both my parents in New Zealand and my sisters in London, for their phone calls and first aid parcels.
* Members of the 1998-9 Fire Engineering course at Canterbury University including the department secretary, Catherine Price. It's been a pleasure working with you all during the past twelve months.

I would also like to acknowledge the New Zealand Fire Service Commission for their financial support of the Fire Engineering program at the University of Canterbury. Without their support the Fire Engineering program and this research would not have been possible.

Table of Contents

List of Figures

List of Tables

Nomenclature

Symbol	Description	Units
a	Dimensionless Constant	(-)
A	Dimensionless Constant	(-)
A	A specific Time to Ignition value used in Scenario F	s
A_0	Initial Pyrolysis Area	m^2
B	A specific Time to Ignition value used in Scenario F	s
c	Specific Heat Capacity	$kJkg^{-1}K^{-1}$
C_1	Constant	m^2s^{-1}
C_2	Constant	s
C_3	Constant	s^{-1}
FFM	Movement description of the flame front	(-)
H	The Height of the combustible material	m
k	Thermal Conductivity of a solid fuel	$kWm^{-1}K^{-1}$
K	Flame Height and Area coefficient which is dependent on the burner location	mkW^{-1} or m^2kW^{-1}
$q_{o,ig}$	Minimum radiant heat flux per area for piloted ignition	(kWm^{-2})
$\dot{q}''$	Radiative Heat Flux per area	kWm^{-2}
$\dot{q}''^*$	Post-ignition Time Adjustment variable	kWm^{-2}
$\dot{q}''^{**}$	Pre-ignition Time Adjustment variable	kWm^{-2}
$\dot{q}''_e$	External radiation heat flux per area	kWm^{-2}
$\dot{q}''_{gc}$	Gas Phase Conduction Heat Flux	kWm^{-2}
$\dot{Q}_b$	Heat Released Rate of the burner	kW
$\dot{Q}_c$	The total heat release rate of the combustible lining material	kW
$\dot{Q}_{cc^*}$	Transient Total Heat Release Rate of the combustible material	kW
$\dot{Q}_{exp}$	Experimental Heat Release Rate	kW

$\dot{Q}_{ND}$	Heat release rate with no decay	kW
$\dot{Q}_{tot}$	Total heat release rate	kW
$\dot{Q}''$	The Average or Maximum Heat Release Rate of the combustible lining material measured in the Cone Calorimeter	kWm^{-2}
$\dot{Q}''$	Energy Release Rate per unit fuel area	kWm^{-2}
$\dot{Q}''_{ave}$	Average Heat Release Rate of the fuel per unit area measured in the Cone Calorimeter at an irradiance level of $50kWm^{-2}$	kWm^{-2}
$\dot{Q}''_{max}$	Maximum Heat Release Rate of the fuel per unit area measured in the Cone Calorimeter at an irradiance level of $50kWm^{-2}$	kWm^{-2}
s_1	Constant	s^{-1}
s_2	Constant	s^{-1}
t	Time	s
t_{ds}	Heat release rate decay time step	s
t_{ig}	The time to ignition of the combustible lining material	s
t_{ig*}	Wall Time to Ignition	s
t_{ig**}	Burner Time to Ignition	s
t_p	Dummy variable of integration	s
t_{pi}	Post-ignition Time	s
t_{step}	Time Step Interval	s
T_0	Ambient temperature	°C or K
T_{ig}	Ignition temperature of a material	°C or K
T_s	Surface Temperature	°C or K
V	The flame spread velocity	m^2s^{-1}
V_c	Transient Flame Spread Velocity value	ms^{-1} or m^2s^{-1}
V_p	Pyrolysis Front Velocity	ms^{-1} or m^2s^{-1}
W	The width of the burner	m
x	Distance	m
x_f	The length of the flame front	m

x_p	The length of the pyrolysis front	m
x_{pc}	Transient Pyrolysis Front Length	m
x_{po}	Initial height of the pyrolysis front	m
x_{po*}	Heat Flux Variation variable	(-)
X	Slope value used in Scenario F	(-)
X1	Constant	(-)
X2	Constant	(-)
y	Distance	m
α	Entrainment coefficient	s^{-1}
α	Constant	s^{-1}
β	Constant	s^{-1}
Δ	Constant	s^{-2}
Δ	Distance	m
Δ	Difference between the calculated and experimental heat release rates	kW
ΔH	Change of Enthalpy	$kJkg^{-1}$
Φ	Flame Heating parameter	kW^2m^{-3}
λ	The Decay coefficient when simulating results from the Cone Calorimeter	s^{-1}
ρ	Density	kgm^{-3}

Subscripts

Symbol	Description
0	Initial
f	Flame
g	Gas
gc	Gas Phase Conduction
ig	Ignition
n	Time Period of current interest
n	Final Time Period in equation (4.24)
p	Pyrolysis
t	Time

1. INTRODUCTION

The research work that is presented in this report is a partial fulfilment of the requirements of the Master of Engineering in Fire Engineering course at the University of Canterbury, Christchurch, New Zealand. Also included in the content is work undertaken by the author following the completion of this degree, carried out at Lund University, Sweden.

1.1 Background

Fires, being defined as the unwanted combustion of materials, are highly likely to be encountered by most individuals at some time or another. Such fires typically have an enormous effect, be that emotionally, physically or financially, on the people involved. But such effects are not restricted to these individuals alone, as the financial cost of any fire is largely met through taxes and/or insurance. It can therefore be seen that a fire is a phenomenon that affects everyone.

In a bid to reduce the public and private cost of fires, improvements in the knowledge on the causes, effects and complex interactions that occur during a fire are constantly being sought. These improvements are obtained from the ongoing work at various research institutions and universities throughout the world. From this gained knowledge, fire safety related legislation, currently incorporated throughout the world, can be improved to ensure that the cost of fires is kept to a minimum.

1.2 Fire/flame Spread on Combustible Materials

Fire statistics from the New Zealand Fire Service [14] have shown that, during the period 1986-1997, approximately 75% of fires occurred within structures. This figure

is expected to be similar throughout many other developed countries in the world and shows that these fires deserve a significant investment in fire safety related research.

Fires in structures are started in numerous places for equally numerous different reasons and are controlled by the highly complex combustion process. This variability and complexity has a dramatic effect on the speed, duration and severity of a given fire. For example, if a fire was to start in a rubbish bin full of paper, the overall severity would likely to be minimised if the bin was of non-combustible construction and was located well away from any other combustible materials, such as furniture and curtains. Such a scenario may result in the fire self-extinguishing before its effect was able to threaten people, and/or property. Such a fire scenario is obviously not always the case and a typical fire, if left uncontrolled by any external means, will generally continue to spread after ignition and is likely to engulf all combustible materials in its path. Such a fire undergoes four specific phases, described by ignition, growth until flashover, full development and decay. These phases can been graphically seen in the figure below.

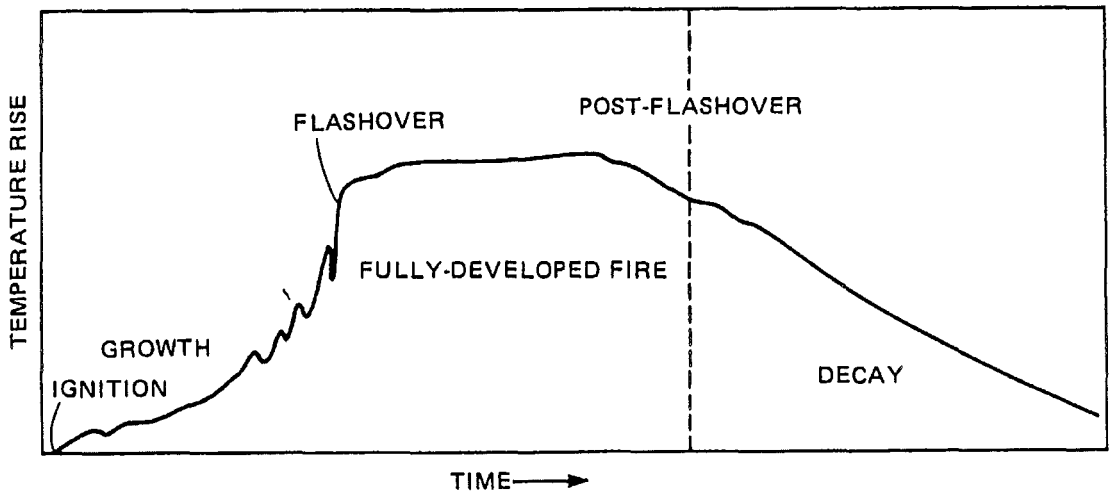

Figure 1.1: General Description of a Compartment Fire in the Absence of Fire Control [22]

One of the main factors that determines the overall effect (severity) that a particular fire has, as shown above, is the growth phase. In this pre-flashover phase, the fire grows primarily as a function of the fuel itself, with little or no influence from the

compartment. This growth occurs by a process known as "surface flame spread". In real fires, it is this flame spread process that is critical to the fire's destiny during the pre-flashover phase.

If a combustible material has a relatively low rate of flame spread over it once ignited, then that material could generally be said, in terms of fire properties, to be a "good" and/or "safe" material to use within a compartment. Such a material would typically exhibit slowly increasing, or more preferably, decelerating flame spread characteristics. Specific materials that have high flame spread characteristics are generally less suited for the use in a compartment where these properties would be detrimental to the occupants and/or the property within after a fire initiation.

Not only are the individual flame spread characteristics significant, but the compartment variability also has a major impact. As the compartments' construction materials are not isolated from one another, the interaction of the materials is also important. The following figure shows some of the main influences on this variability,

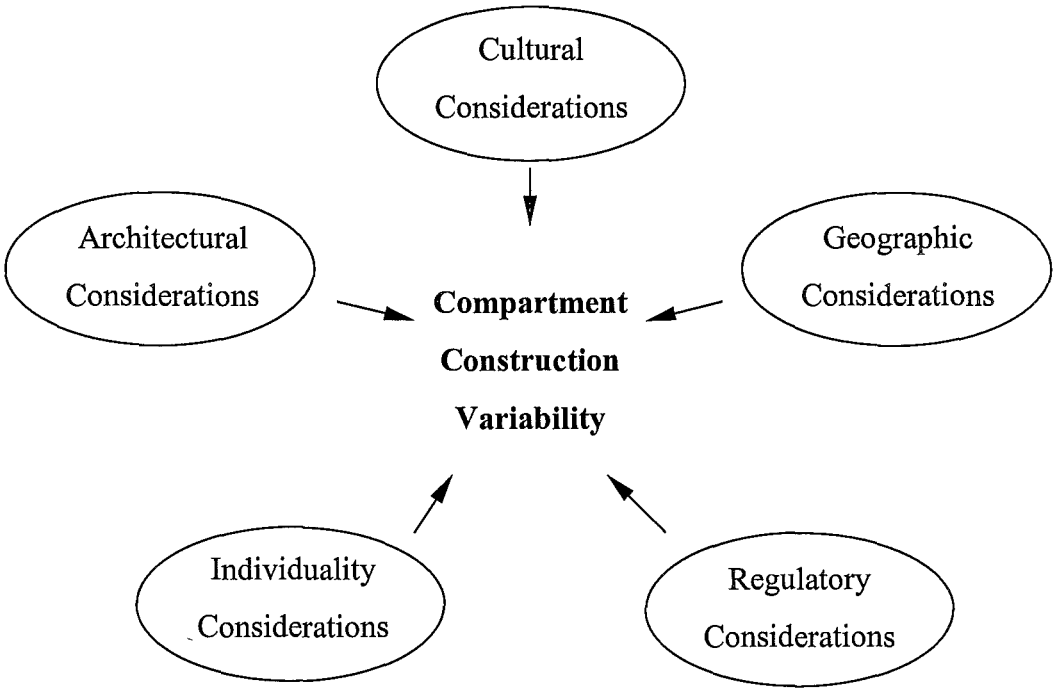

Figure 1.2: Factors that Influence the Variability of the Construction of a Compartment

These factors affect the choice of materials and the construction techniques found in a compartment.

It is this variability described above that often challenges the Fire Engineer when determining the necessary degree of fire protection that a particular room requires to ensure that the fire safety level is maintained. This fire protection is provided as a direct result of the danger that the material represents to the occupants and/or the other materials within the structure.

1.3 Fire Safety Legislation

As mentioned earlier, fire safety legislation, in the form of Building Codes, are currently used as a means of ensuring that buildings are constructed to a publicly acceptable level of safety. Historically, this legislation has been in the form of a prescriptive code that described the specifications that were to be followed in the design of any new structure. Applying these regulations removed the considerations of the designer to what was actually safe, as the level of safety was implicitly embodied in the code. This type of regulation has numerous deficiencies, as they are suited to buildings of a certain type, for which they were initially derived. It was found that if a building did not fit into any standard type, the regulations might force the designer to incorporate too many, too few, or sometimes even inappropriate fire safety measures. It is therefore possible that the safety level may be too low in some buildings that were built under this type of legislation [4].

In a bid to remove these deficiencies of the prescriptive code, so-called performance based building regulations have been developed and implemented in many countries including Australia, Japan, New Zealand, Sweden and the United Kingdom. Performance based regulations define the objective for a certain regulation but do not say how the objective should be accomplished. This type of legislation has generated

more flexible ways of designing buildings and facilitated more cost-effective designs without prejudicing fire safety levels.

1.4 Fire Safety Design Methods

In the move from detailed prescriptive regulations, a functional framework has been set up to facilitate in the fire safety design process. This framework describes ways in which the performance objectives can be met. The following paragraphs include details of the design process in New Zealand. This country has been chosen due to the authors' familiarity with the proceedings in this country but it is expected that similar design methods are available to those other countries that also have performance based codes.

The methods that can be used in the fire safety design process to achieve the requirements of the building code include,

- Acceptable Solutions, or
- Alternative Solutions, which include either "Verification Methods" or "Accreditation".

The Building Industry Authority (BIA) in New Zealand has published "Approved Documents" which include the Acceptable Solution method. This is a prescriptive method of meeting the requirements and is usually a satisfactory approach in the design of small or simple buildings [2].

Specific Fire Engineering design, termed above as "Alternative Solutions", is often used when,

- The Approved Documents are not applicable, e.g. high fire loads, or
- The Approved Documents specify specific Fire Engineering design, or
- The building owner's requirements go beyond those of the Building Code, or

- Addition benefits, generally in cost or safety, will result from a specific design.

The Alternative Solutions require that the designer use established calculation techniques to prove that the performance requirements of the Building Code can be met.

It is often the case, especially in unique or complex designs, that a relatively large calculation effort is needed to prove the fire safety requirements. This effort is generally in terms of time, which directly relates to an increased design cost which often forces design changes and compromises so that a project can be kept within its budget. If the calculation methods used in such design could be simplified, the realistic design possibilities available would be enlarged. One area of current fire research is the development of such engineering calculation techniques. This usually involves experimental and theoretical research. This general statement applies to the development of simple techniques for flame spread design calculations.

1.5 Purpose of the report

The fire spread research presented in this report can be divided into two individual parts, namely,

1. The development of a simplified expression that links the time to ignition of a material to its exposed heat flux level.
2. The incorporation of this time to ignition expression into a model that can analyse the upward flame spread characteristics for various different combustible materials.

The first area of investigation required that a time to ignition equation, based on simplified theory, be modified so that the dependence on the variables in this equation

can be determined. Once this had occurred, various simplifications to this equation were investigated.

The second area aimed to create a practical model for describing the flame spread behaviour on various interior combustible wall linings. The model focused on the dominant phenomena involved, thus removing most of the actual complexity of the "real" situation. This approach is supported by Williams [23] who stated in a 1976 report that,

> *"...there is merit (in neglecting) all but the essential phenomena and in studying thoroughly limiting cases in which different phenomena are controlling."*

To ensure that such a model produced useful results, the calculated values were compared with experimental data from the European Standard Room/Corner and a Finnish Vertical Wall test method. The use for such a model could be to determine whether a particular material, material combination and/or construction technique would be safe to use within a structure. This method could be incorporated as an acceptable engineering calculation technique for the performance based Building Code.

Once the model was established and the values calculated for each material, sensitivity analysis was undertaken so that the influence of each input variable could be determined. This analytical model was constructed in an EXCEL spreadsheet and the sensitivity analysis was undertaken in @RISK.

1.6 Overview of this Report

This research focused on the determining the spread of fire on combustible interior materials. The first chapter of this report, being the introduction, introduces the reader to fire research in general and attempts to provide reasoning for the work undertaken by the author.

Background theory on the spread on fire is presented in the second chapter. Here the theory on flame spread over solids is given and some previous research relevant to this topic is mentioned. The Cone Calorimeter and the Room/Corner test methods are briefly introduced as well as the way that different heat release rate (HRR) representations were used in the developed model.

The third chapter focuses on the first part of the research – the association between the time to ignition of a material and the heat flux level that it is exposed to. Seven different investigations, A to F, are discussed which includes linear regression techniques and variations on the density/heat flux ratio in the governing theoretical equation (see eqn. (2.9)). From these scenario investigations, a simplified equation was found for the time to ignition of various materials which was incorporated into the flame spread model developed in this research.

The second part of the research is the focus of the three following chapters of the report. Chapter four is used to describe the equations and the logic that was incorporated into the model as well as a description of the necessary inputs. Also included in this chapter is a sample spreadsheet of the analytical model so that the reader can establish a mental picture of the model for ease of understanding.

Chapter five describes the experimental studies that have been used as a comparison with the values calculated in the model. These studies include research undertaken in 1997 by the Finnish Technical Research Centre, VTT, as well as by the Swedish Institute for Wood Technology Research (Trätek) and a Nordic fire research program named "EUREFIC".

Chapter six details the assessment of the model, which includes the determination of the optimal values of the four tuning variables incorporated into the model. The results of this assessment are given in the summary at the end of this chapter. This analysis program used in this assessment was @RISK

The conclusions and future research is given in the final chapter of this report.

2. BACKGROUND THEORY

2.1 Introduction

Many people have studied flame spread on solid combustible materials previously to varying extents. These studies have tried to establish the governing equations so that mathematical models can be used to describe this particular aspect of a fire. A selection of this past research has been reviewed in [1]. Numerical and analytical methods have been developed to establish the required solution.

Mainly two types of methods for such predictions have been proposed in the literature in recent years. Firstly, thermal theories for upward flame spread have been used, where input data from the Cone Calorimeter is used to predict the flame spread and the resulting heat release rate (HRR). The large-scale scenario that has been used for the verification of this method has generally been the Room/Corner Test. Secondly, more fundamental work has been carried out using Computational Fluid Dynamic (CFD) and pyrolysis models to predict fire growth for the same full-scale experimental test. Both methods require the properties of the chosen material, which is usually determined from a bench-scale test apparatus, such as the Cone Calorimeter. The parameters needed would generally be thermal properties (such as k, ρ, c, T_{ig}) and properties to do with combustion, such as the heat of combustion and the latent heat of evaporation.

The analysis undertaken in this research has involved the development of an analytical flame spread model. An analytical model was chosen since proposed sensitivity analysis of the variables was planned using the program @RISK. This sensitivity analysis is required as it has been shown in previous research that relatively small variations in data can produce widely differing results in some models. This risk analysis program is designed for spreadsheets and therefore works only with analytical models. Verification of the analytic model has achieved by comparing the calculated values to specific experimental data that has been previously studied.

The following chapter details the theory that has been used in developing the analytical model that describes the flame spread vertically up various interior wall linings and horizontally across ceilings.

2.2 Flame Spread Theory

The growth of a fire in a room is to a considerable extent controlled by the energy released from the burning material and the velocity at which a flame spreads over it. The difficulty of predicting this velocity and the resulting fire growth is a fundamental problem in fire research.

As previously mentioned, many people have studied the flame spread phenomena. From a review on the known flame spread theory, mentioned in [8], it has been found that the process involved in terms of a simple energy conservation principle as given by "the fundamental equation of flame spread". This equation, seen below, states that the heat transferred to the virgin fuel needed to heat the fuel from T_0 to T_{ig} equals its change in enthalpy.

$$\rho V \Delta H_{T_0 \to T_{ig}} = \dot{q}''_{T_0 \to T_{ig}} \qquad \ldots(2.1)$$

where

ρ is the density of the fuel heated to ignition

V is the flame spread rate

ΔH is the change in enthalpy per unit mass of unburnt fuel in going from T_0 to T_{ig}

$\dot{q}''$ is the heat transferred to the unburnt fuel needed to increase the temperature from T_0 to T_{ig}

From the above equation, it is the value of the flame spread rate, V, which is of interest in this research. Usually the density of the fuel is known and assuming that its specific heat capacity, c, is constant with temperature, so that the increase in enthalpy of the material can be written as,

$$\Delta H_{T_0 \to T_{ig}} = c\left(T_{ig} - T_0\right) \qquad \ldots(2.2)$$

Generally, three mechanisms of heat transfer, $\dot{q}''$, would be present during the burning of a material between the flame and the virgin fuel. These mechanisms are convection, radiation and conduction. If such an analytic expression was to be developed to take into account all these mechanisms in the heat transfer, exact solutions would be difficult to set up. To simplify the solving of the analytical expression, only the dominant mode is considered and therefore the flame spread velocity is easily developed and solved using equation (2.1) above.

The dominant mode of heat transfer is the one that produces the largest contribution to $\dot{q}''$. The orientation of the solid fuel and wind conditions are important when determining the dominant mode of heat transfer. The flame spread rate is also dependent on whether the material is thermally thick or thin. Since the materials used throughout this research are thermally thick, only theory for this type of material was considered.

The flame spread equation for a thermally thick material has been found to be,

$$V = \frac{\dot{q}''^2 \Delta}{k\rho c\left(T_{ig} - T_0\right)^2} \qquad \ldots(2.3)$$

2.2.1 Flame Spread over Solids

The following section outlines some aspects of flame spread on solids and the influence that these factors have on the heat transfer, $\dot{q}''$. Generally, flame spread can occur in the presence of ambient wind, be that upwind (oppose flow) or downwind

(wind-aided), and these two categories will be discussed below. This wind may be environmental or fire-induced. Furthermore, flame spread over solids will depend on the geometric orientation (vertical or horizontal) of the materials. [17].

2.2.1.1 Opposed Flow Flame Spread over Thick Solids [8]

By applying the energy conservation equation (2.1), a description of the opposed flow flame spread for thermally thick materials can be obtained. It has been found that the dominant mode of heat transfer in this case is that of gas phase conduction over a short distance, Δ, near the pyrolysis front. In this phenomenon, as seen in the following figure, the flame is tilted which allows the radiation mode to be ignored.

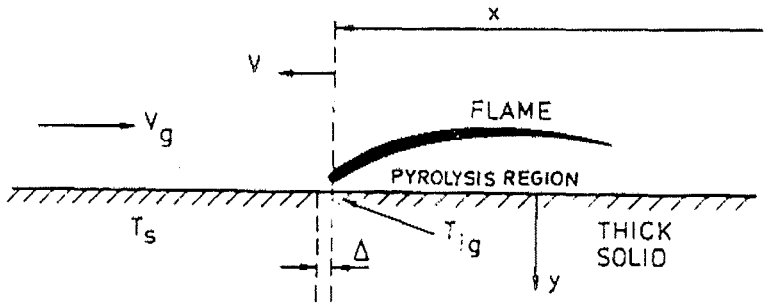

Figure 2.1: Energy Conservation Analysis in Opposed Flame Spread [8]

The gas phase conduction heat flux, $\dot{q}''_{gc}$, is assumed to be constant over the distance, Δ, and zero beyond. This assumption allows equation (2.3) to be rewritten as,

$$V = \frac{\dot{q}''^{2}_{gc}\Delta}{k\rho c\left(T_{ig} - T_0\right)^2} \qquad \ldots(2.4)$$

By defining the properties of the gas and balancing the forward gas phase conduction with the opposed flow convection, the "ideal" velocity can be written as,

$$V = \frac{V_g\left(k\rho c\right)_g\left(T_f - T_{ig}\right)^2}{k\rho c\left(T_{ig} - T_s\right)^2} \qquad \ldots(2.5)$$

Problems arise in determining solutions to this equation, as it is difficult to measure

the flame temperatures when various materials are burning. This problem has alleviated by rewriting this equation as,

$$V = \frac{\Phi}{k\rho c\left(T_{ig} - T_s\right)^2} \qquad \ldots(2.6)$$

where a material property, Φ, which can be determined in a bench-scale test.

2.2.1.2 Wind Aided Flame Spread over Thick Solids

This type of flame spread results from an external wind or the buoyancy-induced flow as a flame spreads up a wall or under a ceiling. The spread can be acceleratory and therefore appears more often than opposed flow flame spread. A similar analysis to that used in the previous section is used to describe this phenomenon.

This analysis considers wind aided flames spread on thermally thick materials, or thin materials attached to a backing board. The theory that has been developed [8] builds on a quasi-steady thermal model and no account of the complex chemical kinetics was included. It was also assumed that the fuel is sufficiently thick so that it is not completely consumed during the flame spread process – this applies that the material does not burn out.

The set-up for this analysis is shown in the figure below,

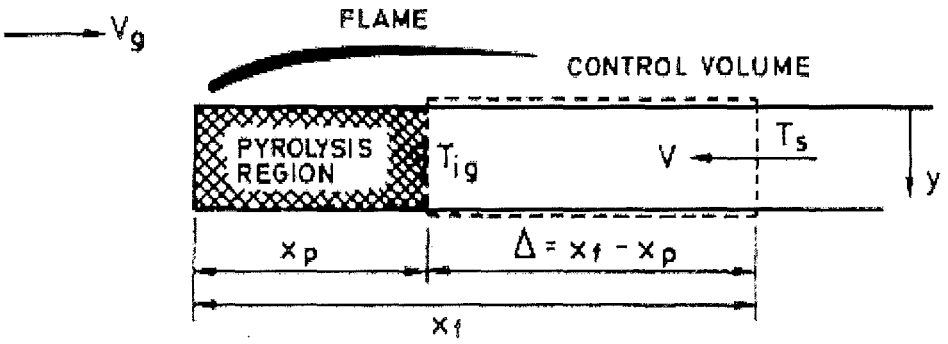

Figure 2.1: Energy Conservation Analysis in Wind-aided Flame Spread [8]

Starting from the general heat conduction equation, (2.1), and by applying the initial condition,

$$T(y,0)=T_0$$

and the boundary condition at y=0 (thus ignoring the convective and radiative cooling and other heat losses),

$$\dot{q}''(0,t) = \dot{q}_e'' = -k\frac{dT}{dy}$$

it is possible to arrive at the following expression for the ignition temperature, T_{ig},

$$T_{ig} - T_0 = \frac{2\dot{q}_e''}{\sqrt{\pi}}\sqrt{\frac{t_{ig}}{k\rho c}} \qquad \ldots(2.7)$$

If the time to ignition, t_{ig}, is replace with the heating distance (assumed to be equal to x_f - x_p) divided by the velocity of the pyrolysis front, an expression for the flame spread velocity can be obtained. This expression, similar to equation (2.3), is given as,

$$V = \frac{4\dot{q}_e''^2(x_f - x_p)}{\pi k\rho c(T_{ig} - T_0)^2} \qquad \ldots(2.8)$$

By rearranging this equation following the method discussed by Saito, Quintiere and Williams [18], an expression for t_{ig}, the time to ignition is obtained. This equation is given by,

$$t_{ig} = \frac{\pi k\rho c(T_{ig} - T_0)^2}{4\dot{q}_e''^2} \qquad \ldots(2.9)$$

given that,

$$V = \frac{x_f - x_p}{t_{ig}} \qquad \ldots(2.10)$$

The time to ignition, t_{ig}, in the equations above depends only on the fuel properties, ambient temperature and the level of heat flux from the flame to the fuel. Inherent in the equations is the assumption that t_{ig} is approximately constant while x_f - x_p varies.

To simplify the underlining theory so a complete expression for V can be written, expressions for x_f and x_p must be found. Saito, Quintiere and Williams [18] found these expressions and developed an equation for V. Certain approximations were required for this solution to be obtained. The main assumptions were;

1. The material is thermally thick, homogeneous and it's thermal properties are constant with temperature.
2. Chemical kinetics are excluded, so that very fast (as well as very slow) rates of spread are not fully dealt with and extinction conditions are therefore only discussed approximately.
3. The flame length, x_f, depends on a power of $\dot{Q}$, the rate of heat release.
4. Heat flux from the flame only occurs at constant flux within the region $x_p < x < x_f$ (see fig 2.3 below).

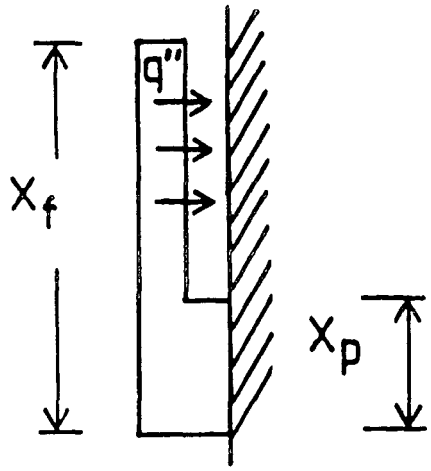

Figure 2.2: Constant Heat Flux Region, $x_p < x < x_f$

As mentioned above, in setting up an equation for the flame spread velocity, V, expressions are needed for x_f and x_p. The height of the pyrolysis zone, x_p, as a function of time, is given by,

$$x_p(t) = x_{po} + \int_0^t V_p(t_p)dt_p \qquad \ldots(2.11)$$

where x_{po} is the value of x_p at an initial time $t = 0$ and t_p is the dummy variable of integration.

The height of the flame is most commonly correlated with the total heat release rate, $\dot{Q}_{tot}$, and takes the form,

$$x_f(t) = K\dot{Q}_{tot}(t) \qquad \ldots(2.12)$$

The value of K depends on the location of the fire scenario, be that under a ceiling, in a corner or on an open wall.

In order to set-up the equation for the time dependent velocity of the pyrolysis front, V(t), steady state assumptions are needed for the initial conditions. The burner output, $\dot{Q}_b$, is assumed to produce a constant, steady flame height in front of the virgin fuel. The flame produces a heat flux that is assumed to be constant over the flame height and zero above it. After a certain time, governed by the a material dependent time to ignition value, the material behind the flame ignites and the pyrolysis height of this region, at $t = 0$, is thus given by,

$$x_f(t_0) = K\dot{Q}_b = x_{po} \qquad \ldots(2.13)$$

The flame height occurring at time, $t = 0$, is termed x_{fo} and is due to the energy released by the burner and the energy released from the initially burning material. The height is this flame at $t = 0$, as opposed to the different flame height before $t = 0$ (given by eqn. (2.13)), is,

$$x_{fo}(t_0) = K\left(\dot{Q}_b + x_{po} W \dot{Q}''(0)\right) \qquad \ldots(2.14)$$

In the above equation, $\dot{Q}''(0)$ is the heat released per unit area by the material at ignition and W is the width of the flame front. It is assumed that the width, W, takes that same value as the width of the burner.

So that the time dependent flame height for $t > 0$ can calculated, equation (2.12) shows that an expression for the total heat release rate, $\dot{Q}_{tot}$, is needed. This expression is influenced by three different sources, namely,

1. The constant output from the gas burner,
2. The initial burning material at time $t = 0$, and
3. The contribution resulting from the upward movement of the pyrolysis front.

By taking these effects into account, the total heat release rate, $\dot{Q}_{tot}$, is given by,

$$\dot{Q}_{tot}(t) = \dot{Q}_b + x_{po} W \dot{Q}''(t) + \int_0^t \dot{Q}''(t - t_p) W V(t_p) dt_p \qquad \ldots(2.15)$$

The heat release rate of the burning material, $\dot{Q}''$, is assumed to change with time, therefore denoted, $\dot{Q}''(t)$, and t_p is the dummy variable of integration.

Now that all the variables in equation (2.10) have been described by obtainable variables, an equation for the flame spread velocity can be derived. This is achieved by substituting equation (2.15) into (2.12), and combining this with (2.11). This substitution arrives at the following Volterra integral equation for the flame spread velocity, V(t),

$$V(t) = \frac{1}{t_{ig}}\left[K\left(\dot{Q}_b + x_{po} W \dot{Q}''(t) + \int_0^t W \dot{Q}''(t - t_p) V(t_p) dt_p\right) - \left(x_{po} + \int_0^t V(t_p) dt_p\right)\right] \qquad \ldots(2.16)$$

The analysis has so far assumed that K has the units of mkW^{-1}. This choice of unit implies that the width of the burning material remains constant. For materials placed under a ceiling, the characteristic width of the flame spread is not constant, therefore a flame spread velocity expression in terms of area is needed. To allow the analysis to continue in a unit area (m^2kW^{-1}) basis as opposed to a unit length (mkW^{-1}), thus incorporating flame spread under ceilings as well as vertically up walls, equation (2.16) is rewritten as,

$$V(t)=\frac{1}{t_{ig}}\left[K\left(\frac{\dot{Q}_b}{W}+x_{po}\dot{Q}''(t)+\int_0^t \dot{Q}''(t-t_p)V(t_p)dt_p\right)-\left(x_{po}+\int_0^t V(t_p)dt_p\right)\right] \quad \ldots(2.17)$$

The first two terms in the brackets on the right hand side represent x_f and x_p respectively and t_p is again, the dummy variable of integration.

Two further assumptions are included in this analysis, being,

1. The initial pyrolysing length, x_{po}, is dependent on the burner output, $\dot{Q}_b$. This output is assumed to be constant at all times.
2. Preheating of the combustible material beyond the flame tip is not accounted for (such as preheating by a hot gas layer). The flame is assumed to be the only source of heat and therefore T_s, as indicated in figure (2.2), is assigned the same value as T_0.

To solve equation (2.17), a mathematical representation is needed for the time dependent heat release rate of the given material. This can be achieved by using Cone Calorimeter data, and developing simple heat release rate expressions. The following sections describe such a technique.

2.2.2 HRR Representations

To solve the equation (2.17), it is necessary to mathematically represent the time dependent heat release rate and the flame length of the material under investigation. From research undertaken in [8], it has been shown that the heat release rate (HRR) of a combustible material can be approximated in one of two ways - a peak followed by an exponential decay (Peak/Decay) or an averaged, straight (Averaged) heat flux. These two HRR representations can be seen graphically in figures (2.4) and (2.6) in the following sections. Note that many other types of mathematical representations can be made [8] but it is these two types that were investigated in this research.

The peak/decay model assumes that the heat flux from the combustible material peaks as the item ignites and then decays exponentially over time. The value of this peak, $\dot{Q}''_{max}$, and the rate of decay, λ, are material dependent and are therefore required input variables in the developed flame spread model.

The averaged model assumes that the exponential decay of the previously described model is so small so that it can be ignored and the material can then be represented by a constant heat flux, $\dot{Q}''_{ave}$. This model holds reasonably well for materials that burn slowly over a relatively long time period.

2.2.2.1 Peak/Decay HRR Representation

As shown in the following figure, materials can be approximated by a Peak/Decay heat release rate mathematical representation. The form of such expression is,

$$\dot{Q}''(t) = \dot{Q}''_{max} e^{-\lambda t}$$

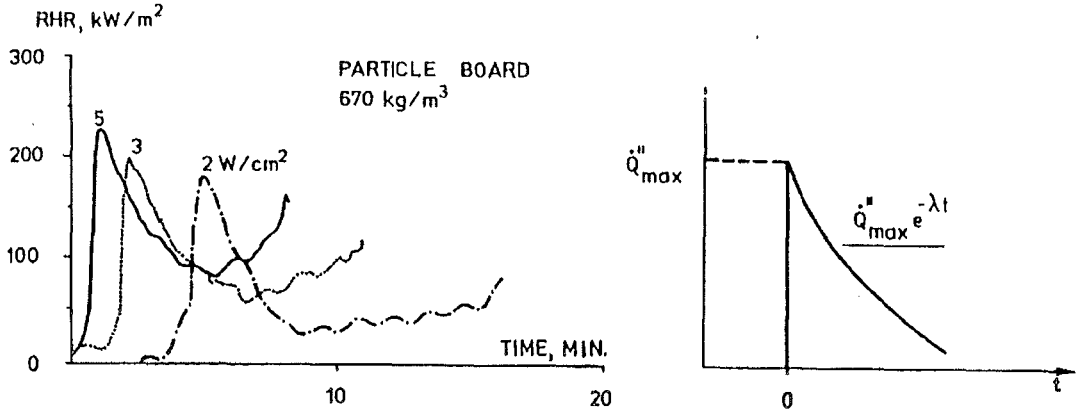

Figure 2.1: Cone Calorimeter Test Results and the Peak/Decay HRR Representation [8]

By applying the assumptions as described previously and taking Laplace transformations, followed by inverse Laplace transforms of equation (2.17), the following equation is obtained for the flame spread velocity, V(t),

$$V(t) = \frac{C_1}{s_2 - s_1}\left[s_2 e^{s_2 t} - s_1 e^{s_1 t}\right] \qquad \ldots(2.18)$$

where,

$$s_{1,2} = -\frac{1}{2t_{ig}}\left(1 - a + \lambda t_{ig}\right) \pm \frac{1}{2}\sqrt{\Delta} \qquad \ldots(2.19)$$

$$\Delta = \frac{1}{t_{ig}^{\,2}}\left(1 - a + \lambda t_{ig}\right)^2 - \frac{4\lambda}{t_{ig}} \qquad \ldots(2.20)$$

$$a = K\dot{Q}''_{max} \qquad \ldots(2.21)$$

and

$$C_1 = \frac{K\dot{Q}''_{max} A_0}{t_{ig}} \qquad \ldots(2.22)$$

The conditions for the velocity to accelerate are that s_1 or s_2 or both are positive, otherwise the velocity decelerates. A decelerating velocity is describe by the

following limits

$$\text{V}(t) \text{ decelerates if} \quad \Rightarrow \quad \left(1-\sqrt{\text{a}}\right)^2 < \lambda t_{ig} < \left(1+\sqrt{\text{a}}\right)^2$$

If the V(t) decelerates, then (2.18) no longer applies and V(t) becomes,

$$\text{V}(t) = \frac{\text{C}_1 e^{\alpha t}}{\beta}\left[\alpha \sin(\beta t) + \beta \cos(\beta t)\right] \qquad \ldots(2.23)$$

where,

$$\alpha = -\frac{1}{2t_{ig}}\left(1 - \text{a} + \lambda t_{ig}\right) \qquad \ldots(2.24)$$

$$\beta = \frac{1}{2}\sqrt{\Delta} \text{ (when } \Delta \text{ is positive)} \qquad \ldots(2.25a)$$

$$\text{or } \beta = \frac{1}{2}\sqrt{-\Delta} \text{ (when } \Delta \text{ is negative)} \qquad \ldots(2.25b)$$

The limits of the accelertory or deceleratory behaviour for the flame spread velocity can be represented graphically in the following figure. Note that in this figure, the symbol τ is used to describe the time to ignition, t_{ig} .

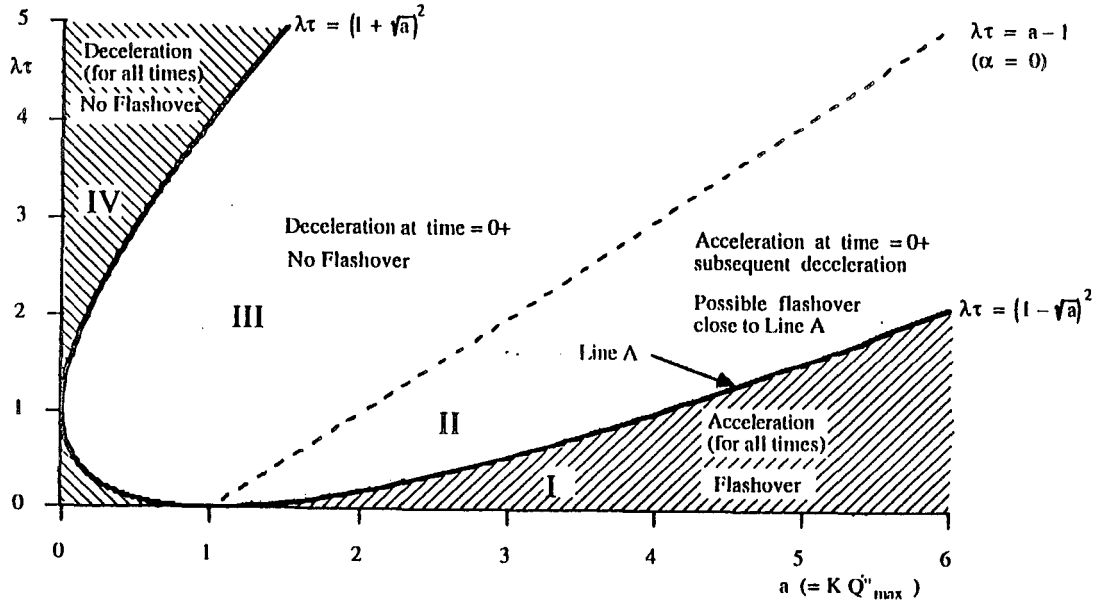

Figure 2.2: Regions of Flame Front Acceleration and Deceleration [8]

Four regions are indicated in the previous figure which depend on the value that the product λt_{ig} takes. The description of the flame spread can be summarised in the following table.

Table 2-1: **Summary of Flame Spread Characteristics**

Region [a]	Expression	Flame Front Description	Graphical Representation
I	$\lambda t_{ig} < \left(1-\sqrt{a}\right)^2$	Acceleration over all times	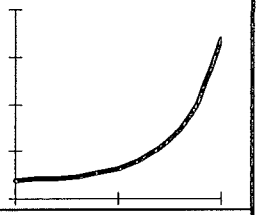
II	$\left(1-\sqrt{a}\right)^2 < \lambda t_{ig} < (a-1)$	Oscillatory decay with initial acceleration	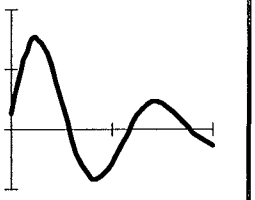
III	$(a-1) < \lambda t_{ig} < \left(1+\sqrt{a}\right)^2$	Oscillatory decay with initial deceleration	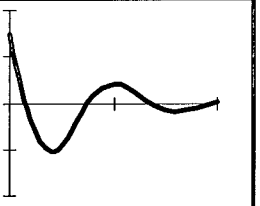
IV	$\lambda t_{ig} > \left(1+\sqrt{a}\right)^2$	Deceleration over all times	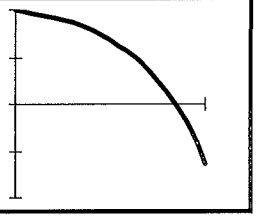

[a] The region described in this column is stated in reference to fig 2.5

Note that the solutions for the flame spread velocity are only valid for positive values of $V(t)$ since the flame height is always considered to be positive. This limitation is of particular importance for oscillatory flame spread described in regions II and III as the validity of $V(t)$ ceases once the velocity becomes negative for the first time.

In order to calculate how far the flame front has travelled and the resulting heat release rate, the expressions, in terms of velocity, for the pyrolysing area, $A_p(t)$, and the heat release rate, $\dot{Q}_c(t)$, must be derived. Again the flame spread behaviour, be that accelertory or deceleratory, must be considered.

The pyrolysing area, $A_p(t)$, with units of m^2, is described by the following equation,

$$A_p(t) = A_0 + \int_0^t V(t_p)dt_p \qquad \ldots(2.26)$$

which has solutions of,

for $\lambda t_{ig} < \left(1-\sqrt{a}\right)^2$, $\lambda t_{ig} > \left(1+\sqrt{a}\right)^2$

$$A_p(t) = A_0 + \frac{C_1}{s_2 - s_1}\left[e^{s_2 t} - e^{s_1 t}\right] \qquad \ldots(2.27)$$

and for $\left(1-\sqrt{a}\right)^2 < \lambda t_{ig} < \left(1+\sqrt{a}\right)^2$

$$A_p(t) = A_0 + \frac{C_1 e^{\alpha t}}{\beta}\sin[\beta t] \qquad \ldots(2.28)$$

where,

$$\alpha = -\frac{1}{2t_{ig}}\left(1-a+\lambda t_{ig}\right) \qquad \ldots(2.29)$$

$$\beta = \frac{1}{2}\sqrt{\Delta} \text{ (when } \Delta \text{ is positive)} \qquad \ldots(2.30a)$$

$$\text{or } \beta = \frac{1}{2}\sqrt{-\Delta} \text{ (when } \Delta \text{ is negative)} \qquad \ldots(2.30b)$$

where Δ is given by equation (2.20).

Similarly, the heat release rate, $\dot{Q}_c(t)$ with units of kW, for the material is described by the following equations;

$$\dot{Q}_c(t) = A_0 \dot{Q}''_{max} e^{-\lambda t} + \int_0^t \dot{Q}''_{max} e^{-\lambda t} V(t_p) dt_p \qquad \ldots(2.31)$$

which has solutions of,

for $\lambda t_{ig} < \left(1-\sqrt{a}\right)^2$, $\lambda t_{ig} > \left(1+\sqrt{a}\right)^2$

$$\dot{Q}_c(t) = A_0 \dot{Q}''_{max} e^{-\lambda t} + \frac{C_1}{s_2 - s_1}\left[\frac{s_2 \dot{Q}''_{max}\left(e^{s_2 t} - e^{-\lambda t}\right)}{s_2 + \lambda} - \frac{s_1 \dot{Q}''_{max}\left(e^{s_1 t} - e^{-\lambda t}\right)}{s_1 + \lambda}\right] \quad \ldots(2.32)$$

and for $\left(1-\sqrt{a}\right)^2 < \lambda t_{ig} < \left(1+\sqrt{a}\right)^2$

$$\dot{Q}_c(t) = A_0 \dot{Q}''_{max} e^{-\lambda t} + C_1 C_2 \dot{Q}''_{max}\left[e^{\alpha t}\left(\cos(\beta t) + \frac{C_3}{\beta}\sin(\beta t)\right) - e^{-\lambda t}\right] \quad \ldots(2.33)$$

where,

$$C_2 = \left[\frac{1}{\lambda}\left(\alpha^2 + \beta^2\right) + 2\alpha + \lambda\right]^{-1} \quad \ldots(2.34)$$

$$C_3 = \frac{1}{\lambda}\left(\alpha^2 + \beta^2\right) + \alpha \quad \ldots(2.35)$$

And C_1, α and β are given by equations (2.22), (2.24), and (2.25a,b) respectively.

2.2.2.2 Average HRR Representation

This analysis, for the Average heat release rate representation, is similar to that described in the previous section for the Peak/Decay representation. The figure below shows an actual heat release rate curve for a particular material, to the left, and a constant representation of the same curve, to the right. The form of the expression for the Average heat release rate representation is,

$$\dot{Q}''(t) = \dot{Q}''_{ave}$$

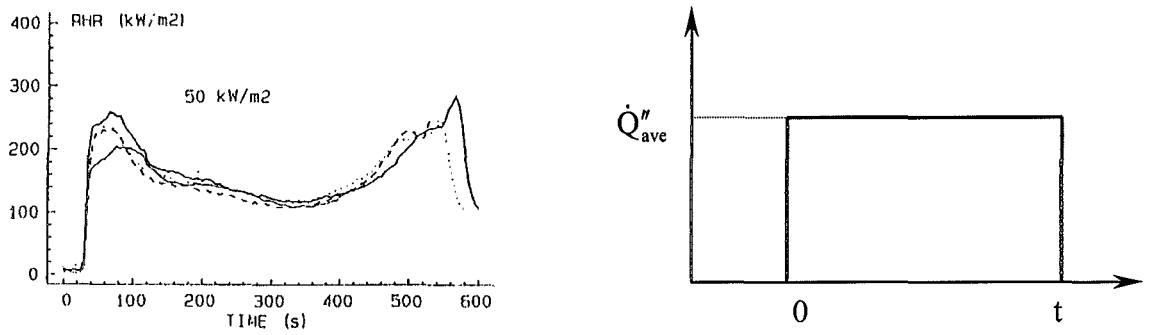

Figure 2.1: Cone Calorimeter Test Results [21] and the Average HRR Representation

By applying the assumptions outlined in the previous section, equation (2.17) can be applied to this particular representation. The following equation is obtained for the flame spread velocity, V(t),

$$V(t) = \frac{K\dot{Q}_b}{t_{ig}} A e^{\frac{(A-1)t}{t_{ig}}} \qquad \ldots(2.36)$$

where,

$$A = K\dot{Q}''_{ave} W \qquad \ldots(2.37)$$

The pyrolysing length, $x_p(t)$, with units of m, can then be described as,

$$x_p(t) = K\dot{Q}_b + \frac{K\dot{Q}_b A}{(A-1)}\left[e^{\frac{(A-1)t}{t_{ig}}} - 1 \right] \qquad \ldots(2.38)$$

Similarly, the heat release rate, $\dot{Q}(t)$, with units of kW, is given by,

$$\dot{Q}(t) = \dot{Q}_b + x_{po}\dot{Q}''_{ave} W + \frac{K\dot{Q}_b A}{(A-1)}\left[e^{\frac{(A-1)t}{t_{ig}}} - 1 \right]\dot{Q}''_{ave} W \qquad \ldots(2.39)$$

3. IGNITION TIME/HEAT RELEASE ASSOCIATION

3.1 Introduction

Many different variables are needed to fully describe the flame spread process during any given test. Such variables include the properties, location and orientation of the material, the properties of the testing equipment as well as various environmental factors to name but a few. In an attempt to develop a simple model that focuses on the dominant phenomena and therefore reduces the number of necessary inputs, a simple expression which linking the time to ignition of a material to its exposed heat flux level was needed. The determination of such an expression is the topic of this chapter.

3.1.1 Background

The heat flux exposed to a material, from an experimental apparatus such as the Cone Calorimeter, can be varied over a considerable range, typically from around 0 to 110 kWm^2 for the standard bench scale device. It is this change in radiated heat flux level that obviously plays a significant role in the time that a given material would take to ignite. An equation has been established in the previous chapter, which can be used to describe this time duration, namely equation (2.9). This equation, as developed in the previous section, is given by,

$$t_{ig} = \frac{\pi k\rho c\left(T_{ig} - T_0\right)^2}{4\dot{q}_e''^2} \qquad \ldots(3.1)$$

and is a solution of the one-dimensional heat conduction equation, using relatively simple initial and boundary conditions. The material properties are included in the terms "$k\rho c$" and T_{ig}, and the apparatus term is given by $\dot{q}_e''$. The ambient temperature, T_0, also introduces an environmental term.

This equation, though relatively simple, was expected to contain more variables than needed. The dominant variables were thus sought so that further simplifications could be possibly made.

From previous testing, results had shown that for cellulosic materials the value of $(T_{ig} - T_0)^2$ varies to a lesser extent than for the other variables, since T_{ig} is typically in the range 350-450°C. In general, it can be assumed that the conductivity, k, increases with density, ρ. From this, it was anticipated that the time to ignition may be able to be satisfactory represented by some form of the equation,

$$t_{ig} = C\frac{\rho^{X1}}{\dot{q}_e''^{X2}} \qquad \ldots(3.2)$$

where the constant C incorporated the less dominant variables of eqn. (3.1) and X1 and X2 were some powers associated with the two remaining dominant variables.

One method of determining the three unknowns values in this form of equation is by Linear Regression.

Equation (3.2) is not the only equation that can be used to determine the time to ignition at various heat fluxes. Other possible calculation forms could include a decaying exponential equation, as it has been found from plots of these two dominant variables, that the time exhibits this type of behaviour as the heat flux increases.

These simplified equations were investigated so that the "best" expression could be incorporated into the developed flame spread model.

3.1.2 Materials Investigated

Thirteen different materials studied by the Swedish Institute of Wood Technology Research were investigated in this analysis. To simplify the analysis in the following section, the materials used have been abbreviated. Further details of the materials can be found in [8].

Table 3-1: Swedish Data Abbreviations used in this Section

Material Number	Building Material
S1	Insulating Fibre Board
S2	Medium Density Fibre Board
S3	Particle Board
S4	Gypsum Board
S5	Plastic Wall-covering on Gypsum Board
S6	Paper Wall-covering on Gypsum Board
S7	Textile Wall-covering on Gypsum Board
S8	Textile Wall-covering on Rockwool
S9	Melamine-faced Particle Board
S10	Expanded Polystyrene
S11	Rigid Polyurethane Foam
S12	Wood Panel (Spruce)
S13	Paper Wall-covering on Particle Board

3.2 Analysis

In this section, seven different analyses are documented. Again, as for the previous table, an abbreviation has been made for the descriptions of the investigations, as follows,

Table 3-1: **Investigation Descriptions**

Scenario	Description
A and B	Linear Regression: $t_{ig} = C\frac{\rho^{X1}}{\dot{q}_e''^{X2}}$ Equation
C	Linear Regression: $t_{ig} = C\frac{1}{\dot{q}_e''^{X3}}$ Equation
D	$t_{ig} = C\frac{\rho}{\dot{q}_e''^{2}}$ Equation Investigation
E	$t_{ig} = C\frac{\rho^{2}}{\dot{q}_e''^{2}}$ Equation Investigation
F	$t_{ig\,A} = Xt_{ig\,B}$ Equation Investigation
G	Averaged Exponential Trendline Analysis

3.2.1 Scenarios A, B and C

Scenario A:

Equation (3.2) indicates that the time to ignition can be calculated by multiplying a constant, C, with a density/heat flux term raised to certain powers. The first of three different Linear Regression Analyses undertaken involved finding the values of the constant C and the powers X1 and X2.

The Linear Regression technique used in this report was undertaken in EXCEL and verified by Matlab. Both programs gave identical results.

The analysis, as previously mentioned, was carried out on the combined group of Swedish materials. The results of this analysis are detailed below.

The output results indicated that the density variable had less influence than that of the heat flux variable. A summary of the findings of the Regression Analysis is given in the following table.

Table 3-1: Dependent Variable Values for Materials S1-13 Combined

Variable	Regression Results
Constant, C	21822.0
Density Power, X1	0.344
Heat Flux Power, X2	2.307

From the values given in the table above the equation (3.2), i.e.,

$$t_{ig} = C\frac{\rho^{X1}}{\dot{q}_e''^{X2}}$$

can now be written as;

$$t_{ig} = 21822\frac{\rho^{0.344}}{\dot{q}_e''^{2.307}} \qquad \ldots(3.3)$$

The results from this combined Liner Regression were then used to assess the ability of equation (3.3) to map the calculated time to ignition values to the actual time to ignition values determined in a experimental apparatus, namely the Cone Calorimeter. The results of this analysis are given in the table below.

Table 3-2: Scenario A Time to Ignition Comparison

Material Number	Cone Calorimeter Data: Actual t_{ig} (s) @q (kWm^{-2})						Calculated Values: t_{ig} (s) using the Linear Regression Equation Values @q (kWm^{-2})						Results: %^{age} Error in Comparing the Cone Data and Calculated Values @q (kWm^{-2})						
	20	25	30	35	50	75	20	25	30	35	50	75	20	25	30	35	50	75	Average
S1	92	43			12	6	145	87	57	40	18	7	58	102			46	15	55
S2	223	123			28	14	196	117	77	54	24	9	-12	-5			-15	-34	-16
S3	255	123			34	16	212	127	83	58	26	10	-17	3			-25	-37	-19
S4				112	34	13	207	124	81	57	25	10				-49	-26	-24	-33
S5	126	41	28		10	4	205	123	81	56	25	10	63	199	188		148	143	148
S6		106	101		21	6	206	123	81	57	25	10		16	-20		18	62	19
S7		115	82		20	7	206	123	81	57	25	10		7	-1		25	40	18
S8	49	30			11	9	131	78	51	36	16	6	167	161			44	-31	85
S9			498		42	12	218	130	85	60	26	10			-83		-37	-14	-45
S10	873	223			39		61	36	24	17	7	3	-93	-84			-81		-86
S11	12	4			2		70	42	28	19	8	3	484	947			323		585
S12	525	169	79		21	11	188	112	74	52	23	9	-64	-34	-7		8	-19	-23
S13	603	139	111		27	12	210	125	82	58	25	10	-65	-10	-26		-6	-17	-25
																		Average of the averaged %^{age} errors above:	51

Note that the percentage error values can often be misleading due to the range values that they are expressing, i.e. for large values, the percentage error will be less than for smaller values that have the same difference in their absolute values.

From the values obtained in the table above, a plot that compares the experimental data with the results of equation (3.3) was produced. The following figure shows this comparison.

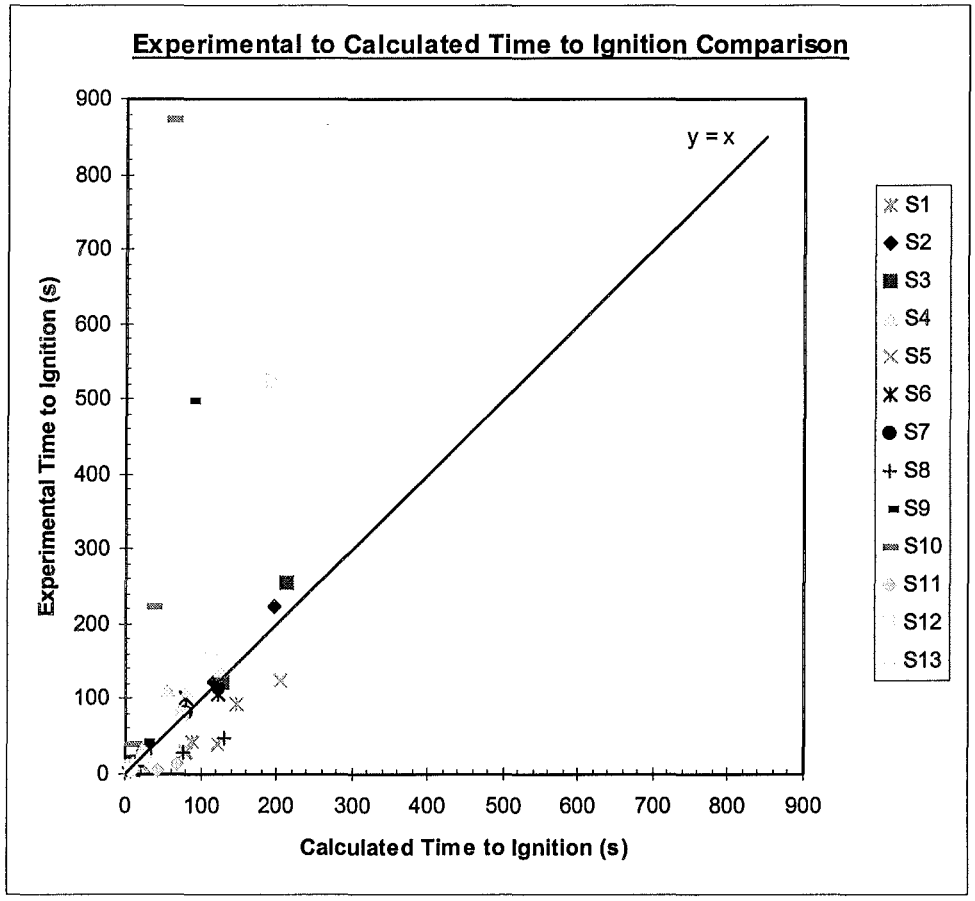

Figure 3.1: Scenario A Time to Ignition Comparison

From this graph it is possible to see that the some errors occur when this technique is applied. It can also be seen that some materials are not suited for this equation, e.g. S10, which has a much larger slope than the other materials.

The table and figure above show that this method can only give representative values of the time to ignition for all the materials. Some selected materials could be acceptable for the used of the equation, such as materials S2 and S3. The average value of the averaged percentage error values is 51%. The results show that this mapping technique works best for materials S2-4, S6, S7, S12 and S13.

Scenario B:

From the previous analysis, it was found that materials S1, S5, S8, S10 and S11, in particular, did not compare well to the rest of the materials as their percentage errors were generally larger, so further analysis was carried out which excluded these materials. This analysis involved recalculating the C, X1 and X2 values in equation (3.2).

The results from the regression analysis from materials S2-4, S6-7, S9 and S12-13 are,

Table 3-3: Dependent Variable Values for Materials S2-4, S6-7, S9 and S12-13 Combined

Variable	Refined Regression Results
Constant, C	2607.8
Density Power, X1	0.853
Heat Flux Power, X2	2.567

Equation (3.3) can now be rewritten for this group of materials as,

$$t_{ig} = 2607.8 \frac{\rho^{0.853}}{\dot{q}_e''^{2.567}} \qquad \ldots(3.4)$$

This equation differs from its previous form (3.3) by,

- The constant, C, reducing (21822 → 2607.8),
- X1 increasing (0.344 → 0.853), and
- X2 increasing (2.307 → 2.567).

The results from this combined Linear Regression of the reduced number of materials was then used to assess the ability of equation (3.4) to map the calculated time to ignition values to the actual time to ignition values determined in a experimental apparatus, namely the Cone Calorimeter. The results of this analysis are given in the table below.

Table 3-4: Scenario B Time to Ignition Comparison

Material Number	Cone Calorimeter Data: Actual t_{ig} (s) @q (kWm^{-2})						Calculated Values: Linear Regression Equation t_{ig} (s) Values @q (kWm^{-2})						Results: %age Error in Comparing the Cone Data and Calculated Values @q (kWm^{-2})						
	20	25	30	35	50	75	20	25	30	35	50	75	20	25	30	35	50	75	Average
S1	*92*	*43*			*12*	*6*	*132*	*75*	*47*	*31*	*13*	*4*	*44*	*74*			*5*	*-26*	*24*
S2	223	123			28	14	279	158	99	66	27	9	25	28			-5	-33	4
S3	255	123			34	16	338	191	119	80	32	11	33	55			-5	-29	13
S4				112	34	13	319	180	113	76	30	11				-32	-11	-18	-20
S5	*126*	*41*	*28*		*10*	*4*	*312*	*176*	*110*	*74*	*30*	*10*	*147*	*329*	*293*		*197*	*162*	*226*
S6		106	101		21	6	312	176	110	74	30	11		66	9		42	75	48
S7		115	82		20	7	315	178	111	75	30	11		55	36		50	51	48
S8	*49*	*30*			*11*	*9*	*102*	*58*	*36*	*24*	*10*	*3*	*108*	*92*			*-12*	*-62*	*32*
S9			498		42	12	361	204	127	86	34	12			-74		-18	1	-30
S10	*873*	*223*			*39*		*15*	*9*	*5*	*4*	*1*	*1*	*-98*	*-96*			*-96*		*-97*
S11	*12*	*4*			*2*		*22*	*12*	*8*	*5*	*2*	*1*	*81*	*206*			*3*		*97*
S12	525	169	79		21	11	250	141	88	59	24	8	-52	-17	12		13	-24	-13
S13	603	139	111		27	12	329	185	116	78	31	11	-45	33	5		16	-8	0
																			Average of the averaged %age errors above: 25

Note:

1. The rows that are in *italics* (i.e. materials S1, S5, S8, S10 and S11) were excluded from the Linear Regression Calculation since they exhibit different characteristics from the other data.
2. The percentage error values can often be misleading due to the range values that they are expressing, i.e. for large values, the percentage error will be less than for smaller values that have the same difference in their absolute values.

From the values obtained in the table above, a plot that compares the experimental data with the results of equation (3.4). The following figure shows this comparison.

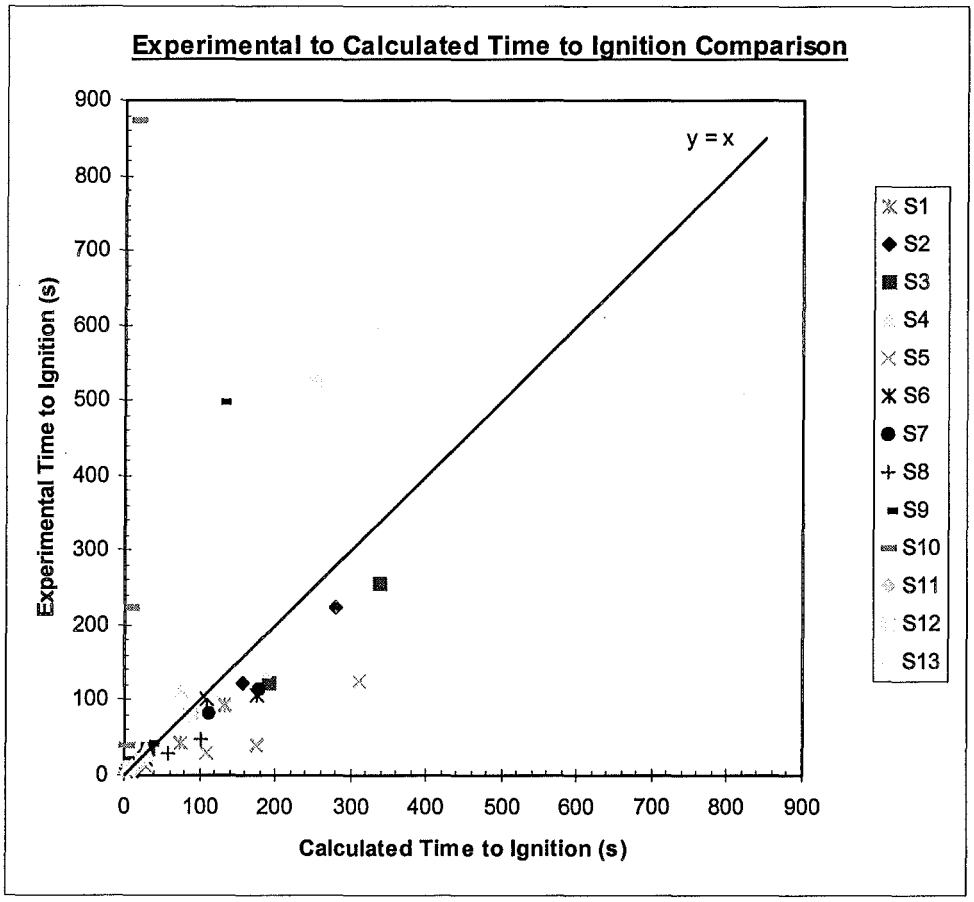

Figure 3.2: Scenario B Time to Ignition Comparison

Smaller percentage errors were found in this scenario B analysis compared to those found in the first (A) linear regression results were materials S1, S5, S8, S10 and S11 were included.

The table and figure above show that this method can give reasonable values for the time to ignition when this technique is applied for most of the Swedish materials. From the graph it can be expected that the calculated times for materials S5 and S10 would produce poor results, as the averaged percentage errors for these materials were -97 and +226% respectively. The average of the averaged percentage error values is 25%.

Scenario C:

In an attempt to simplify equation (3.2) even further, the density variable was removed. The Linear Regression analysis of this scenario is detailed below.

With the density variable removed, the scenario equation in which the unknown variables were to be determined, became,

$$t_{ig} = C\frac{1}{\dot{q}_e''^{X3}}$$

Linear regression analysis was performed on all the Swedish materials so that C and X3 could be found. The solutions are shown in the following table.

Table 3-5: Dependent Variable Values for all Materials Combined

Variable	Final Regression Results
Constant, C	55468.7
Heat Flux Power, X3	2.030

Equation (3.2) can now be rewritten for this scenario as;

$$t_{ig} = 55468.7\frac{1}{\dot{q}_e''^{2.030}} \qquad \ldots(3.5)$$

The calculated time to ignition results from this equation on the Swedish materials was compared to the actual time to ignition values. The results of this analysis are given in the table below.

Table 3-6: Scenario C Time to Ignition Comparison

Material Number	Cone Calorimeter Data: Actual t_{ig} (s) @q (kWm^{-2})						Calculated Values: Linear Regression Equation t_{ig} (s) Values @q (kWm^{-2})						Results: %^{age} Error in Comparing the Cone Data and Calculated Values @q (kWm^{-2})						
	20	25	30	35	50	75	20	25	30	35	50	75	20	25	30	35	50	75	Average
S1	92	43			12	6	127	81	56	41	20	9	38	88			65	45	59
S2	223	123			28	14	127	81	56	41	20	9	-43	-34			-29	-38	-36
S3	255	123			34	16	127	81	56	41	20	9	-50	-34			-42	-46	-43
S4				112	34	13	127	81	56	41	20	9				-64	-42	-33	-46
S5	126	41	28		10	4	127	81	56	41	20	9	1	97	99		98	117	82
S6		106	101		21	6	127	81	56	41	20	9		-24	-45		-6	45	-7
S7		115	82		20	7	127	81	56	41	20	9		-30	-32		-1	24	-10
S8	49	30			11	9	127	81	56	41	20	9	159	169			80	-4	101
S9			498		42	12	127	81	56	41	20	9			-89		-53	-28	-56
S10	873	223			39		127	81	56	41	20	9	-85	-64			-49		-66
S11	12	4			2		127	81	56	41	20	9	958	1917			888		1254
S12	525	169	79		21	11	127	81	56	41	20	9	-76	-52	-29		-6	-21	-37
S13	603	139	111		27	12	127	81	56	41	20	9	-79	-42	-50		-27	-28	-45
																		Average of the averaged %^{age} errors above:	88

Note that the percentage error values can often be misleading due to the range values that they are expressing, i.e. for large values, the percentage error will be less than for smaller values that have the same difference in their absolute values.

The following figure shows the comparison between the actual experimental values for the time to ignition and the values calculated using this technique.

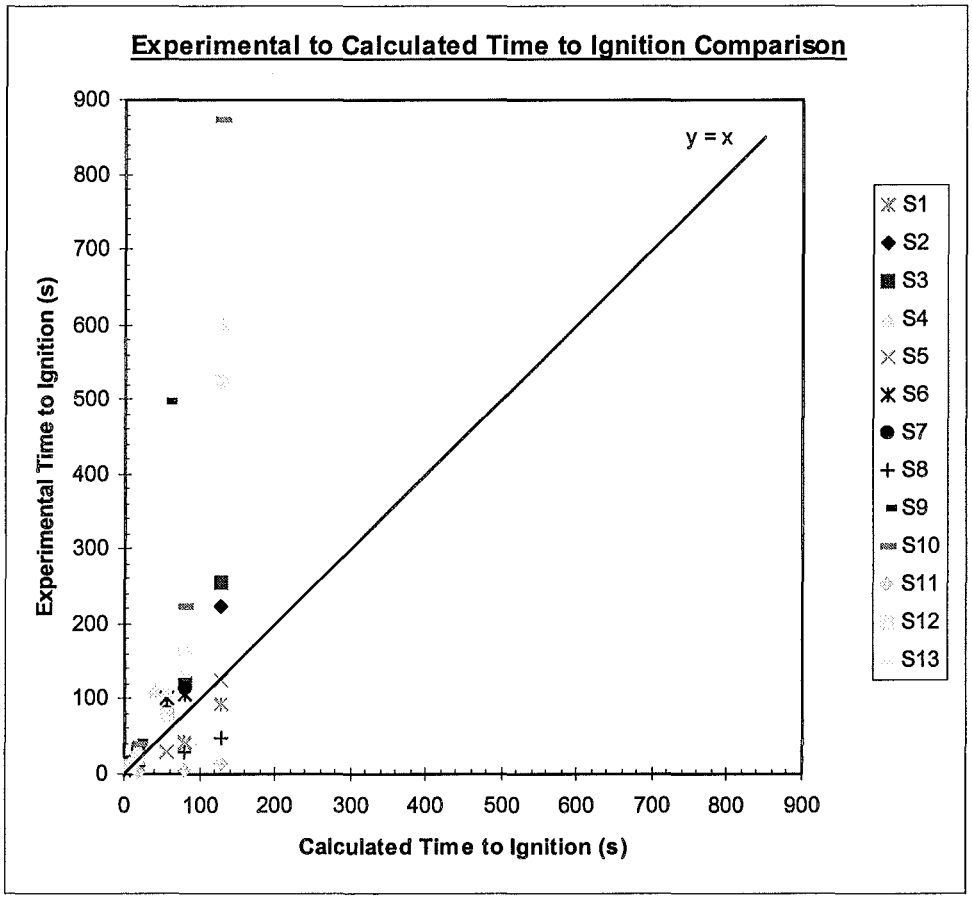

Figure 3.3: Scenario C Time to Ignition Comparison

The tabulated results from this analysis show that with the material dependence removed, i.e. the density of the material, from the time to ignition calculation, the comparison between the actual and calculated values deteriorates. This is clearly indicated by the increase of the averaged percentage error to 88%. The increase in this averaged error is highly influenced by the extremely large errors that occur for material S11. The results show that this mapping technique works "best" for materials S1-4, S6-7, S9-10 and S12-13.

3.2.2 Scenario D

Once it was expected that sufficient results were obtained from Linear Regression, a different approach to finding a mapping technique for the time to ignition at different heat fluxes was investigated. This scenarios approach was derived from the observations of the form of equation (3.1).

The first equation to be investigated in this new approach was a relationship between the time to ignition and the ratio of the material density to the exposed heat flux level squared. The form of such equation was,

$$t_{ig} = C\frac{\rho}{\dot{q}_e''^2}$$

The results of this investigation are given below.

The first step taken in the investigation was to plot the materials so that the slope, C, of the trendlines, linking the points of each material, could be determined. The time to ignition of the materials was plotted on the y-axis and the known density to the exposed heat flux squared value was plotted on the x-axis. The following graph shows this technique.

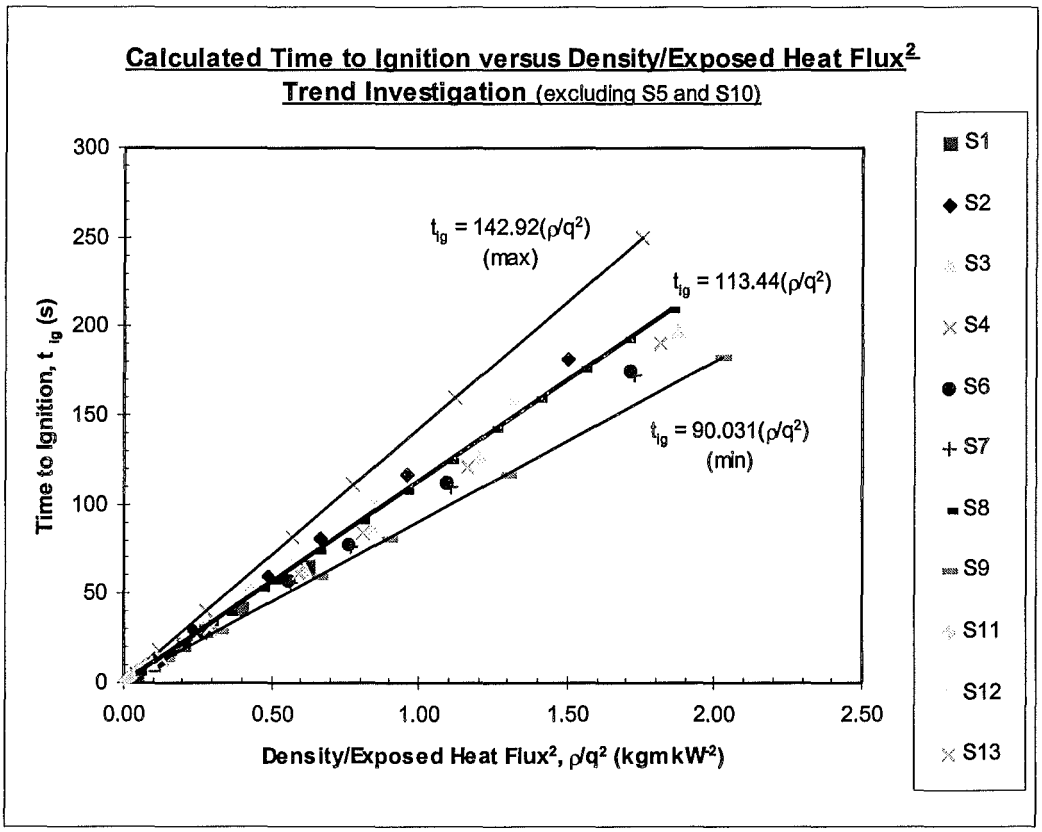

Figure 3.1: Time to Ignition, t_{ig}, versus $\frac{\rho}{\dot{q}_e''^2}$ Investigation

It can be seen from this figure that the materials plotted have C values that are similar. The central thick line in the figure above shows the average trendline of the grouped materials. The trendlines above and below this line indicate the maximum and minimum values of C. These trendlines nicely bound all of the data points, except S5 and S10, on the figure and the following table gives the actual values of the constant C as well as the percentage deviation that each material exhibits from the averaged C values.

Table 3-1: Constant Value for the Swedish Data

Material Number	Constant Value, C	%age Error
S1	104.09	-8.2
S2	121.12	6.8
S3	105.08	-7.4
S4	142.92	26.0
S5	*37.23*	*-67.2*
S6	102.34	-9.8
S7	99.55	-12.2
S8	114.66	1.1
S9	90.03	-20.6
S10	*2503.82*	*2107.3*
S11	141.57	24.8
S12	121.91	7.5
S13	104.54	-7.8
Averages	**113.44**	**0.00**

Note that the values in *italics* have been left out of the average calculation

Note that in the previous figure, materials S5 and S10, plastic wall-covering on gypsum board and expanded polyurethane foam, have been ignored. This is due to the fact that their points lie well away from the maximum and minimum trendlines that are indicated. This fact can also be seen in the table above where the slopes for S5 and S10 are 37.23 and 2503.82 respectively.

The average percentage change in the table above is zero, which shows that this particular equation holds well for the given data as the entire points lie within a relatively narrow band. It is this compactness of the data that indicates that this investigation should produce satisfactory results.

From the figure above the average value of the constant, C, was obtained, being equal to 113.44. By using this value to calculate the time to ignition at varying heat fluxes,

it was possible to determine the reliability of the estimation that this equation gave. The results when this equation was compared to experimental values are given in the following figure.

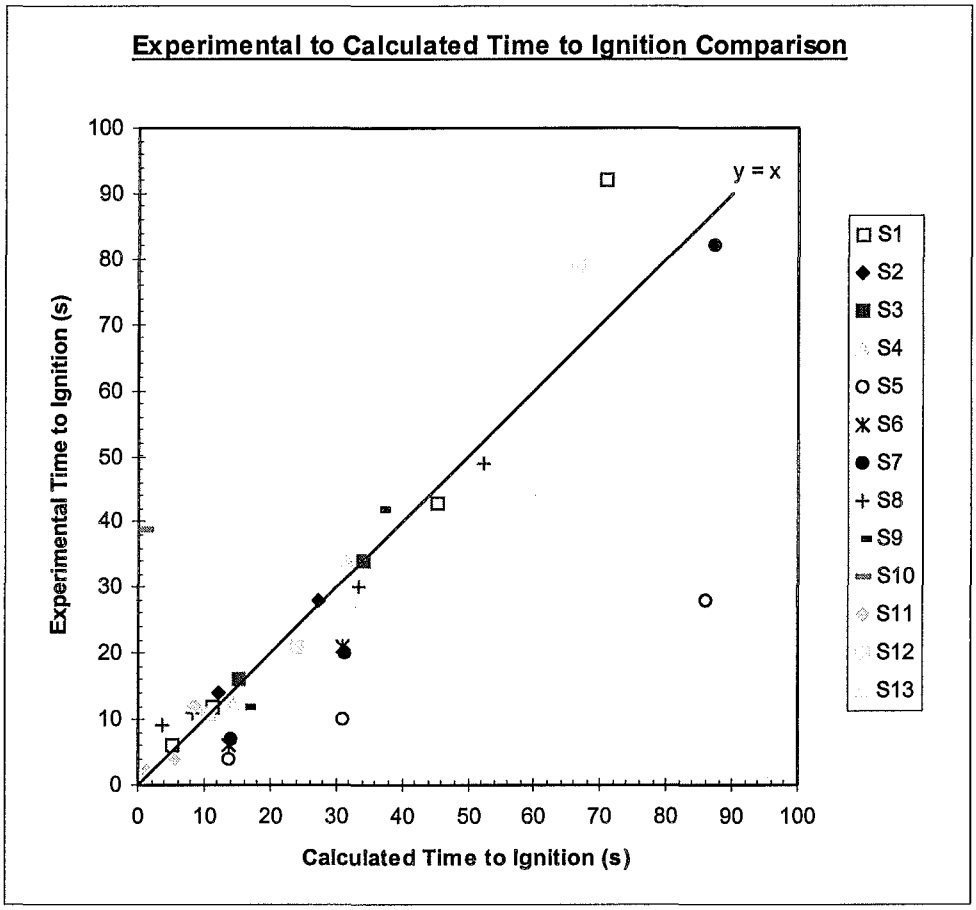

Figure 3.2: Scenario D Time to Ignition Comparison

The values graphed in the figure above are from the following table, which tabulates the results of the analysis of equation (3.6).

Table 3-2: Scenario D Time to Ignition Comparison

Material Number	Cone Calorimeter Data: Actual t_{ig} (s) @q (kWm^{-2})						Calculated Values: Calculated t_{ig} (s) using C=113.44 @q (kWm^{-2})						Results: %^{age} Error in Comparing the Cone Data and Calculated Values @q (kWm^{-2})						
	20	25	30	35	50	75	20	25	30	35	50	75	20	25	30	35	50	75	Average
S1	92	43			12	6	71	45	32	23	11	5	-23	6			-5	-16	-10
S2	223	123			28	14	170	109	76	56	27	12	-24	-11			-3	-14	-13
S3	255	123			34	16	213	136	95	69	34	15	-17	11			0	-5	-3
S4				112	34	13	199	127	88	65	32	14				-42	-7	9	-13
S5	*126*	*41*	*28*		*10*	*4*	*193*	*124*	*86*	*63*	*31*	*14*	*53*	*202*	*207*		*209*	*244*	*183*
S6		106	101		21	6	194	124	86	63	31	14		17	-15		48	130	45
S7		115	82		20	7	196	125	87	64	31	14		9	6		57	99	43
S8	49	30			11	9	52	33	23	17	8	4	6	11			-24	-59	-16
S9			498		42	12	230	147	102	75	37	16			-79		-12	36	-19
S10	*873*	*223*			*39*		*6*	*4*	*3*	*2*	*1*	*0*	*-99*	*-98*			*-98*		*-98*
S11	12	4			2		9	5	4	3	1	1	-29	36			-32		-8
S12	525	169	79		21	11	149	96	66	49	24	11	-72	-43	-16		14	-3	-24
S13	603	139	111		27	12	206	132	92	67	33	15	-66	-5	-18		22	22	-9
																			Average of the averaged %^{age} errors above: -2

Note:

1. The rows that are in *italics* (i.e. materials S5 and S10) are excluded from all calculations since they exhibit extremely different characteristics from the other data and are only show to indicate the extent of their differences.
2. The percentage error values can often be misleading due to the range values that they are expressing, i.e. for large values, the percentage error will be less than for smaller values that have the same difference in their absolute values.

The results of the comparison show that the equation $t_{ig} = C\frac{\rho}{\dot{q}_e''^2}$ represents the Swedish data relatively well for heat flux ranges from 20 to 75kWm^{-2}. The bottom right-hand value on the previous table shows that when all the average percentage error values are averaged, the result equals -2. This indicates that overall the Swedish data is evenly distributed about the average value for this investigation.

A similar investigation was carried out by not only ignoring materials S5 and S10, but also S4, S9 and S11. It was found that the value of the constant changed from 113.44 to a value of 109.16. A similar comparison between the calculated time to ignition values versus those actual times given by the Cone Calorimeter was undertaken. The results of this comparison showed that this new value of C gave only an extremely small improvement to the time to ignition calculated values for the seven remaining materials.

It is recommended that the constant C value of 113.44 should be used if this type of mapping technique is to be used on this specific group of materials, i.e.,

$$t_{ig} = 113.44\left(\frac{\rho}{\dot{q}_e''^2}\right) \qquad \ldots(3.6)$$

Care should be observed when applying this equation as the desired accuracy and consistency of the time to ignition values are yet to be proven when this particular mapping technique is used.

3.2.3 Scenario E

Another variation on simplification of equation (3.1) is detailed in this section and involves the analysis of the equation $t_{ig} = C\frac{\rho^2}{\dot{q}_e''^2}$. This equation, similar to the equation investigated in the previous section except the density term is squared, was expected to give similar results to the previous equation but this was proved incorrect.

This following section outlines the analysis and the results achieved.

The same technique was performed in the this analysis as previously used, that is to plot the two known terms on the x and y axis and determine the resulting slope of the trendline which linked the individual points on the graph, i.e. the unknown term C. It was found by plotting the materials in the way described above, that the C term became an exponential equation. The table below gives the values of the exponential equation that was found for each individual material.

Table 3-1: Graph Trendline Equations (including $q_{o,ig}$ values)

Material Number	Exponential Equation	First Term	$\%\Delta_{ave\ 1st\ term}$	Power	$\%\Delta_{ave\ 2nd\ term}$
S1	*$y = 4.4581e^{0.0266x}$*	*4.458*	*-50.3*	*0.027*	*483.9*
S2	$y = 12.743e^{0.0038x}$	12.743	42.0	0.004	-16.6
S3	$y = 14.56e^{0.0024x}$	14.560	62.3	0.002	-47.3
S4	$y = 5.9527e^{0.0083x}$	5.953	-33.7	0.008	82.2
S5	$y = 3.5228e^{0.0036x}$	3.523	-60.7	0.004	-21.0
S6	$y = 7.8853e^{0.0037x}$	7.885	-12.1	0.004	-18.8
S7	$y = 7.9747e^{0.0036x}$	7.975	-11.1	0.004	-21.0
S8	*$y = 5.0794e^{0.0394x}$*	*5.079*	*-43.4*	*0.039*	*764.9*
S9	$y = 7.0859e^{0.0059x}$	7.086	-21.0	0.006	29.5
S10	*$y = 19.232e^{4.0463x}$*	*19.232*	*114.3*	*4.046*	*88721.2*
S11	*$y = 1.6112e^{0.764x}$*	*1.611*	*-82.0*	*0.764*	*16670.7*
S12	$y = 9.3454e^{0.0065x}$	9.345	4.2	0.007	42.7
S13	$y = 11.686e^{0.0032x}$	11.686	30.2	0.003	-29.8
	Averaged Values:	**8.973**		**0.005**	

Note 1) In this table, y is the time to ignition, t_{ig}, and x is the ratio $\frac{\rho^2}{\dot{q}_e''^2}$.

2) The rows that are in *italics* (i.e. materials S1, S8, S10 and S11) are excluded from all calculations since they exhibit extremely different first and/or second term values from the other data and are only shown to indicate the extent of their differences.

3) The equations in this table use the materials' q_o value. It is assumed that t_{ig} equals 1500 seconds at q_o

From the table above, the unknown terms in the equation have been found. The form of the equation given above is now,

$$t_{ig} = 8.973e^{0.005\left(\frac{\rho^2}{\dot{q}''^2}\right)} \qquad \ldots(3.7)$$

It can be noted that this equation is no longer in the similar mathematical form as equation (3.2). This change is due to the resulting trendlines that are averaged when the data was plotted with the time to ignition on the y-axis the ratio $\frac{\rho^2}{\dot{q}_e''^2}$ on the x-axis.

This equation was now applied to each of the materials and the calculated values were compared to the actual time to ignition values obtained from the Cone Calorimeter data. The results from this analysis are given below.

Table 3-2: Scenario E Time to Ignition Comparisons

	Cone Calorimeter Data							**Calculated Averaged Exponential Equation Values**						**Error in the t_{ig} (Exponential Eqn.) values versus the Cone data (%) @q (kWm^{-2})**						
Material	t_{ig} (s) @q (kWm^{-2})							t_{ig} (s) @q (kWm^{-2})						%^{age} Error @q (kWm^{-2})						
Number	$q_{o,ig}$	20	25	30	35	50	75	20	25	30	35	50	75	20	25	30	35	50	75	Average
S1	*1500*	*92*	*43*			*12*	*6*	*18*	*14*	*12*	*11*	*10*	*9*	*-80*	*-67*			*-16*	*57*	*-41*
S2	1500	223	123			28	14	541	124	56	34	17	12	143	1			-38	-14	24
S3	1500	255	123			34	16	5434	541	155	73	25	14	2031	340			-26	-12	772
S4	1500				112	34	13	2380	319	107	56	22	13				-50	-36	3	-43
S5	1500	126	41	28		10	4	1793	266	94	51	21	13	1323	549	237		109	227	492
S6	1500		106	101		21	6	1849	272	96	51	21	13		156	-5		0	118	120
S7	1500		115	82		20	7	2064	291	101	53	21	13		153	23		7	89	133
S8	*1500*	*49*	*30*			*11*	*9*	*13*	*11*	*11*	*10*	*10*	*9*	*-73*	*-62*			*-13*	*2*	*-49*
S9	1500			498		42	12	15779	1071	248	103	30	15			-50		-29	27	-29
S10	*1500*	*873*	*223*			*39*		*9*	*9*	*9*	*9*	*9*	*9*	*-99*	*-96*			*-77*		*-93*
S11	*1500*	*12*	*4*			*2*		*9*	*9*	*9*	*9*	*9*	*9*	*-24*	*126*			*349*		*88*
S12	1500	525	169	79		21	11	212	68	37	25	15	11	-60	-60	-54		-29	2	-47
S13	1500	603	139	111		27	12	3630	418	129	64	23	14	502	201	16		-13	15	181
																			Average %^{age} Error:	116

Note: 1) The rows that are in *italics* (i.e. materials S1, S8, S10 and S11) are excluded from all calculations since they exhibit extremely different first and/or second term values from the other data and are only show to indicate the extent of their differences.

2) This table includes the q_o value. It is assumed that t_{ig} equals 1500 seconds at q_o.

3) The percentage error values can often be misleading due to the range values that they are expressing, i.e. for large values, the percentage error will be less than for smaller values that have the same difference in their absolute values.

It can be seen from the table above that the average percentage error was 116%.

The following figure shows the comparison between the actual experimental values for the time to ignition and the values calculated using this technique.

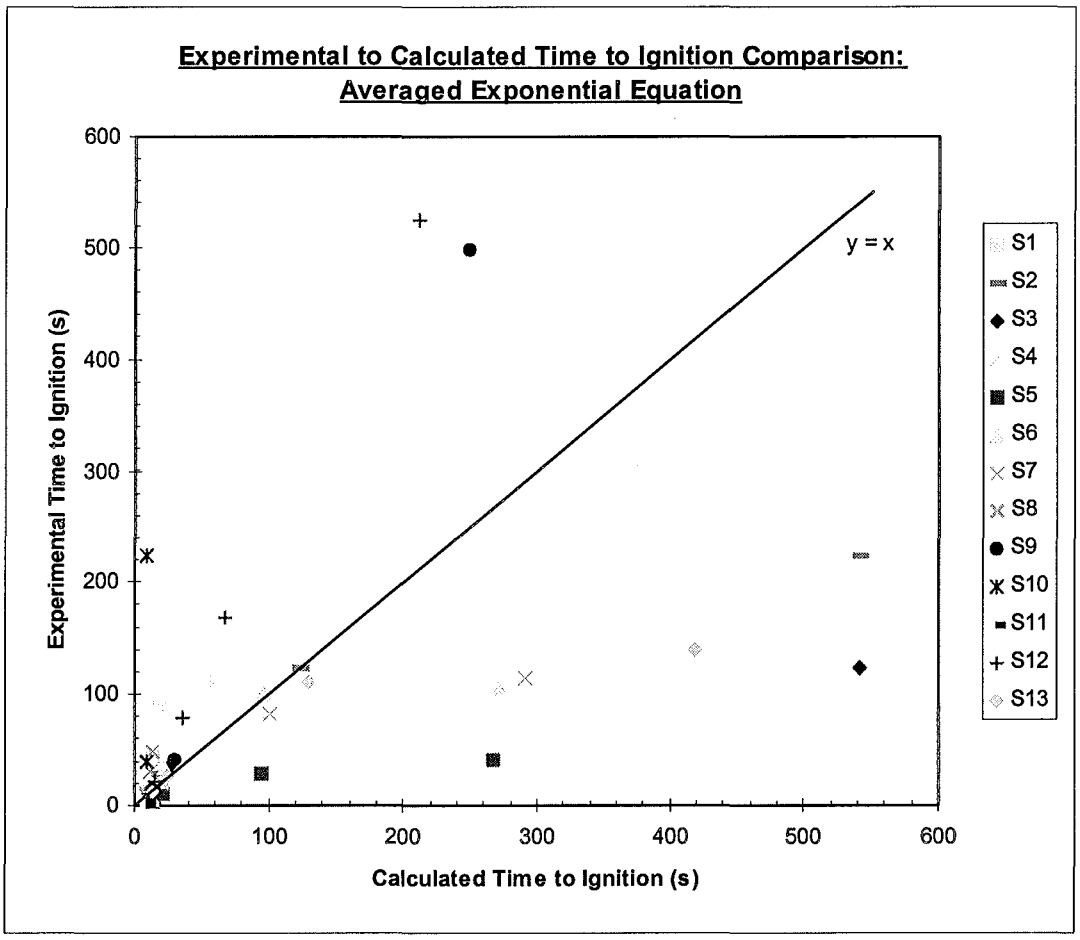

Figure 3.1: Scenario E Time to Ignition Comparison

As mentioned below the table, materials S1, S8, S10 and S11 have been excluded from all calculations undertaken in this analysis. This is due to the large errors that each of these materials exhibit when their calculated time to ignition values are compared to those materials which are included in the analysis. The exclusion limit involved removing all materials that had a percentage deviation in their first or second term values greater than ±100% in table (3.12).

The analysis showed that this form of simplified mapping technique gives poor representative values for the time to ignition of the selected material group over the exposed heat flux range of 20-75kWm^{-2}.

3.2.4 Scenario F

This investigation looked at the errors associated with finding a constant, X, which would directly be used to map that time to ignition of any material at a given heat flux to a time to ignition at a different heat flux, i.e.

Material 1: $t_{ig@50kWm^{-2}} = A \quad \Rightarrow \quad t_{ig@25kWm^{-2}} = XA$

Material 2: $t_{ig@50kWm^{-2}} = B \quad \Rightarrow \quad t_{ig@25kWm^{-2}} = XB$

The heat flux levels, as shown above, that were of particular interest was 50 and 25kWm^{-2}.

The technique that was implemented in this analysis involved first finding the slope for each material when going from the time to ignition at 25kWm^{-2} to the corresponding value at 50kWm^{-2}. These slopes were then averaged and this averaged value of the slope was then used as the value for X, in the equations above.

In an attempt to improve the estimation that this mapping technique gave, a second (Slope2) and third (Slope3) slope was found. These slopes where calculated by excluding certain materials that were found to have slopes that were significantly different from the previous averaged slope calculation.

The results from this method are given in the following tables:

Table 3-1: **Slope Calculations for Scenario F**

Material Number	**Cone Calorimeter Data t_{ig} (s) @ $\dot{q}''_e$ (kWm^{-2})**		**Calculated Slope Values, (=-1/X)**		
	25	**50**	**Slope1**	**Slope2**	**Slope3**
S1	43	12	-1.24	-1.24	x [a]
S2	123	28	-3.8	-3.8	-3.8
S3	123	34	-3.56	-3.56	-3.56
S4	-	34	- [b]	-	-
S5	41	10	-1.24	-1.24	x
S6	106	21	-3.4	-3.4	-3.4
S7	115	20	-3.8	-3.8	-3.8
S8	30	11	-0.76	x	x
S9	-	42	-	-	-
S10	223	39	-7.36	x	x
S11	4	2	-0.08	x	x
S12	169	21	-5.92	-5.92	x
S13	139	27	-4.48	-4.48	-4.48
Average Slope Values, (=-1/X)			-3.07	-3.43	-3.81
Actual Slope Values, X			**0.325**	**0.292**	**0.263**

[a] x indicates that the material has been excluded from the averaged calculation
[b] - indicates that no Cone Calorimeter data was available

The results from the table above show that three different slopes, X, have been found, each of which describes a different selection of materials. The first value of X, namely X = 0.325, describes the materials S1-3, S5-8 and S10-13. Materials S4 and S9 have been excluded from this selection since no data was given for them at a heat flux level of 25kWm^{-2}. The second slope value, X = 0.292, describes fewer materials than the previous selection. At was hoped that by excluding those materials that were used for the first slope value but not in the second slope value would improve the mapping of the time to ignition for the included materials. The exclusion process has been on the basis that the materials exhibit individual slopes that are relatively far

from the mean slope. The third slope value includes the smallest number of materials, i.e. only S2, S3, S6, S7 and S13. This material selection has a slope value of X = 0.263.

Once the slope values were obtained, analysis on the reliability of these values was undertaken. The following table details the results when the actual Cone Calorimeter values for each material was compared to the values calculated by equation $t_{ig_A} = Xt_{ig_B}$. Here t_{ig_A} represents the calculated time to ignition value at 50kWm^{-2} and t_{ig_B} represents the known time to ignition value at 25kWm^{-2} which was multiplied by the given slope values, X.

Table 3-2: Scenario F Time to Ignition Comparison

Material Number	Actual Cone Data [a]	Calculated Values [a]			%[age] Change in the Values		
		Slope1	Slope2	Slope3	Slope1	Slope2	Slope3
S1	12	14	13	x [b]	17	4	
S2	28	40	36	32	43	28	15
S3	34	40	36	32	18	5	-5
S4	34	- [c]	-	-			
S5	10	13	12	x	33	20	
S6	21	34	31	28	64	47	33
S7	20	37	34	30	87	68	51
S8	11	10	x	x	-11		
S9	42	-	-	-			
S10	39	73	x	x	86		
S11	2	1	x	x	-35		
S12	21	55	49	x	162	135	
S13	27	45	41	37	68	50	35
				Average %[age] Error:	47	45	26

[a] Values are at a heat flux level of 50kWm^{-2}
[b] x indicates that the material has been excluded from the averaged calculation
[c] - indicates that no Cone Calorimeter data was available

The table above shows that as the number of materials is reduced in a particular selection, the average percentage error in the mapping technique reduces. It should be noted that the technique generally seems to over estimate the actual time to ignition.

The following three figures show the comparison between the actual experimental values for the time to ignition and the values calculated using this technique for each of the three different slopes, namely slope 1, 2 and 3.

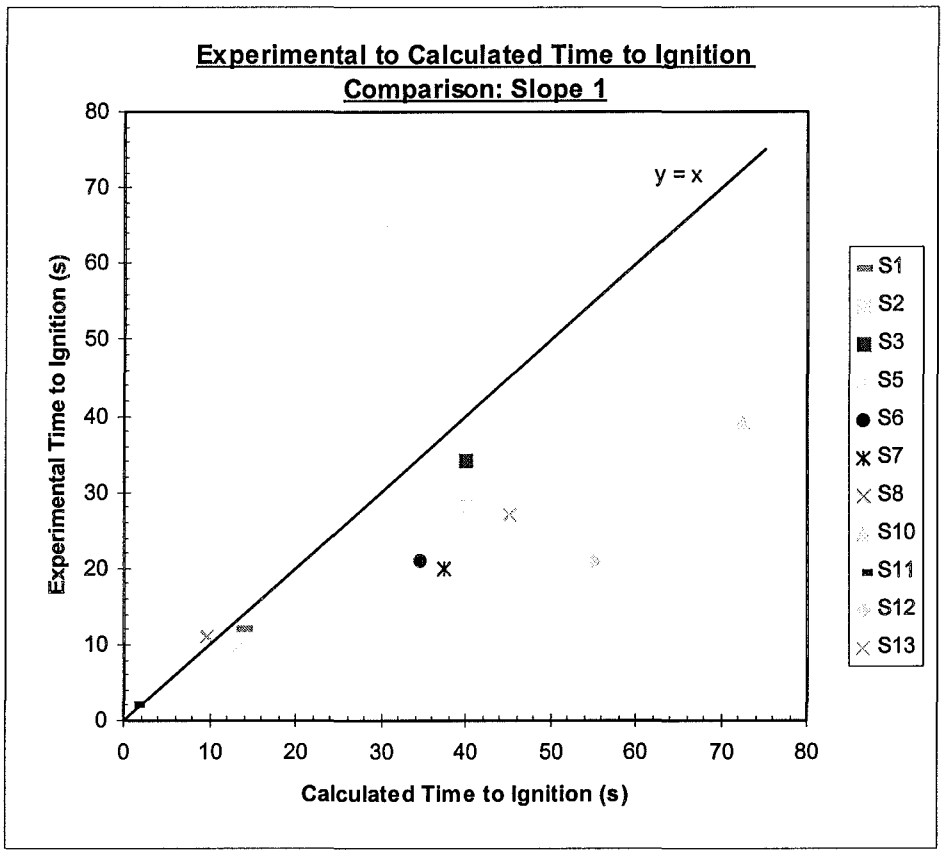

Figure 3.1: Slope 1 Time to Ignition Comparison

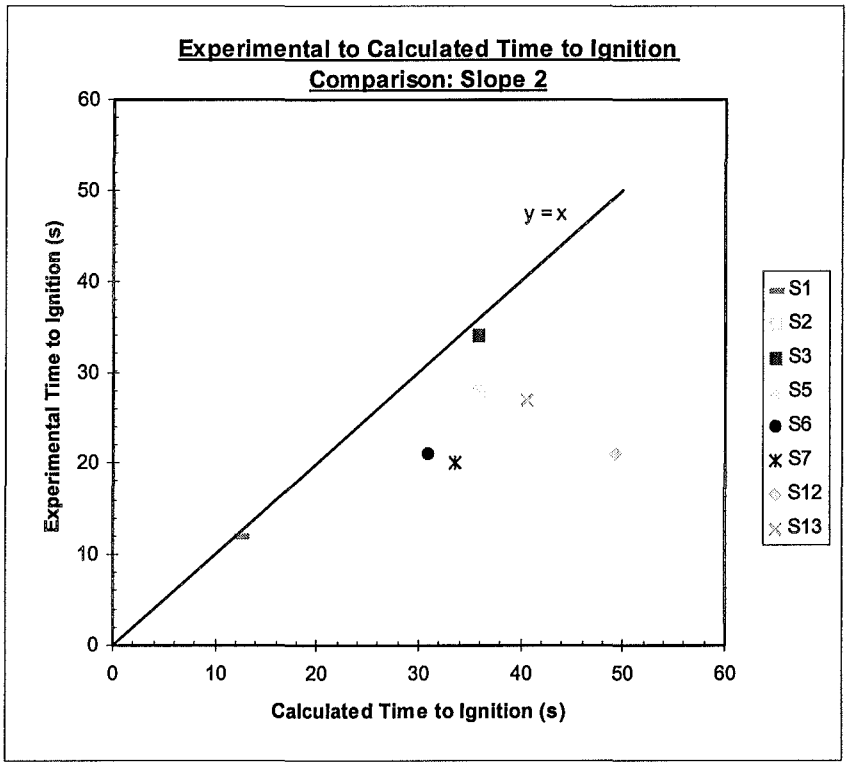

Figure 3.2: Slope 2 Time to Ignition Comparison

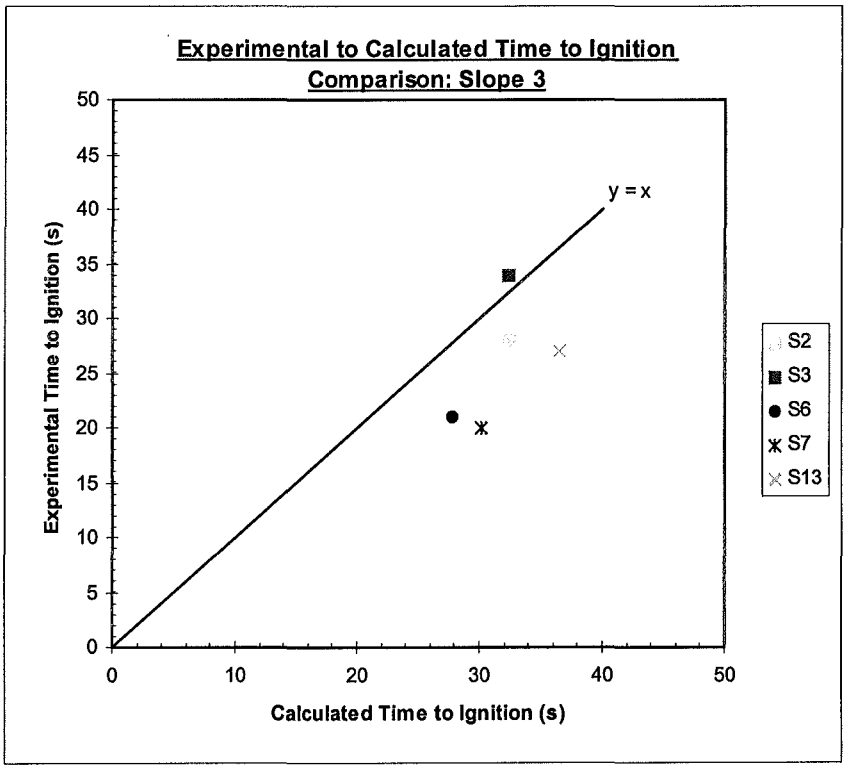

Figure 3.3: Slope 3 Time to Ignition Comparison

The following figure summarises the results from this investigation using the $t_{ig_A} = Xt_{ig_B}$ technique to determine the time to ignition. The first column for each material type gives the actual Cone Calorimeter value and the columns to the right of this represent the calculated time to ignition values using the different slope (X) values. Since the different slope values have been obtained by excluding some of the materials from the selection the calculated the slope, it can be seen that the number of columns for each of the materials is not constant.

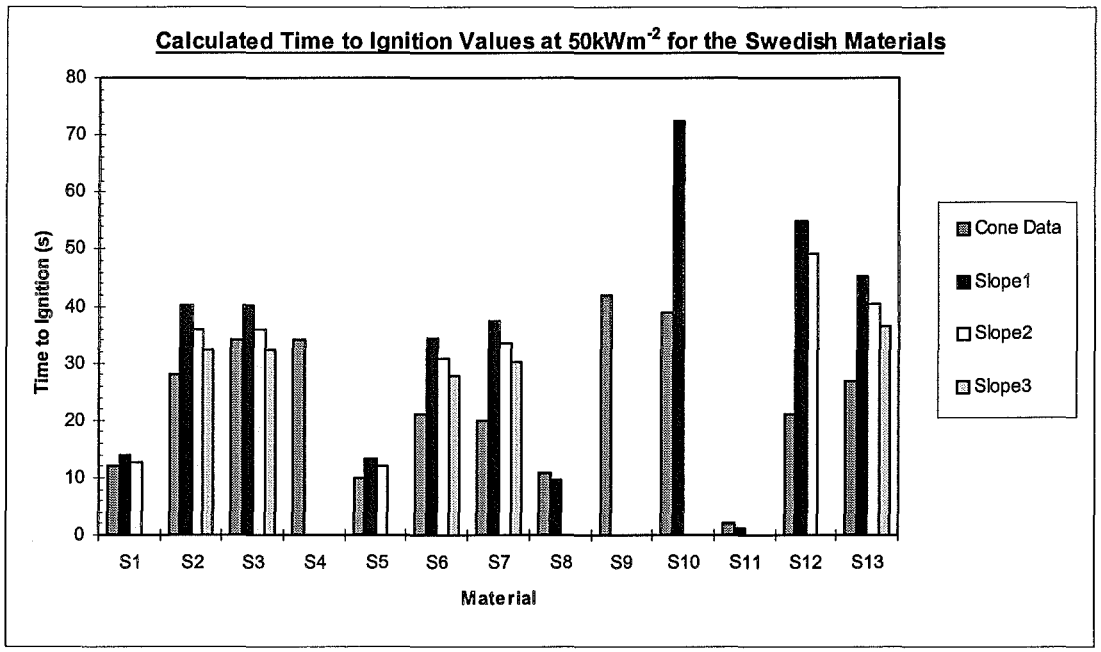

Figure 3.4: Scenario F Time to Ignition Comparison

It can be seen from this graph that materials S4 ands S9 should be initially excluded since no Cone data was available for these materials at 25kWm^{-2}. The materials S10 and S12 should also be excluded as their calculated values differ largely from their actual values when this technique is used.

It can be concluded from this analysis that this technique for mapping the time to ignition at one heat flux level to another should be used with considerable caution. The material selection that is used to determine the average slope, X, will be highly influential on the results that can be obtained by this technique.

3.2.5 Scenario G

In a final attempt to find a satisfactory equation that could be used to map the time to ignition, t_{ig}, of a material at different heat fluxes, $\dot{q}_e''$, various trendlines were fitted to the raw Swedish data. These lines were fitted by using the trendline function in EXCEL. This function places a line through the data as well giving the corresponding equation of this line.

The initial analysis involved applying different trendlines to the data so that the general type of equation could be determined which could be used to describe all of the selected materials. Once the type of equation was known, sensitivity analysis was performed in a bid to optimise the variables in the equation.

Five types of equations were initially tried, which included exponential, polynomial, linear, logarithm and power. It was found that the best type of equation for the given data was exponential, as previously used in this investigation chapter. The following table gives the individual exponential equations of each material as well as the averaged equation for all the materials, which was achieved by averaging each of the numerical terms in the individual equations.

Table 3-1: Exponential Equations for the Swedish Data

Material Number	Exponential Equation [a, b]	First Term	$\%\Delta_{ave\ 1st\ term}$	Power	$\%\Delta_{ave\ 2nd\ term}$
S1	$y = 793.19e^{-0.0715x}$	793.19	-38.2	-0.0715	-9.6
S2	$y = 1315e^{-0.0662x}$	1315	2.5	-0.0662	-16.3
S3	$y = 1341.8e^{-0.0641x}$	1341.8	4.6	-0.0641	-18.9
S4	$y = 5474.6e^{-0.087x}$	*5474.6*	*326.8*	*-0.087*	*10.0*
S5	$y = 767.73e^{-0.0781x}$	767.73	-40.2	-0.0781	-1.2
S6	$y = 1880.3e^{-0.0822x}$	1880.3	46.6	-0.0822	3.9
S7	$y = 1682.3e^{-0.0795x}$	1682.3	31.1	-0.0795	0.5
S8	$y = 436.42e^{-0.06x}$	436.42	-66.0	-0.06	-24.1
S9	$y = 10997e^{-0.096x}$	*10997*	*757.3*	*-0.096*	*21.4*
S10	$y = 6907.5e^{-0.1061x}$	*6907.5*	*438.5*	*-0.1061*	*34.2*
S11	$y = 723.75e^{-0.1377x}$	723.75	-43.6	-0.1377	74.1
S12	$y = 1915.8e^{-0.0767x}$	1915.8	49.3	-0.0767	-3.0
S13	$y = 1971.5e^{-0.0748x}$	1971.5	53.7	-0.0748	-5.4
	Averaged Values:	**1282.779**		**-0.07908**	

[a] These equations include the q_o value and it is assumed that t_{ig} equals 1500 seconds at q_o

[b] The y term in the equations is the time to ignition, t_{ig}, and the x term is the heat flux, $\dot{q}''_e$

Note: The rows that are in *italics* (i.e. materials S4, S9 and S10) are excluded from all calculations since they exhibit extremely different first and/or second term values from the other data and are only shown to indicate the extent of their differences.

From the table above, the averaged exponential equation for mapping the time to ignition values to the heat flux values. The form of this equation is,

$$t_{ig} = 1282.779e^{-0.07908\dot{q}''} \qquad \ldots(3.8)$$

Due to the nature of the exponential function, any material that has values which deviate significantly from the numerical values of the averaged exponential equation would be expected not be suited for this equation. This was actually the case, as is described below.

Equation (3.8) was applied to the selected group of materials so that the reliability of the calculated values could be determined. The following table and graph illustrate the position each material with respect to this equation.

Table 3-2: Scenario G Time to Ignition Comparison

Material Number	Cone Calorimeter Data: Actual t_{ig} (s) @q (kWm^{-2})						Calculated Values: Calculated t_{ig} (s) using Averaged Exponential Values @q (kWm^{-2})						Results: %age Error in Comparing the Cone Data and Calculated Values @q (kWm^{-2})						
	20	25	30	35	50	75	20	25	30	35	50	75	20	25	30	35	50	75	Average
S1	92	43			12	6	264	178	120	81	25	3	187	313			105	-43	96
S2	223	123			28	14	264	178	120	81	25	3	18	44			-12	-76	-21
S3	255	123			34	16	264	178	120	81	25	3	4	44			-28	-79	-28
S4				*112*	*34*	*13*	*264*	*178*	*120*	*81*	*25*	*3*				*-28*	*-28*	*-74*	*-55*
S5	126	41	28		10	4	264	178	120	81	25	3	110	333	327		146	-15	137
S6		106	101		21	6	264	178	120	81	25	3		68	18		17	-43	-4
S7		115	82		20	7	264	178	120	81	25	3		55	46		23	-51	-2
S8	49	30			11	9	264	178	120	81	25	3	438	492			124	-62	183
S9			*498*		*42*	*12*	*264*	*178*	*120*	*81*	*25*	*3*			*-76*		*-41*	*-72*	*-70*
S10	*873*	*223*			*39*		*264*	*178*	*120*	*81*	*25*	*3*	*-70*	*-20*			*-37*		*-52*
S11	12	4			2		264	178	120	81	25	3	2098	4341			1130		1877
S12	525	169	79		21	11	264	178	120	81	25	3	-50	5	51		17	-69	-21
S13	603	139	111		27	12	264	178	120	81	25	3	-56	28	8		-9	-72	-30
																			Average of the averaged %age errors above: 155

Note:

1) The rows that are in *italics* (i.e. materials S4, S9 and S10) are excluded from all calculations since they exhibit extremely different characteristics from the other data and are only show to indicate the extent of their differences.
2) The percentage error values can often be misleading due to the range values that they are expressing, i.e. for large values, the percentage error will be less than for smaller values that have the same difference in their absolute values.

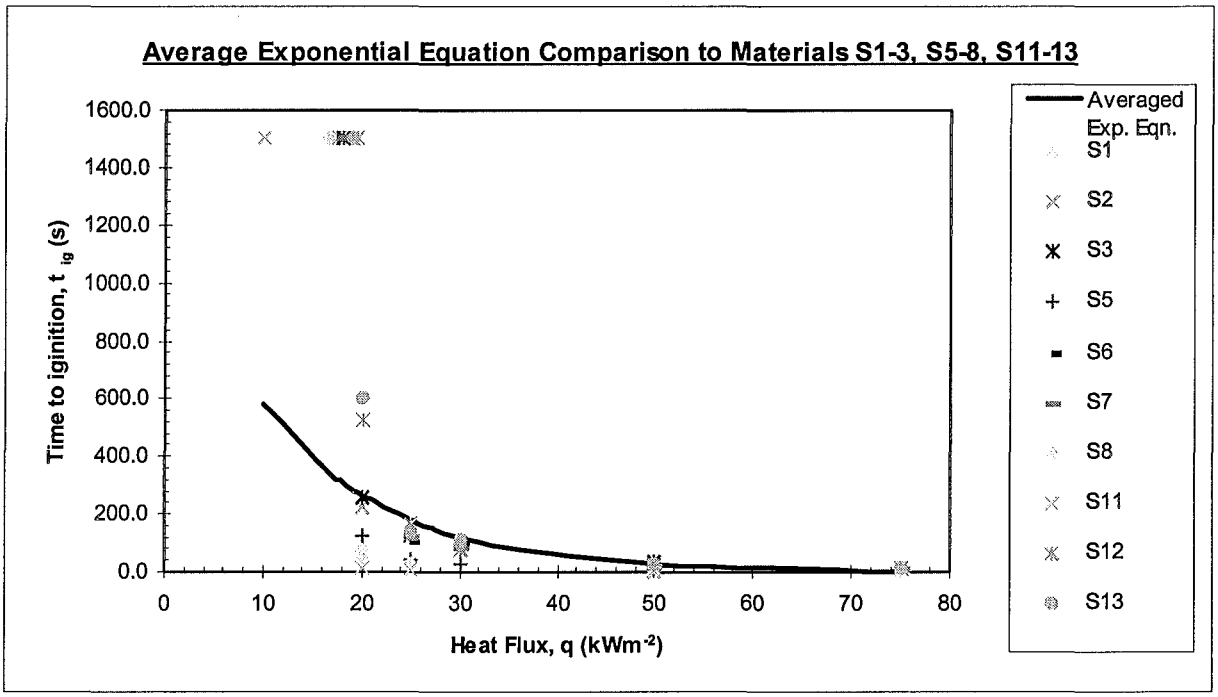

Figure 3.1: Scenario G Equation Comparison

It can be noted from the table above that since the averaged exponential equation does not include any individual material variables, such as the density as seen in previous investigations, each calculated time to ignition values are the same. This result would expect to give values that were a poor correlation when used across the selection of materials, as was found. Many of the materials are found to exhibit average percentage errors greater than ±50%. Particularly notable is material S11 which had percentage errors >1000%. This large discrepancy is because this material has very different actual time to ignition values at the investigated heat fluxes than is seen in the other materials.

The following figure shows the spread of data when the actual experimental values for the time to ignition and the values calculated using this technique are compared.

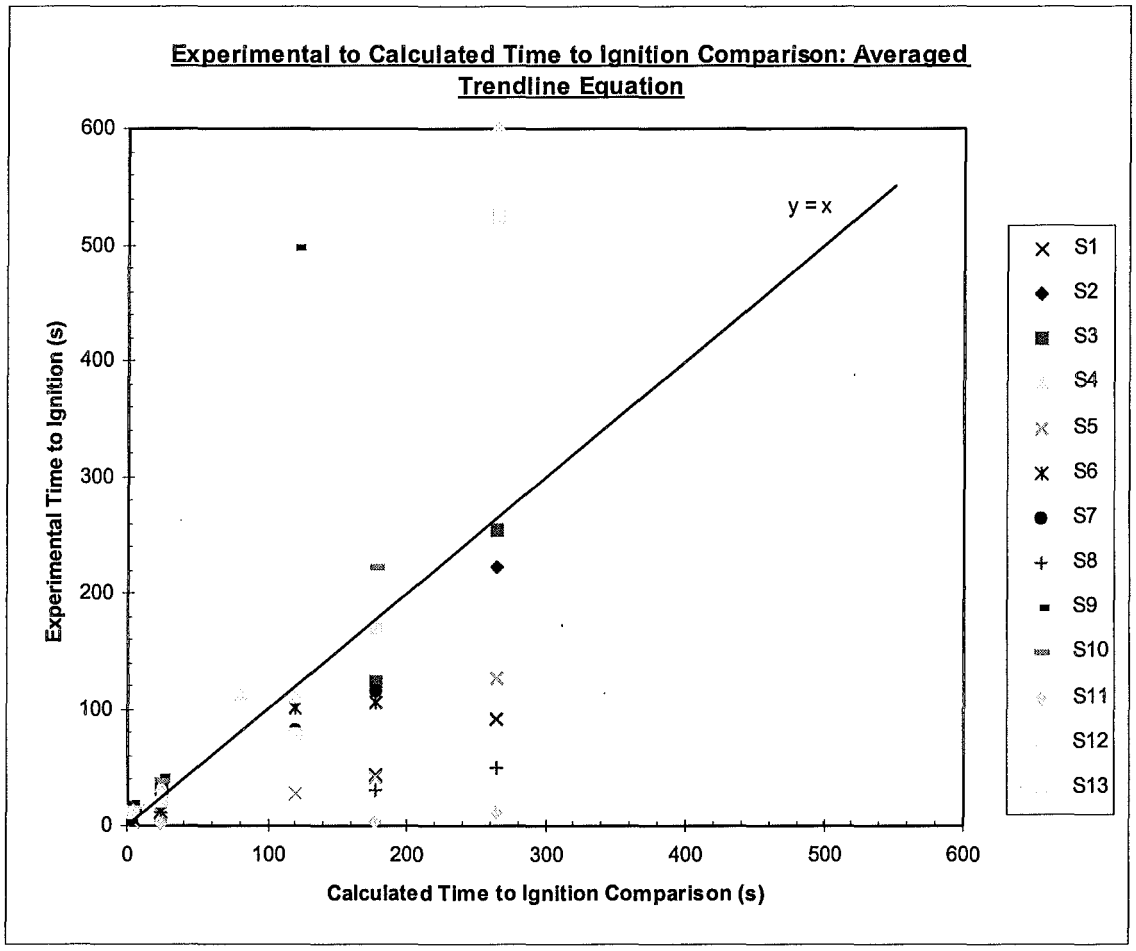

Figure 3.2: Scenario G Time to Ignition Comparison

This figure shows how poorly this technique maps the time to ignition values to the actual values.

In conclusion, this mapping technique has been shown to give poor representations of the time to ignition values for the selected materials at heat fluxes from 20-75kWm^{-2}.

3.3 Analysis Results

It was found from the analysis undertaken in this section that modifying the time to ignition equation (2.9) worked to varying extents. It was generally found that by increasing the mathematical complexity of the simplified time to ignition equation, e.g. using a exponential form, the fewer the number of materials that can be grouped

together and used, but the better the estimation is for these materials. There is a trade off between the quality of the mapping and the quantity of the materials that can be used in the mapping. The next step in the research involved using the best equation from this section in a model to determine the upward flame spread for different materials. The errors that occurred in the simplified investigation may or may not be detrimental to the flame spread calculations.

Conclusions

The conclusions that can could be drawn from the initial linear regression analysis, scenario A, is that this method only gives representative values for the calculated time to ignition. The averaged percentage errors were found be between -86 and +85 for materials S1-4, S6-10 and S12-3. The other Swedish materials gave values that were unreliable as they lay outside this already large range. The average of the averaged percentage error values was 51%. The heat flux range used in this and all the calculations was from 20-75kWm^{-2}.

Scenario B involved a similar analysis except that some materials (S1, S5, S8, S10 and S11) were excluded form the linear regression. These materials were excluded on the basis that their percentage errors in the previous analysis were significantly larger than the other materials. It was found that this analysis gave improved results for the time to ignition calculation and reduced the averaged percentage errors in the mapped values to between -30 and +48%. It was shown that this method could give reasonable values when this technique is applied. The materials particularly suited for this analysis were S1-4, S6-9 and S12-3. The average of the averaged percentage error values was 25%.

The final linear regression analysis undertaken was scenario C. This investigation differed from the two previous by the removal of the material dependence, namely the density variable, in the time to ignition equation. By removing this variable, the governing expression was simplified further but it was found that in doing so the averaged percentage errors increased. The error increased to an average of 88% and it was found that this technique was best suited for materials S1-7, S9-10 and S12-3.

Scenario D involved investigating the relationship between the time to ignition and the density/heat flux squared ratio. This analysis was similar to scenarios A and B except that the powers of the density and heat flux were fixed and were not calculated by linear regression. This scenario was found to give satisfactory results for most materials, being S1-4, S6-9 and S12-3. The error reduced to and average of –2% which emphasises the suitability of equation (3.6) to model to times to ignition at heat flux varying between the range of 20-75kWm^{-2}.

The E scenario changed on the previous investigation by increasing the density power to a value of two. The resulting points on the time to ignition versus density/heat flux ratio plot exhibited exponential trends. This observation meant that the time to ignition equation also changed to an exponential form. The resulting values from applying this equation to the Swedish materials produced relatively large errors when compared to some other scenarios. It was found that the averaged errors obtained were over a range of –49 to +88% but the overall averaged value was 116%. Only materials S1-2, S4, S8-9 and S11-2 could possibly be represented by the equation developed from this analysis.

The scenario F investigation of the $t_{ig_A} = Xt_{ig_B}$ equation found that the slope, X, of the equation could take values of 0.326, 0.292 and 0.263. The value 0.326 could be used to describe the materials S1-3, S5-8 and S9-13 and gave a average percentage error in the calculation of around 47%. This slope covers the most materials but it was found that by choosing one of the other slopes the percentage error in the calculation could be reduced. The percentage error for the 0.292 slope is around 45% and can be used for materials S1-3, S5-7, S12 and S13. The best percentage error, of 26%, was when the slope equalled 0.263 but this value only included materials S2, S3, S6, S7 and S13.

The final scenario, G, investigated averaging the exponential trendlines as given by EXCEL. This analysis showed that using this type of technique only gave representative values and introduced significant errors. Many of the materials exhibited average percentage errors greater than ±50%. Particularly notable is material S11 which has percentage errors >1000% when this technique was applied.

This large discrepancy is because this material has very different actual time to ignition values at the investigated heat fluxes than is seen in the other materials. The average percentage error of all the selected materials (S1-3, S5-8, S11-13) when the averaged exponential equation was used was found to be 155%. Since this technique produced the largest errors of any of the scenarios investigated, it should not be used.

The following table gives a summary of the results from the investigations undertaken in this chapter,

Table 3-1: Time to Ignition versus Heat Flux Relationship Investigation Summary

Scenario	Description	Result			Acceptable Results?
		Variable Values	Comparison [a]	Materials Included [b]	
A	Linear Regression, $t_{ig} = C\frac{\rho^{X1}}{\dot{q}_e''^{X2}}$	C = 21822.0 X1 = 0.344 X2 = 2.307	Average $\%^{age}$ error = 51 Range (-86 - +85)	S1-4, S6-10, S12-13	No
B	Linear Regression, $t_{ig} = C\frac{\rho^{X1}}{\dot{q}_e''^{X2}}$	C = 2607.778 X1 = 0.853 X2 = 2.567	Average $\%^{age}$ error = 25 Range (-30 - +48)	S1-4, S6-9, S12-13	No
C	Linear Regression, $t_{ig} = C\frac{1}{\dot{q}_e''^{X3}}$	C = 55468.66 X3 = 2.030	Average $\%^{age}$ error = 88 Range (-66 - +82)	S1-7, S9-10, S12-13	No
D	$t_{ig} = C\frac{\rho}{\dot{q}_e''^2}$	C = 113.44	Average $\%^{age}$ error = -2 Range (-24 - +45)	S1-4, S6-9, S12-13	Yes
E	$t_{ig} = C\frac{\rho^2}{\dot{q}_e''^2}$	$t_{ig} = 8.973e^{0.005\left(\frac{\rho^2}{\dot{q}''^2}\right)}$	Average $\%^{age}$ error = 116 Range (-49 - +88)	S1-2, S4, S8-9, S11-12	No
F	$t_{ig_A} = Xt_{ig_B}$	X = 0.325 (Slope1) X = 0.292 (Slope2) X = 0.263 (Slope3)	Average $\%^{age}$ error: 47 (Slope1) 45 (Slope2) 26 (Slope3)	S1-3, S5-8, S9-13 S1-3, S5-7, S12. S13 S2, S3, S6, S7, S13	No (Slope1) No (Slope2) No (Slope3)
G	Exponential Trendlines	$t_{ig} = 1282.779e^{-0.07908\dot{q}''}$	Average $\%^{age}$ error = 155 Range (-70 - +96)	S1-4, S6-7, S9-10, S12-13	No

[a] This column gives the results from the comparison between the calculated and experimental time to ignitions for all the various Swedish Materials.

[b] These materials represent those that show "satisfactory" mapping of the times to ignition for the given scenario.

3.4 Summary

This chapter has attempted to develop a simplified equation for the time to ignition for various materials at different heat flux values. Seven different scenarios were analysed and the results have been presented.

It was found, from scenario D investigations, that the following equation gives satisfactory calculated times when they are compared to actual experimental values. This equation is,

$$t_{ig} = 113.44\left(\frac{\rho}{\dot{q}_e''^2}\right)$$

The averaged errors when this equation is applied to the thirteen Swedish materials were found to be –2%. This equation, since satisfactory, was incorporated into the second part of this research, namely the development of a model to calculated the upward flame spread on interior combustible materials. The following chapters of this report are dedicated to this flame spread model.

4. ANALYTICAL MODEL

The second part of this research was to establish an analytical model to determine the flame spread characteristics for various materials. The following chapter gives details of the equations and the logic incorporated in the model. A sample of the developed spreadsheet is also given in this section so that the readers can familiarise themselves with the format that was used.

4.1 Analytical Model Equations

It was observed during the initial part of the investigation, that the Average HRR representation was in fact simply a special case of the Peak/Decay HRR case where the $\dot{Q}''_{max}$ equalled $\dot{Q}''_{ave}$ and the decay coefficient, λ, equalled zero. It was therefore obvious that by modifying the Peak/Decay equations, both representations could be catered for in the model. The HRR representation is now carried out by replacing the variables described above with $\dot{Q}''$ and λ.

The equations in the following section are derived from a modified version of equation (2.17). One notable change was in the time to ignition variable, t_{ig}, which was modified to t_{ig*}. This new variable is described later in this chapter. It is these changes that are described in the following section.

The final equations used in the analytical model are,

Flame Spread Velocity, $V(t)$***, with units of*** ms^{-1}***;***

for $\lambda t_{ig*} < \left(1-\sqrt{a}\right)^2$ and $\lambda t_{ig*} > \left(1+\sqrt{a}\right)^2$

$$V(t) = \frac{C_1}{s_2 - s_1}\left[s_2 e^{s_2 t} - s_1 e^{s_1 t}\right] \qquad \ldots(4.1)$$

and for $\left(1-\sqrt{a}\right)^2 < \lambda t_{ig^*} < \left(1+\sqrt{a}\right)^2$

$$V(t) = \frac{C_1 e^{\alpha t}}{\beta}\left[\alpha \sin(\beta t) + \beta \cos(\beta t)\right] \qquad \ldots(4.2)$$

where,

$$\dot{Q}_b = \frac{A_o}{K} \qquad \ldots(4.3)$$

$$x_{po} = \frac{K\dot{Q}_b}{W} \qquad \ldots(4.4a)$$

which changed to the following equation when the tuning variable was included

$$x_{po} = \frac{x_{po^*} K\dot{Q}_b}{W} \qquad \ldots(4.4b)$$

$$C_1 = \frac{K\dot{Q}'' x_{po}}{t_{ig^*}} \qquad \ldots(4.5)$$

$$a = K\dot{Q}'' \qquad \ldots(4.6)$$

$$\Delta = \frac{1}{t_{ig^*}^{\ 2}}\left(1 - a + \lambda t_{ig^*}\right)^2 - \frac{4\lambda}{t_{ig^*}} \qquad \ldots(4.7)$$

$$s_{1,2} = -\frac{1}{2t_{ig^*}}\left(1 - a + \lambda t_{ig^*}\right) \pm \frac{1}{2}\sqrt{\Delta} \qquad \ldots(4.8)$$

$$\alpha = -\frac{1}{2t_{ig^*}}\left(1 - a + \lambda t_{ig^*}\right) \qquad \ldots(4.9)$$

$$\beta = \frac{1}{2}\sqrt{\Delta} \text{ (when } \Delta \text{ is positive)} \qquad \ldots(4.10a)$$

$$\text{or } \beta = \frac{1}{2}\sqrt{-\Delta} \text{ (when } \Delta \text{ is negative)} \qquad \ldots(4.10b)$$

for the complex solution, i.e. when Δ is negative, $s_{1,2}$ becomes complex and is written in the form, $\alpha \pm i\beta$.

Pyrolysing Length, $x_p(t)$***, with units of m;***

for $\lambda t_{ig^*} < \left(1-\sqrt{a}\right)^2$ and $\lambda t_{ig^*} > \left(1+\sqrt{a}\right)^2$

$$x_p(t) = x_{po} + \frac{C_1}{s_2 - s_1}\left[e^{s_2 t} - e^{s_1 t}\right] \qquad \ldots(4.11)$$

and for $\left(1-\sqrt{a}\right)^2 < \lambda t_{ig^*} < \left(1+\sqrt{a}\right)^2$

$$x_p(t) = x_{po} + \frac{C_1 e^{\alpha t}}{\beta}\sin\left[\beta t\right] \qquad \ldots(4.12)$$

Flame Front Length, $x_f(t)$***, with units of m;***

$$x_f(t) = K\dot{Q}_c(t) \qquad \ldots(4.13)$$

Heat Release Rate, $\dot{Q}_c(t)$***, with units of kW;***

for $\lambda t_{ig^*} < \left(1-\sqrt{a}\right)^2$ and $\lambda t_{ig^*} > \left(1+\sqrt{a}\right)^2$

$$\dot{Q}_c(t) = W\left[x_{po}\dot{Q}'' + \frac{C_1}{s_2 - s_1}\left(\frac{s_2\dot{Q}''\left(e^{s_2 t} - e^{-\lambda t}\right)}{s_2 + \lambda} - \frac{s_1\dot{Q}''\left(e^{s_1 t} - e^{-\lambda t}\right)}{s_1 + \lambda}\right)\right] \qquad \ldots(4.14)$$

and for $\left(1-\sqrt{a}\right)^2 < \lambda t_{ig^*} < \left(1+\sqrt{a}\right)^2$

$$\dot{Q}_c(t) = W\left[x_{po}\dot{Q}''e^{-\lambda t} + C_1C_2\dot{Q}''\left[e^{\alpha t}\left(\cos(\beta t) + \frac{C_3}{\beta}\sin(\beta t)\right) - e^{-\lambda t}\right]\right] \quad \ldots(4.15)$$

where,

$$C_2 = \left[\frac{1}{\lambda}\left(\alpha^2+\beta^2\right) + 2\alpha + \lambda\right]^{-1} \quad \ldots(4.16)$$

$$C_3 = \frac{1}{\lambda}\left(\alpha^2+\beta^2\right) + \alpha \quad \ldots(4.17)$$

And C_1, α and β are given by equations (4.5), (4.9) and (4.10a,b) respectively.

4.2 Sample Spreadsheet Model

The following figure shows the arrangement of the analytical flame spread model in the EXCEL spreadsheet. It should also be noted that this is actually only the top part of the model, as the flame spread calculations are undertaken for approximately six hundred seconds (Post-ignition time).

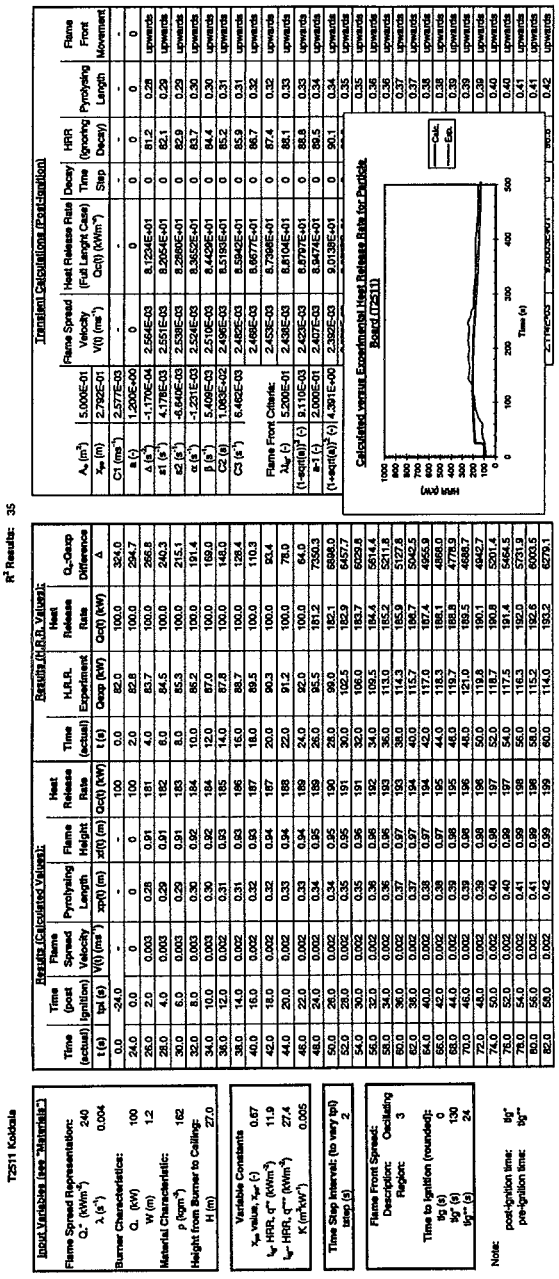

Figure 4.1: Analytical Flame Spread Model for a Typical Material

4.3 Spreadsheet Model Description

This flame spread analysis was undertaken in EXCEL and utilised many different functions. On particular function that was used frequently was the IF statement. This statement specifies a logical test to perform and takes the following form,

$$\text{"IF" statement} = \text{IF}[\text{logical test}, \text{value if true}, \text{value if false}]$$

The following section describes the logic behind the inputs, outputs and transient calculations that were incorporated into the model. This spreadsheet analysed the calculated Upward Flame Spread values and compared them to the data found from various experiments, including VTT (Kokkala et al.) [10, 11], Swedish [8] and EUREFIC [8, 20] results. For a full description of the origin of the equations used in this model, the reader is directed to chapter 2 - being the section on "Background Theory". The actual form of the spreadsheet model can be seen in figure (4.1).

4.3.1 Input Variables

A few input variables were needed in this model, which were used to describe such things as the material being investigated, the location of the material, the burner characteristics as well as some constants for the heat flux and time to ignition considerations. These variables are described below.

4.3.1.1 Flame Spread Representation

Heat Flux, $\dot{Q}''$ ***:***

This variable assumed a single quantity of the heat flux produced by the material in the Cone Calorimeter test as described by either the Peak/Decay or the Average heat

release rate representation. Details of this representation technique are described in chapter 2. The units if this variable are kWm^{-2}. The value of this variable for each material investigated was obtained by a curve fitting technique from the Cone Calorimeter data and the results can be found in appendix A.

Decay Coefficient,* λ*:

This value describes the materials' exponential rate of decay of the heat released during burning. For a material represented by the constant heat release rate, this value should be set to zero but since this creates infinity errors in the model, a value of should be used. Again, details of this representation technique are described in chapter 2. The units if this variable are s^{-1}. The value of this variable for each material investigated was obtained by a curve fitting technique from the Cone Calorimeter data and the results can be found in appendix A.

4.3.1.2 Burner Characteristics

Burner Output, :

The heat output of the burner is governed by the standard test method, NT FIRE, which indicates that the burner should be set to 100kW. This value remains constant for the first ten minutes of the test, which is the time period of interest in this model.

Burner Width,* W*:

The width of the burner is taken as the total distance that the burner is attached to the wall. This is particularly important as if the square burner is placed in a corner of the compartment, as this width is the length of two sides as opposed to just a single side when the burner is placed along a wall. This variable has units of metres, m.

4.3.1.3 Material Characteristics

Density, ρ***:***

The density of the material is generally given as part of the results from the Cone Calorimeter tests. The value of the variable has sometimes been difficult to establish, especially for composite materials and determination for such materials has involved a taking a mass weighting of the individual densities of the components. This method induces some uncertainty in the calculation, but sensitivity analysis of this variable or establishing the actual value would quantify this uncertainty. The units for the density are kgm^{-3}.

4.3.1.4 Height from the Burner to Ceiling

Material Height, H***:***

This value is needed so that the total distance that the flame, the pyrolysis length, can spread can be limited. The height is calculated by dividing the total assumed surface area of the material by the width of the burner. The total surface area is assumed to be the sum of the ceiling area and the wall area. The wall area equals the distance from the top of the burner/base of the flame to the ceiling multiplied by the width of the pyrolysis front (assumed to be equal to the burner width). This calculation can be described by,

$$\text{Material Length} = \frac{\text{Total Pyrolyised Area}}{\text{Pyrolysis Width}}$$

where the total pyrolyised area is given by

$$\text{Total Pyrolyised Area} = (\text{Ceiling Length} \times \text{Ceiling Width}) + (\text{Wall Height} \times \text{Burner Width})$$

The dimensions of the test compartment are 3.6m long, 2.4m wide and 2.4m high. Such dimensions and a burner width of 0.34m give a total height of approximately 27m. This length has assumed that the flame pyrolysis width remains constant.

4.3.1.5 Variable Constants

To allow for "tuning", due to the unknowns in the model, the following constants have been developed. This tuning process, to account for the removed complexity, allows the development of simple models that focuses on the dominant phenomena. This approach is supported by Williams [23] who stated in a 1976 report that,

> *"...there is merit (in neglecting) all but the essential phenomena and in studying thoroughly limiting cases in which different phenomena are controlling."*

The variable constants used in the model are described below.

Heat Flux Variation, x_{po*}***:***

In the applied theory, it is assumed that the initial heat flux, prior to the burning of the material, is constant across the gas burner flame height and zero below it (see fig. (2.3)). Since this assumption over-estimates the heat transferred from the burner flame to the material, this factor has been incorporated to more closely represent reality. The value of x_{po*}, due to this overestimation, is between 0 and 1.

Post-ignition Time Adjustment, q"***:***

This factor is used to describe the heat flux level for the time to ignition value, t_{ig*}, used in the transient model equations. This is based on the result from the initial analysis in this research, which found a dependence on the assumed exposed heat flux (see chapter 3). The unit of this flux is kWm^{-2}.

Pre-ignition Time Adjustment, q"**:

Once the burner is started, the material being tested takes a period of time to ignite. The simplified time to ignition equation derived in the previous section is used to describe this time, t_{ig**}, and q"** is the heat flux level used in this equation. The unit of this flux is kWm^{-2}.

Flame Area Coefficient, K:

This factor is burner location dependent and assumes values depending on the original flame spread experimental test method. The location of the burner in this research is either in a corner or on a wall.

4.3.1.6 Time Step Interval

Time Step, t_{step}:

To allow for simple modification of the calculation times (t_{pi}), this factor has been introduced. The value, in seconds, that this variable takes is generally dependent on the speed of the flame spread, as if the time step is set too large, important changes may be under or overestimated.

4.3.2 Output Variables

The constructed spreadsheet model gives various outputs. The following section describes each of these outputs.

4.3.2.1 Flame Front Spread

In the hope of adding clarity for the reader, in terms of the movement of the flame

front, these two outputs have been included to determine the characteristics of the overall flame spread, as indicated by the regions I, II, III and IV in figure (2.5).

Description:

This calculation looks at the numerical result from the following "Region" calculation and gives a written statement on the flame spread velocity characteristic. The equation used for this calculation is,

IF("Region"=1,"Accelerating",IF("Region"=4,"Decelerating","Oscillating"))

Region:

In the figure (2.5), mentioned above, four specific regions are identified. The IF statement, below, is used to determine which region the flame spread velocity is situated.

$$\text{Region} = \text{IF}\left[\lambda t_{ig^*} \le \left(1-\sqrt{\text{a}}\right)^2, 1, \text{Region}_\text{a}\right]$$

$$\text{Region}_\text{b} = \text{IF}\left[\lambda t_{ig^*} \le (1-\text{a}), 2, \text{Region}_\text{c}\right]$$

$$\text{Region}_\text{c} = \text{IF}\left[\lambda t_{ig^*} \le \left(1+\sqrt{\text{a}}\right)^2, 3, 4\right]$$

where "a" is described by equation (4.6).

4.3.2.2 Time to Ignition

The follow section details the different times to ignition incorporated into the model. These times were rounded to the nearest second to simplify the calculation of the average R^2 value.

In the model, two different ignition times have been used. The first ignition time, $t_{ig^{**}}$, is used to describe the time it takes for the material to ignite. Before this time, the

only heat that is being released is that from the gas burner. The second ignition time, t_{ig*}, is used in the transient calculations of the model and describes the post-ignition time behaviour of the material. For the specific use of this variable, the reader is directed to the previous section 4.1.

The following figure indicates the effects that these two ignition times can have on the heat release rate for a typical material.

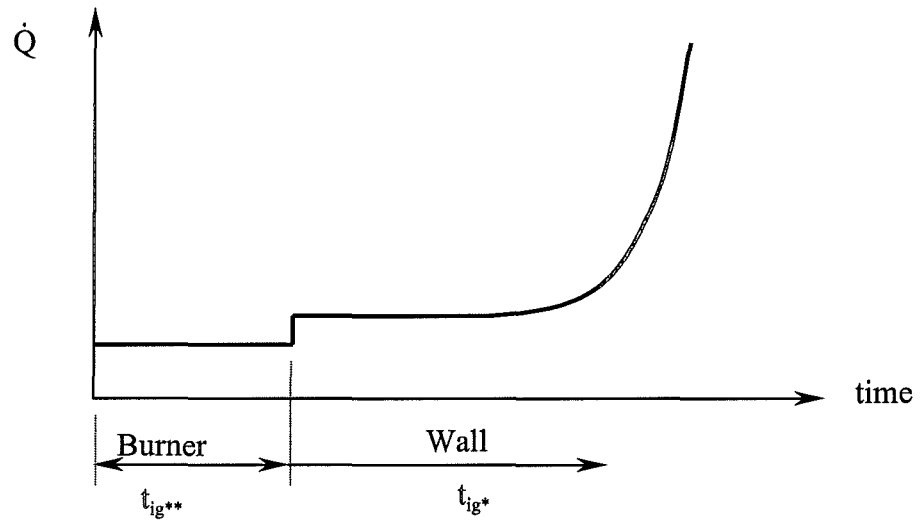

Figure 4.1: Characteristic Representation of the Different Ignition Times

Material Time to Ignition, t_{ig}:

This time is not actually used in the flame spread model itself and isn't seen in the figure above, but has been shown since this value can be compared to the ignition time found in the Cone Calorimeter test. This value uses the ignition time equation derived in the previous chapter and is calculated in the spreadsheet by the following equation,

$$t_{ig} = 113.44\left(\frac{\rho}{\dot{Q}''^2}\right)$$

Burner Time to Ignition, t_{ig**}:

In the full scale Room/Corner and Vertical Wall tests, described in the next chapter, a 100kW gas burner is placed in the corner of the room. This results in a corner flame, which nearly reaches the ceiling of the compartment. For simplicity, it is assumed that the burner flame gives a constant irradiant heat flux to the material behind the burner over an area, A_w. This area assumes the value of $0.75m^2$ in the full scale test and is equal to twice the burner width (0.17m) times the height from the top of the burner to the ceiling. It is the time to ignition of this area that is of interest and is calculated by using this Burner Time to Ignition value, t_{ig**}.

Previous research [8] has shown that using the total incident heat flux from the burner, i.e. 100 kW, to describe the time to ignition of the material gives incorrect results and improved values were obtained by using approximately $40kWm^{-2}$ at 1.6m above the floor. Because of these inaccuracies, the same general time to ignition approximation equation is used to describe is value. In the model, this equation is given as,

$$t_{ig**} = 113.44\left(\frac{\rho}{q''^{**2}}\right)$$

Wall Time to Ignition, t_{ig*}:

Once the burner has ignited the wall, this value was used in the models transient calculations as described in the previous sections. The equation used in the model was,

$$t_{ig*} = 113.44\left(\frac{\rho}{q''^{*2}}\right)$$

Time (Actual), t:

This time scale is the basis for comparison with the experimental data. The time used in the calculation procedure is added to the time to ignition for the material. As a result, the following equation is used for the actual time, t, namely,

$$t = t_{pi} + t_{ig**}$$

The total time for this model must not exceed ten minutes (600 seconds). This limitation is due to the experimental testing procedure of increasing the burner output to 300 kW if the material has not reached flashover by this stage. It should also be noted that this is a pre-flashover model so if flashover occurs within this ten minutes, the values after this event are also invalid.

Time (Post Ignition), t_{pi}:

If a flame spread calculation requires a time, it is this value that is used. This time is governed by two simple equations in the spreadsheet, one being for the initial time and the second for the times following this. The initial time value is negative as it describes the time from the start of the burner to the time when the material ignites, which occurs at $t = 0$. These equations are,

Initial Time Value;

$$t_{pi} - t_{ig**}$$

where the t_{pi} value in this calculation equals zero.

Following Time Values;

$$(0, 1, 2, 3 ...) \times t_{step}$$

This equation is incorporated into the model so that the post-ignition time interval can be changed.

4.3.2.3 Calculated Values

The four variables below are the main outputs of interest in this model. These time dependent variables are directly used to compare the validity of the model with the experimental results.

Flame Spread Velocity, $V(t)$***:***

The general statements used for the calculation of this velocity are:

$$V(t) = IF("Flame\ Front\ Movement"="invalid",0,V_1(t)) \quad ...(4.18)$$

$$V_1(t) = IF("Pyrolysing\ Length"="H",0,V(t_n)) \quad ...(4.19)$$

To ensure that the spread does not continue past the height of the wall, the requirement that the velocity equals zero at this point has been used. Any combustion of surfaces above the wall material of interest is not included in this analysis.

This statement above, applies to the two equations (4.1) and (4.2) which calculates the Flame Spread Velocity, $V(t)$, of the flame. This velocity has units of ms^{-1}.

Pyrolysing Length, $x_p(t)$***:***

The following statements are used to describe the length of the pyrolysis front at a given time, t_n.

$$x_p(t_n) = IF\left[MIN(V_c(t_0):V_c(t_n)) < 0, x_p(t_{n-1}), x_{p1}(t_n)\right] \quad ...(4.20a)$$

$$x_{p1}(t_n) = IF\left[x_{pc}(t-1) \geq H, H, x_{p2}(t_n)\right] \quad ...(4.20b)$$

$$x_{p2}(t_n) = IF\left[MIN(x_{pc}(t_0):x_{pc}(t_n)) < 0, MAX(x_p(t_0):x_p(t_{n-1})), x_{p3}(t_n)\right] ...(4.20c)$$

$$x_{p3}(t_n) = IF\left[\left(MAX\left(x_{pc}(t_0) : x_{pc}(t_{n-1})\right) > x_{pc}(t_n)\right), MAX\left(x_p(t_0) : x_p(t_{n-1})\right), x_{p4}(t_n)\right] \quad ...(4.20d)$$

$$x_{p4}(t_n) = IF\left[\left(x_{pc}(t_n) > H\right), H, x_{pc}(t_n)\right] \quad ...(4.20e)$$

These equations above ensure that the pyrolysing length, $x_p(t)$, never decreases, as this would imply that the material was becoming unburnt, or becomes larger than the actual height of the wall, H.

The subscript "(t_0)" indicates the initial value and "(t_{n-1})" indicates the previous value of the pyrolysing length. The subscript c, added to the pyrolysing length symbol, x_p, and the velocity, V, indicates that the value is taken from the transient calculations. This difference is due to limitations of the theory and due to the logic that has been imposed in the calculations. This subscript is also used for other variables in the spreadsheet.

The logic equations above are applied to equation (4.11) or (4.12), which calculates the pyrolysing length, $x_p(t)$, of the flame. This length has units of metres, m.

Heat Release Rate, $\dot{Q}_c(t)$***:***

The following statements are used to describe the heat release rate of a material at a given time, t_n.

$$\dot{Q}_c(t_n) = IF\left["\text{Flame Front Movement}"="\text{invalid}", \dot{Q}_{cc*}(t_n)e^{-\lambda t} + \dot{Q}_b, \dot{Q}_{c1}(t_n)\right] .. \quad (4.21a)$$

$$\dot{Q}_{c1}(t_n) = IF\left[x_p(t_n) = H, \dot{Q}_{cc*}(t_n)e^{-\lambda t} + \dot{Q}_b, \dot{Q}_{c2}(t_n)\right] \quad ...(4.21b)$$

$$\dot{Q}_{c2}(t_n) = IF\left["\text{Decay TimeStep}" = 0, \dot{Q}_{cc*}(t_n) + \dot{Q}_b, \dot{Q}_{cc*}(t_n)e^{-\lambda t} + \dot{Q}_b\right] \quad ...(4.21c)$$

The subscript "c*" on $\dot{Q}_c(t)$ indicates that it is the heat release rate value where the pyrolysing length, $x_p(t)$, stops increasing. This value is needed so that the λ decay can start once the pyrolysing length stops increasing.

These statements are applied to equations (4.14) or (4.15) which calculates the Heat Release Rate, $\dot{Q}_c(t)$, of the flame. The unit for this variable is kW.

Flame Height, $x_f(t)$***:***

This variable has been described after the heat release rate as this variable is used in the calculation. The flame height is governed by the following simple equation;

$$x_f(t) = K\dot{Q}_c(t) \qquad \ldots(4.22)$$

4.3.2.4 Experimental Results

The experimental results collected for this research are given in these columns of the spreadsheet and are described below.

Time (actual), t_{exp}***:***

This column contains the raw experimental times.

Experimental Heat Release Rate, Exp. HRR***:***

Again the data given here is directly taken from the experiments. The unit of this variable is kW. To provide some baseline for the experimental values, all this heat release data was time shifted so that the heat release rate was 80kW at the start of the experiment, i.e. $t = 0$. This shift is designed to take the experimental measurement time lag into account

4.3.2.5 Comparison Result

A value was needed which could describe the degree of fit that the calculated heat release rate had with the experimental results. This value was used as the output variable in the sensitivity analysis of the model which was undertaken in @RISK. The following variables and equations were used in the determination of this value,

Difference, Δ:

The technique that was incorporated in this analysis was a R^2 approach. This method first squared the differences between the two heat release rate values during the same time period and then took the square root of the average of all the times stepped difference values. This method was broken down into two steps. Firstly, the squares of the differences were calculated and then these values were averaged and square rooted in the second step. The equations for the first step, as described by this variable, Δ, are shown below, at the given time, t_n.

$$\Delta_n = \mathrm{IF}\left[\Delta_1, 0, \left(\dot{Q}_{exp}(t_n) - \dot{Q}_c(t_n)\right)^2\right] \quad \ldots(4.23a)$$

$$\Delta_1 = \mathrm{OR}\left[\dot{Q}_{exp}(t_n) = 0, t_n > 600, \mathrm{AND}\left(\dot{Q}_c(t_0 : t_n) > 1000, \dot{Q}_{exp}(t_0 : t_n) > 1000\right)\right] \ldots(4.23b)$$

The logic applied to these equations were,

- Limiting the experimental heat release rate data when the values became zero - once the end of the experimental data was reached, no comparison can be further made.
- Limiting the time period of interest – only the first 600 seconds of the model can be used to describe the flame spread behaviour of the material in question due to the burner output change.
- Limiting the maximum heat release rate to 1000kW – once the flashover occurs (approximately 1000kW), the model is no longer valid.

All these logic steps result in a zero value for Δ that would remove the influence on the comparison for the particular time period in question.

R^2 Results:

The second part of the comparison equation gives the actual result that is used in the sensitivity analysis. It is this value which is minimised to calculate when the experiment and calculated values have the closest fit. The equation used is shown below and includes the sum of the difference values (Δ) from the first time period, t_0, to the final time, t_n. The units of this term is kW.

$$\mathrm{R}^2 \text{ Result} = \mathrm{SQRT}\left[\frac{\mathrm{SUM}(\Delta_0 : \Delta_n)}{\mathrm{COUNTIF}((\Delta_0 : \Delta_n),"> 0")}\right] \qquad \ldots(4.24)$$

4.3.3 Transient Variables

Transient calculations were used in the model, as seen in figure (4.1), primarily to keep the equations in each cell to a manageable size. The secondary reason was that some equations, such as that describing the heat release rate, involved rather complex theory which gave the author no option other than using these extra transient columns.

While the inclusion of such columns removes the "cleanliness" of the model, they provide extra insight into the specific behaviour/values of parts of the theory at the given calculated times.

Some of these variables are detailed below.

4.3.3.1 Decay Time Step, $t_{\mathrm{ds}}(t_n)$

This variable is used in the heat release rate column. It's purpose is to count the number time periods after the pyrolysis front has reached the top of the material. The logic used is given by the equations below,

$$t_{ds}(t_n) = \text{IF}\left[\text{x}_\text{p}(t_n) = \text{H}, \text{COUNTIF}\left(\text{x}_\text{p}(t_n) = \text{H}\right), t_{ds1}(t_n)\right] \quad \ldots(4.25)$$

$$t_{ds1}(t_n) = \text{IF}\left[\text{FFM} = \text{"Upwards"}, 0, t_{ds}(t_{n-1}) + 1\right] \quad \ldots(4.26)$$

4.3.3.2 HRR(No Decay), $\dot{\text{Q}}_{\text{ND}}(t)$

This variable is used in conjunction with the previous one in the heat release rate calculation. The value of this variable never decreases and it remains constant once the pyrolysis front starts to mathematically decrease. The governing equations are,

$$\dot{\text{Q}}_{\text{ND}}(t_n) = \text{IF}\left[\text{x}_\text{p}(t_n) - \text{x}_\text{p}(t_{n-1}) = 0, \dot{\text{Q}}_{\text{ND}}(t_{n-1}), \dot{\text{Q}}_{\text{ND1}}(t_n)\right] \quad \ldots(4.27)$$

$$\dot{\text{Q}}_{\text{ND1}}(t_n) = \text{IF}\left[\dot{\text{Q}}_{\text{cc*}}(t_{n-1}) \geq 1 \times E + 300, 1 \times E + 300, \dot{\text{Q}}_{\text{ND2}}(t_n)\right] \quad \ldots(4.28)$$

$$\dot{\text{Q}}_{\text{ND1}}(t_n) = \text{IF}\left[\dot{\text{Q}}_{\text{cc*}}(t_{n-1}) \leq -1 \times E + 300, 1 \times E + 300, \dot{\text{Q}}_{\text{c}}(t_n)\right] \quad \ldots(4.29)$$

These final two equations ensure that the upper and lower number limits in EXCEL at not reached, therefore removing such possible sources of error.

4.3.3.3 Flame Front Movement, FFM.

The description of the movement of the flame front, given by the equations below, are used by most of the other variables in the model to ensure that the movement is still valid. These equations firstly check to see that the velocity is positive, then that the pyrolysis front isn't at the top of the material and finally that the pyrolysis front direction is still upwards (positive).

$$\text{FFM}(t_n) = \text{IF}\left[\text{MIN}\left(\text{V}(t_0^*) : \text{V}(t_n^*)\right) < 0, \text{"invalid"}, \text{FFM}_1(t_n)\right] \quad \ldots(4.30)$$

$$\text{FFM}_1(t_n) = \text{IF}\left[\text{x}_\text{p}(t_n) = \text{H}, \text{"stopped"}, \text{FFM}_2(t_n)\right] \quad \ldots(4.31)$$

$$\text{FFM}_2(t_n) = \text{IF}\left[\text{MAX}\left(\text{x}_\text{p}(t_0^*) : \text{x}_\text{p}(t_n^*)\right) > \text{x}_\text{p}(t_n^*), \text{"backwards"}, \text{"upwards"}\right] \quad \ldots(4.32)$$

5. COMPARISON EXPERIMENTS

In the development of a model, various checks must be made to ensure that it satisfactory represents what actually happens in the "real" world. One way these checks can be made involves the comparison of the calculated values to actual results from experiments. This chapter describes the particular experiments that were used for comparison in this research.

5.1 Introduction

Various experimental tests have been carried out throughout the world, which have looked at the spread of flames on walls of internal compartments. So that the model that has been developed in this research can be validated, it has been constructed which mimics this previous experimental research.

The experiments that have been used as a comparison in this report include work undertaken in 1997 by the Finnish Technical Research Centre, VTT [10, 11], as well as by the Swedish Institute for Wood Technology Research (Trätek) [8] and a Nordic fire research program named "EUREFIC [8, 20].

The Finnish research data in this report has been obtained from a report written by Kokkala et al and because of this, all future references to this research will be named "Kokkala et al". Similar simplifications have been made for the two other test results and the future references to the Swedish and EUREFIC tests will be by the names "Swedish" and "Eurefic" respectively. A description of each of these experiments is given below.

5.2 Background to Experiments

The three different experimental results used in this report give details of specific fire behaviour for numerous materials. This behaviour is primarily in terms of,

1. The quantity of energy that is released by a material, and
2. The way in which flames spread over the material.

A bench scale apparatus such as the Cone Calorimeter or the ISO Ignitibility Test generally describes the first behaviour. The second behaviour has been described for the given materials by a Room/Corner test or similar apparatus.

These two behaviours are fundamental in the development of the analytic model described in this report. The energy release rate prediction found from the initial test method is a required input into the model and without the second test, experimental comparison with the model could not be easily made.

Each result from the three experiments were found by slightly different methods. These differences are described in the following three sections of this chapter and further information can be found in the given references.

5.3 Kokkala et al Experiments

These experiments on combustible materials were carried out to investigate the upward flame spread on certain materials when ignited by a propane burner. The experimental set-up is described as a Vertical Wall test. The materials were mounded on a vertical timber framed sample holder and the burner, with a heat output of between 70 – 100 kW, was placed at the base. The materials examined and used in this research are given in the table below.

Table 5-1: Materials used from the Kokkala et al Experiments

Kokkala et al Materials		
Test No.	Product	Backing
T0412	Porous Fibre Board	Mineral Wool
T2312	Particle Board	Calcium Silicate Board
T2511	Particle Board	Mineral Wool
T1301	Textile Wall Covering on Calcium Silicate Board	Mineral Wool
T1002	Particle Board	Mineral Wool
T0203	Wood with Horizontal Grooves	Mineral Wool
T0903	Wood with Vertical Grooves	Mineral Wool

Measurements in the tests comprised of the temperatures, heat flux levels and various combustion properties. The experimental set-up is shown in the following figure.

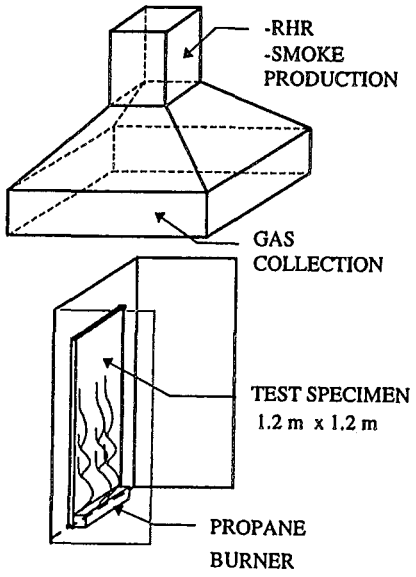

Figure 5.1: A Schematic view of the Vertical Wall Experimental Set-up [10]

To characterise the burning behaviour of the materials, Cone Calorimeter tests were undertaken. The Cone Calorimeter apparatus utilises the principle of oxygen consumption to calculate the heat released by the material. The results from this test are thus, for each exposure level, the time to ignition, mass loss rate and the rate of heat release.

This device was used, not only in the Kokkala et al study but also in the Swedish and Eurefic experiments. The typical set-up of this device, in the horizontal orientation, is seen if the following figure.

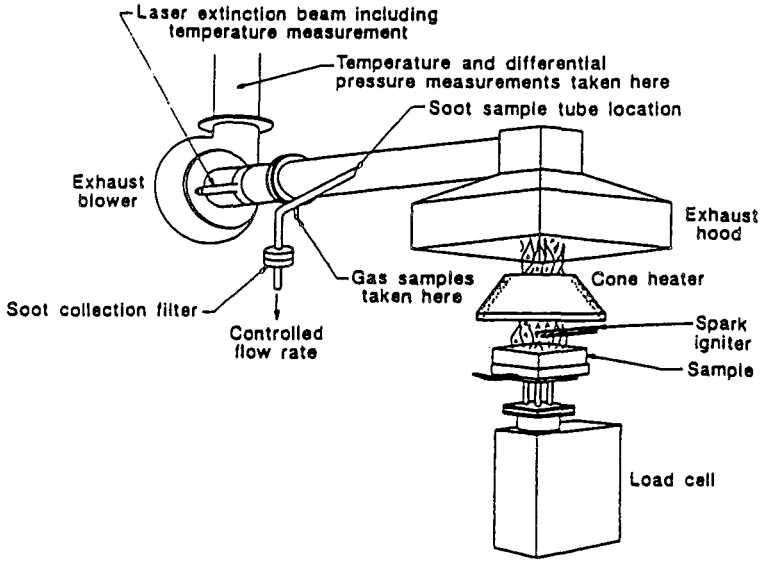

Figure 5.2: Typical Cone Calorimeter Experimental Set-up [8]

5.4 Swedish Experiments

The Swedish, as well as the Eurefic experiments incorporated the European Standard Room/Corner test. This is a large-scale test method for the measurement of the burning behaviour of surface lining materials used in buildings. The test apparatus consists of a small compartment (3.6m long, 2.4m wide and 2.4m high) with one open door and a gas burner. A gas collection system is also supplied with the necessary instrumentation to measure the fire gas properties. The Swedish and Eurefic data used in this report are just a small collection of the many different materials that have been investigated in this apparatus. The experimental set-up for the Room/Corner test is shown in the figure below.

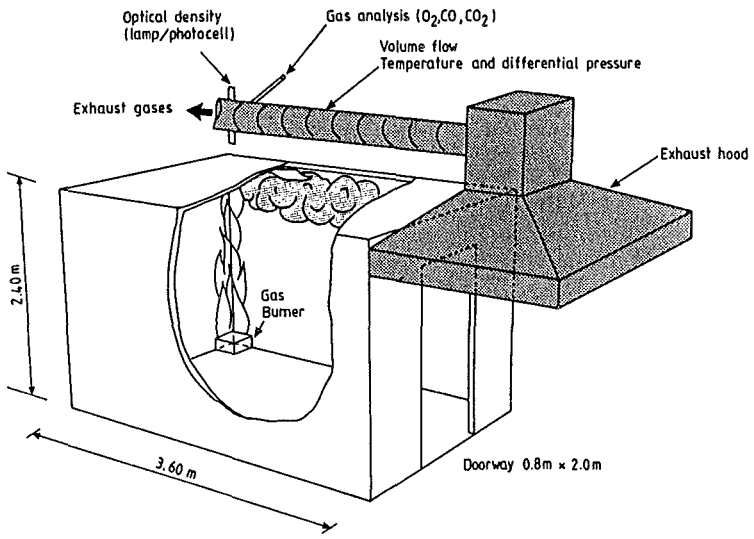

Figure 5.1: Room/Corner Experimental Set-up [19]

Thirteen different materials from this study have been incorporated into this research. Again, as mentioned previously, the materials were also tested in the Cone Calorimeter at irradiance levels of between 25–75kWm^{-2}. These materials, given in table (5.2), were fixed to the ceiling and to the walls, excluding the wall where the door was located.

The ignition source in these tests was a propane gas burner placed on the floor in one corner of the room. During the first ten minutes of the test, the burner was run at 100kW and after ten minutes, if flashover had not occurred in the compartment, was increased to 300kW.

The combustion products leaving the room through the door from this test were collected in a hood connected to an exhaust system. The rate of heat released from the fire was calculated within this system by the same principle as in the Cone Calorimeter test, namely, oxygen consumption.

The materials used in this Swedish study are given in the following table.

Table 5-1: **Materials used in Swedish Experiments**

Swedish Materials	
Material No.	Material Name
S1	Insulating Fibre Board
S2	Medium Density Fibre Board
S3	Particle Board
S4	Gypsum Plasterboard
S5	PVC covering on S4
S6	Paper covering on S4
S7	Textile covering on S4
S8	Textile covering on Mineral Wool
S9	Melamine-faced Particle Board
S10	Expanded Polystyrene
S11	Rigid Polyurethane Foam
S12	Wood Panel (Spruce)
S13	Paper covering on S3

5.5 Eurefic Experiments

The Eurefic data is from the Nordic research program "EUREFIC - EUropean REaction to FIre Classification". This program is managed by the co-operation of the institutes in Denmark, Finland, Norway and Sweden. The purpose of the tests incorporated into this research was to gain sufficient data for the use in the development and validation of a calculation model for scaling test results from the Cone Calorimeter to large scale test results of the room fire test, NT FIRE 025.

The eleven different materials included from this study have only been those tested in the horizontal orientation in the Cone Calorimeter, since this was the case for the Swedish materials. These materials are described in the table below.

Table 5-1: Materials used in Eurefic Experiments

Eurefic Materials	
Material No.	Material Description
E1	Painted Gypsum Paper Plaster Board
E2	Ordinary Plywood
E3	Textile Wall-covering on Gypsum Paper Plaster Board
E4	Melamine Faced High Density Non-combustible Board
E5	Plastic Faced Steel Sheet on Mineral Wool
E6	FR Particle Board - type B1
E7	Faced Rockwool
E8	FR Particle Board
E9	Polyurethane Foam Covered with Steel Sheet
E10	PVC-wall Carpet on Gypsum Paper Plaster Board
E11	FR Polystyrene

The experimental flame spread data for these materials was obtained from the Room/Corner Test apparatus.

6. MODEL ASSESSMENT

Once the model had been written and the comparison materials determined, an assessment of the performance of the model was undertaken. This assessment involved the determination of the best values for the four variable constants. This task and the results of the comparison are given in this chapter.

6.1 Introduction

To determine the variation that would occur in the results of the analytical flame spread model when the values of the different variables were modified, sensitivity analysis was undertaken. This analysis was performed in a risk analysis package called @RISK. It was the desire to pursue such analysis that was instrumental in the creation of the analytical, as opposed to a numerical, model that was developed in this research. The following section describes the sensitivity analysis undertaken.

6.1.1 Background to Sensitivity Analysis and @RISK

Sensitivity Analysis

In any modelling approach, many different variables are used to describe the outputs and for most situations, these variables are often not known with complete certainty. These outputs will therefore also include this degree of uncertainty.

Often, this uncertainty is small, which generally occurs when all the variables can be simply described, but it can often become very significant when a complex phenomenon is being described. Uncertainty in the values of the input variables can also arise due to their values being based on either objective or subjective decisions.

For the uncertainty of a model to be quantified, all the possible values of the variables which influence the outputs needs to be investigated. This process is termed "Sensitivity Analysis".

One technique that can be used to perform sensitivity analysis is to describe the input variables by probability distributions. There are many different types of probability distributions available which can describe the range of possible values and their likelihood of occurrence for each input variable.

One program that can be used for this type of sensitivity analysis is @RISK. This program was utilised in this report so that the uncertainty variables within the upward flame spread model could be assessed.

@RISK

@RISK is used in conjunction with either Lotus 1-2-3 or Microsoft Excel (used in this research) and applies a quantitative procedure that determines the likely range of outcomes for a given scenario. In general, the technique encompasses:

- **Developing a Model**, by defining the activity in a spreadsheet.
- **Identifying the Uncertainties**, by providing probability distributions for the models uncertain input variables.
- **Analysing the Model by Simulation**, which determines the values and distribution(s) of the selected output(s). This is accomplished by calculating the summary statistics of many iterations of the model. Each iteration selects a different input value governed by the distribution associated to the particular input variable.

The results from the simulation of the model can then be used to determine the most appropriate course of action that should next be taken. This method clarifies the behaviour of the model to any changes in the values of the input variables.

6.1.2 Simulation Inputs

The purpose of the simulation was to determine the values of the four particular variables that are incorporated in the flame spread model. A range of possible values for these input variables was known from previous research and by examining their specific definitions. These variables are described in the previous analytical model chapter and the values and distributions that they took are described below.

Heat Flux Variation, x_{po*}:

This variable is used to reduce the heat transfer overestimation that occurs in the initial phases of the model. The range of values that this variable is assumed to take is between 0.05 and 0.95.

As previously mentioned, @RISK requires that the variables be given a distribution that describes their uncertainty. The choice of these distributions was made difficult due to the complexity of the model. This complexity is not only in terms of the phenomenon that is being analysed but also in terms of the interaction that occurs between the simplified equations. Since the influence that each variable has is uncertain, a uniform distribution has been chosen for all four input variables. The shape of this simple distribution function is given in the figure below.

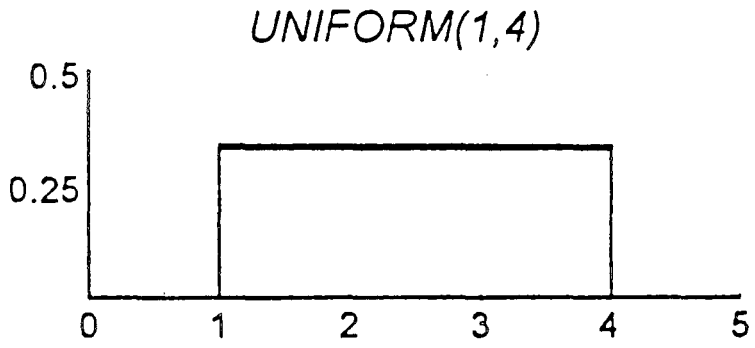

Figure 6.1: A Uniform Probability Distribution [15]

It is assumed in using this function that the probability of any value throughout its range is equal.

Ignition Time Adjustments, q"* and q"**:

These time to ignition factors are assumed to be covered by a range of between 5 and 70 kWm^{-2}. Again, a uniform distribution was applied to these variables.

Flame Area Coefficient, K:

This factor is burner location dependent and is assumed to have values ranging from between 0.003 to 0.03 m^2kW^{-1}. This area coefficient is also given a uniform distribution.

6.1.2.1 Summary

The values that were used in the initial analysis of the flame spread model are summarised in the following table,

Table 6-1: Flame Spread Model Input Variables

Input Variable	Units	Values		
		Minimum	Maximum	Distribution
x_{po*}	-	0.05	0.95	Uniform
q"*	kWm^{-2}	5	70	Uniform
q"**	kWm^{-2}	5	70	Uniform
K	m^2kW^{-1}	0.003	0.03	Uniform

6.1.3 Simulation Outputs

The main reason for performing the sensitivity analysis was to optimise the variables so that the heat release rate calculated in the model would fit the experimental data to its best ability. Because of this, the output of particular interest was the comparison equation, "R^2 Results". This value was calculated for the each individual materials as

well as being averaged over all of the materials. The philosophy used in this optimisation was to;

"obtain the four input variable values when the R^2 value, averaged over all the materials, was minimised."

These values would therefore indicate the best fit of all the materials to their individual experimental data.

The technique used in @RISK to implement this philosophy was to;

1. Sort the summary simulation data in ascending order so that the minimum value of the averaged R^2 value could be obtained, as well as the iteration that it occurred.
2. View the data from the iteration, found in step 1, and determine the values of the four input variables.

6.1.4 Simulation Settings

@RISK allows various settings to be chosen for a simulation. These options include varying,

- the number of iterations performed,
- the sampling type,
- convergence monitoring parameters, and
- the (random) seed number generation setting.

During the model simulation the following settings and values were chosen,

Table 6-1: Simulation Settings Summary

Setting	Values: Model A[1]	Values: Model B[2]
Iteration Number	5000	7500
Seed	1	1
Sampling Technique	Latin Hypercube	Latin Hypercube
Standard Recalc.	Expected Value	Expected Value
Convergence Limit	Every 100 iterations	Every 100 iterations

[1] The Room/Corner tests involving the Swedish and Eurefic materials
[2] The Vertical Wall test involving the Kokkala et al materials

6.2 Input Analysis Rsults

This section of the report details the base case analysis of the developed flame spread model. The input, output and simulation settings used in this section are those that were described above.

Using the computer program @RISK, the required average R^2 value and the distribution of this value was found. From this result, the value of the input variables could be ascertained. Sensitivity results were also collected to determine what influence each input had on the output, namely, the averaged R^2 value.

Two separate analyses were undertaken for this report – Model A and Model B. Model A combined the materials that were tested by the Room/Corner test method (i.e. Swedish and Eurefic materials) and Model B investigated the Vertical Wall test of the Kokkala et al materials.

6.2.1 Model A Base Case Analysis

The @RISK simulation predicted a minimum averaged R^2 value of 364, with a mean of 1.55×10^{15} and a standard deviation of 1.8×10^{16}. This large standard deviation was influenced by the large upper limit, of 4.4×10^{17}, for R^2. Some of these values can be

seem in the following figure, which focuses on the lower end of the averaged R^2 distribution result,

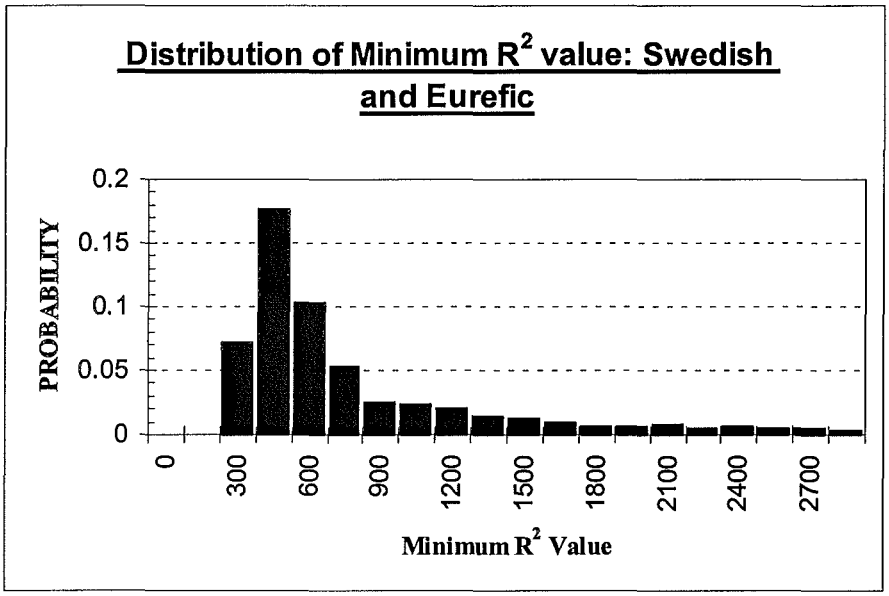

Figure 6.1: Minimum Average R^2 Distribution for Model A

It can be seem from the figure above that the average R^2 value exhibits a lognormal type of distribution.

The corresponding correlation analysis of the base case indicated that the averaged R^2 value is most sensitive to the variation of the value of the Flame Area Coefficient, K, and the value of the Pre-ignition Time Adjustment variable, q"**. The Post-ignition Time Adjustment variable, q"* and the Heat Flux Variation variable, x_{po*} were found to have a smaller influence on the value of the average R^2 value for model A. These results can be seem in the following figure,

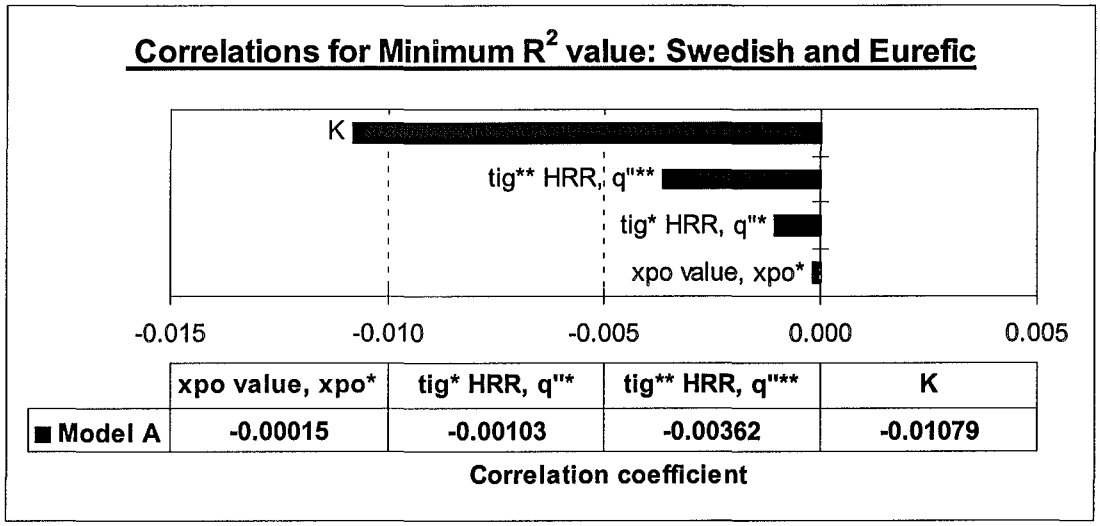

Figure 6.2: Minimum Average R^2 Correlation Results for Model A

From the results that were obtained by this analysis, "best" values for the four input variables could be found. These values would give the closest comparison between the experimental and calculated heat release rate values. The method used to find these input values has been previously described. The results using this technique are presented in the table below,

Table 6-1: Minimum Input Values for Model A

Input Variable	Symbol	Value
Heat Flux Variation variable	x_{po*}	0.18
Post-ignition Time Adjustment variable	q"*	30.4
Pre-ignition Time Adjustment variable	q"**	47.2
Flame Area Coefficient	K	0.018

6.2.2 Model B Base Case Analysis

This model, as could be expected, produced a different mean Averaged R^2 value than in the previous @RISK analysis. The minimum value was found to be 54.8, with a mean of 2552 and the standard deviation of 2408. The shape of the distribution for this output, as shown in the figure below, was very different to the previous analysis.

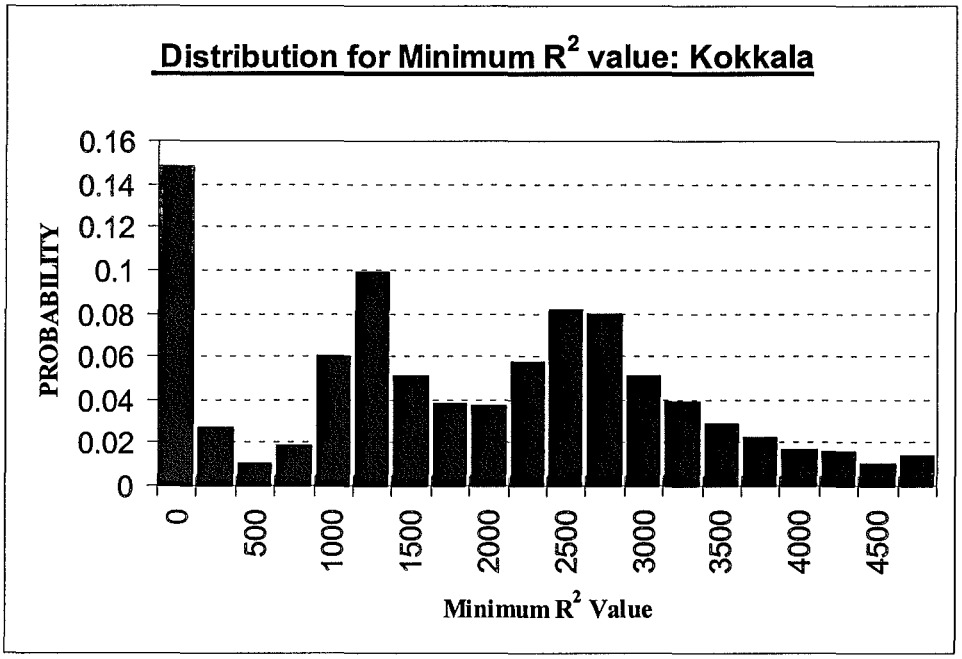

Figure 6.1: Minimum Average R^2 Distribution for Model B

The correlation analysis for this case exhibited different results to those found in model A. This time, the Flame Area Coefficient, K, and the Post-ignition Time Adjustment variable, q"* were shown to have the most significant influence on the value of the minimum average R^2 value and the other two variables exhibited less significance. These results are shown in the following figure,

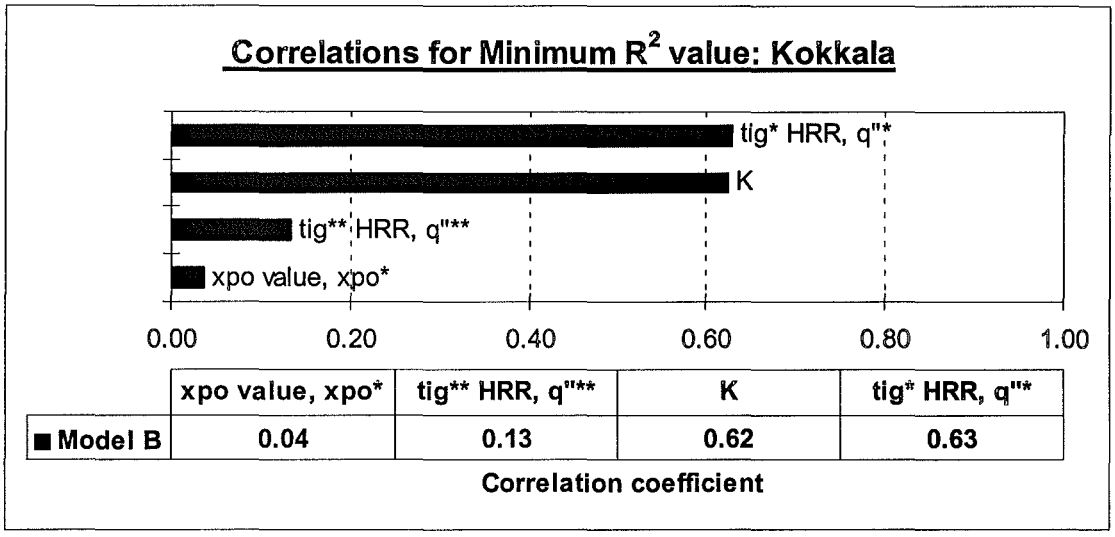

Figure 6.2: Minimum Average R^2 Correlation Results for Model B

The "best" values for the inputs were found for this model using the same technique applied in model A. These values, corresponding to the optimum fit between the experimental to calculated heat release rate, were applied to the model and a description of the actual effect that this had is described in the next section. The results from the analysis in this section is given in the table below,

Table 6-1: Minimum Input Values for Model B

Input Variable	Symbol	Value
Heat Flux Variation variable	x_{po*}	0.67
Post-ignition Time Adjustment variable	q"*	11.9
Pre-ignition Time Adjustment variable	q"**	27.4
Flame Area Coefficient	K	0.005

6.3 Modelling Initial Optimised Input Values

Once the optimal input values were found from the @RISK analysis, they could be incorporated into the models. At this point, verification of the flame spread model to the experimental data could be made. If the values were found to be similar, then the @RISK simulation technique for finding to particular values of the input variables would have been successful.

6.3.1 Model A

In model A, using the Room/Corner experiment results, very good overall comparison was found between the calculated heat release rate and the corresponding experimental results for the Swedish and Eurefic materials. An example of the success of the model is shown in the figure below, which shows material S3 (Particle Board).

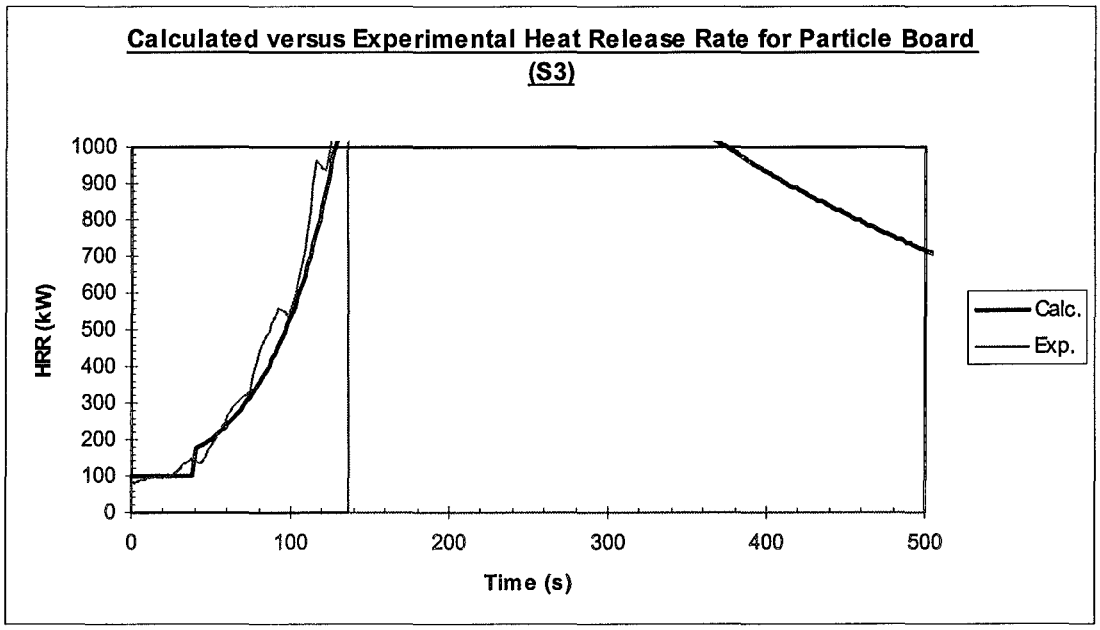

Figure 6.1: Model A Comparison for Material S3

This figure clearly shows the individual aspects of the modelled heat release rate. It can be seen in the initial phase that the calculated heat release rate is constant at 100kW. This constant value continues until the material behind the burner ignites. After approximately forty (40) seconds, the material ignites and heat release rate rapidly raises to a peak value and is followed by an exponential decay. This peak and some of the exponential decay is off the graph, but is of little interest in this pre-flashover model, as once the heat release rate exceeds 1000kW, flashover is said to occur and the model is no longer valid. Flashover can be seen to occur in both the calculated and experiment in approximately 130 seconds.

A complete set of figures for the Swedish and Eurefic materials can be seen in appendices D and E.

6.3.2 Model B

The application of the input variable values into Model B, using the Vertical Wall test, also gave very good results. The material T2511, indicated in the figure below, again

shows the success that the model has in calculating the heat release rate values. This material, as with all the Kokkala et al materials, did not go to flashover.

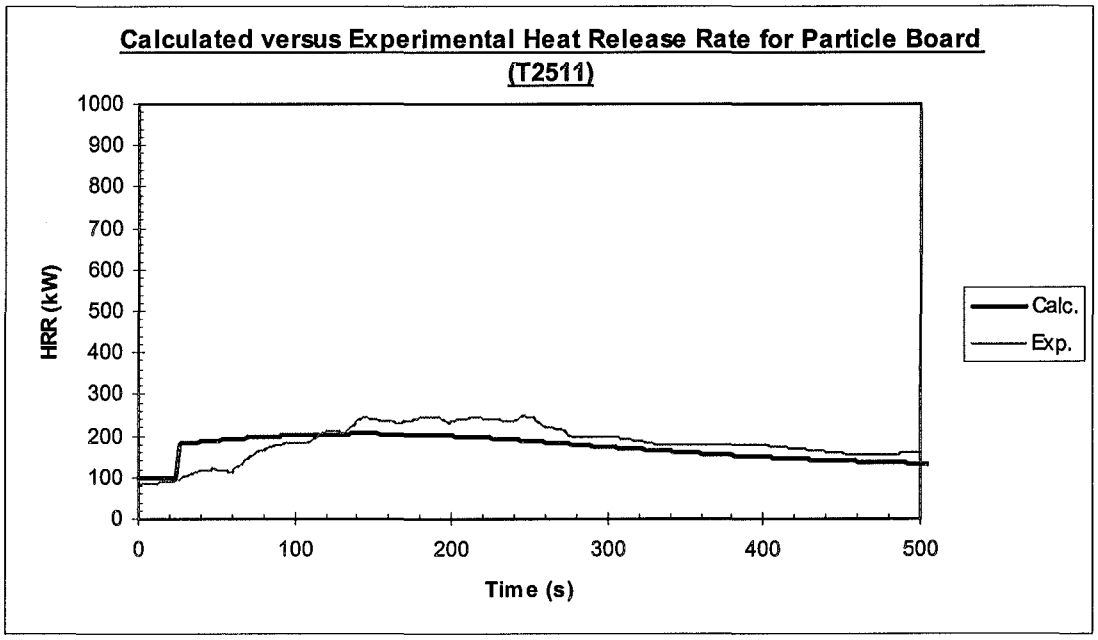

Figure 6.1: Model B Comparison for Material T2511

A complete set of figures for the Kokkala et al materials can be seen in appendix C.

6.3.3 Time to Ignition Comparison

Since the time that a material will take to go to flashover in a compartment is very important, a comparison between the experimental and calculated time to flashover was made. Flashover is assumed to occur when the heat release rate exceeds 1000kW. This comparison is made in the following figure.

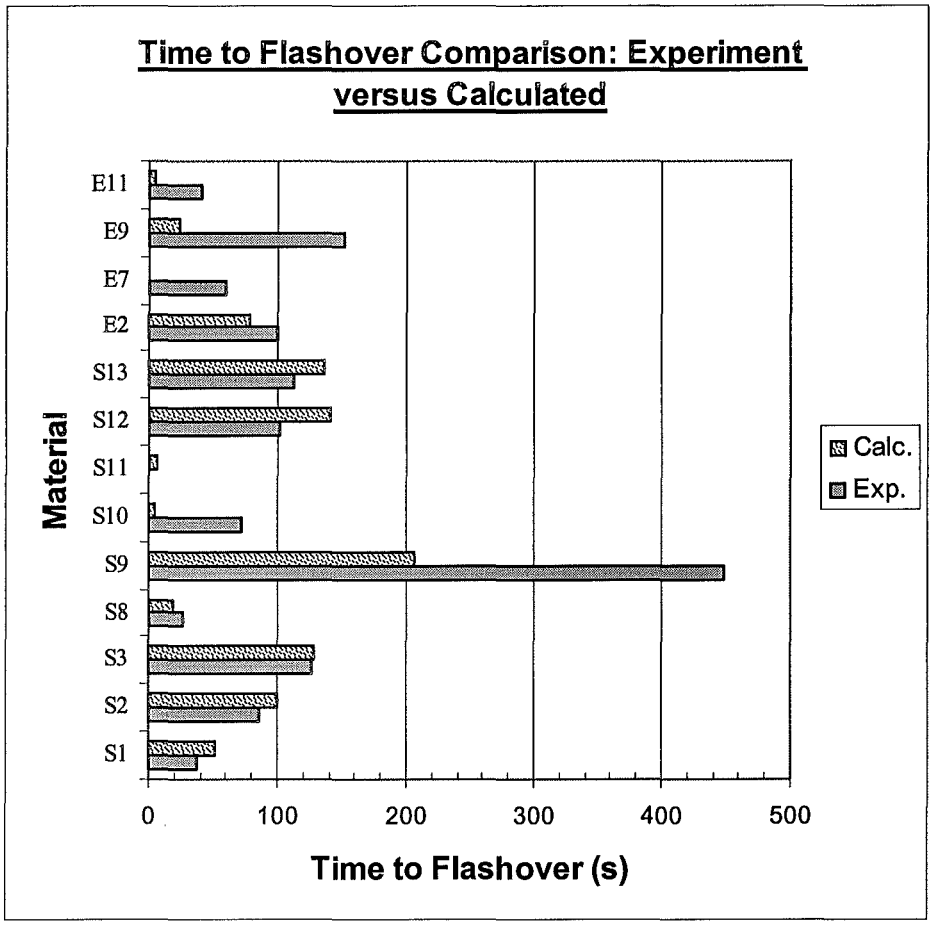

Figure 6.1: Calculation to Experimental Time to Ignition Comparison

The materials in the figure above only come for model A, the Room/Corner test, as no Kokkala materials went to flashover. It can be seen that the model was generally very good at predicting the time to flashover.

6.4 Summary

In the assessment of the two models, A and B, to their experimental studies, sensitivity analysis was applied so that the optimal values of the four input tuning variables could be determined. It was found from the analysis that the values of these variables differed between that of the model A, which incorporated the Swedish and Eurefic materials, and model B, which investigated the Kokkala et al materials. The values of these variables are summarised in the following table,

Table 6-1: Optimal Input Values for Model A and B

Input Variable	Symbol	Model A Values	Model B Values
Heat Flux Variation variable	x_{po*}	0.18	0.67
Post-ignition Time Adjustment variable	q"*	30.4	11.9
Pre-ignition Time Adjustment variable	q"**	47.2	27.4
Flame Area Coefficient	K	0.018	0.005

It was found by using the Regression Correlation function in @RISK that each input value influenced the average R^2 result to differing extents. For both models, the flame area coefficient, K, was found to have the most influence on the minimum average R^2 result. Both of the ignition time adjustment variables were also significant and the heat flux variation variable found to have the least influence on the minimum average R^2 result.

The optimised R^2 values of these variables were found to give very good comparisons between the calculated and experimental heat release rate for each of the two models. The model can therefore be used to satisfactorily calculate the flame spread characteristics for the materials investigated.

7. CONCLUSIONS

Part 1: Time to Ignition Equation Investigation

In the first part of the research, a simplified expression for the time to ignition of a material, based on an equation derived in [8], was developed. This development involved the investigation of several possibilities but all but one of these was excluded since their performance was found to be poor. The simplified equation that was finally chosen was incorporated into the analytical flame spread model. The analysis undertaken for this equation used only the Swedish materials and the initial results in the comparison between the calculated and experimentally determined time to ignition values were found to be very satisfactory.

The form of this time to ignition equation was,

$$t_{ig} = 113.44\left(\frac{\rho}{\dot{q}_e''^2}\right)$$

The averaged errors when this equation is applied to the thirteen Swedish materials were found to be –2%.

Further investigation into the applicability of this equation for the Eurefic and Kokkala et al materials would hopefully determine the level of confidence that could be assumed when applying this equation.

Part 2: Analytical Flame Spread Model Development and Assessment

As with most models of complex phenomenon, many simplifications were incorporated into the model developed in this research. These simplifications neglect all but the essential aspects of vertical flame spread on combustible materials in an attempt to make the model easy to use and so that the sensitivity analysis performed would be relatively computationally inexpensive.

One of these simplifications involved representing the experimentally determined heat release rate of each material by a mathematical expression. This expression was either described as a Peak/Decay or an Average representation.

Tuning of the model was undertaken by four input variables that were optimised by sensitivity analysis. This optimisation compared the fit of the calculated values to the experimental data collected from three different studies. Two of the studies, namely the Swedish and Eurefic tests, used the European standard Room/Corner test method. The other study on the Kokkala et al materials used a Vertical Wall test method.

The results from using the analytical model described in the report to represent the complex phenomena of upward flame spread on solid materials were found to be very satisfactory based on the generally close comparison between the calculated and experimental values.

8. REFERENCES

1) Brenton, J.R., Drysdale, D.D., *Upward Flame Spread over Vertical Fuel Surfaces*, Submitted to the Fire Safety Journal.

2) Buchanan A.H (Editor), *Fire Engineering Design Guide*, Centre for Advanced Engineering, University of Canterbury, July 1994.

3) Cooper, L.Y., Compartment Fire-Generated Environment and Smoke Filling, *The SFPE Handbook of Fire Protection Engineering*, National Fire Protection Association, Quincy, Second Edition, Section 3, Chapter 10, 1995.

4) Frantzich, H., *Uncertainty and Risk Analysis in Fire Safety Engineering*, Report TVBB-1016, Department of Fire Safety Engineering, Lund University, Sweden, 1998.

5) Hakkarainen, T., Oksanen, T., Mikkola, E., *Fire Behaviour of Facades in Multi-storey Wood-framed Houses*, VTT Research Notes 1823, Technical Research Centre of Finland, 1997.

6) Höglander, K. Sundström, B, *Design Fires for Pre-flashover Fires - Characteristic Heat Release Rates of Building Contents*, SP Swedish National Testing and Research Institute, SP Report 1997:36, Sweden, 1997.

7) International Organisation for Standardisation (ISO), *Fire Safety Engineering – Part 1: The Application of Fire Performance Concepts to Design Objectives*, Committee Draft, Report ISO/PDTR 13387-1, 1998.

8) Karlsson, B. *Modelling Fire Growth on combustible Wall Lining Materials in Enclosures*, Report TVBB-1009, Department of Fire Safety Engineering, Lund University, Sweden, 1992.

9) Karlsson, B. Quintiere, J.G., *Enclosure Fire Dynamics - A First Draft of a Student Textbook*, Department of Fire Safety Engineering, Lund University, Sweden, August 1998.

10) Kokkala, M., Göransson, U., Söderbom, J., *Five Large-scale Room Fire Experiments, Project 3 of the EUREFIC Fire Research Programme*, VTT Publication 104, Technical Research Centre of Finland, Espoo 1992.

11) Kokkala, M., Mikkola, E., Immonen, M.; Juutilainen, H., Manner, P., Parker, W. J. *Large-scale Upward Flame Spread Tests on Wood Products*, VTT Research Notes 1834, Technical Research Centre of Finland, 1997.

12) Lie, T.T., Fire Temperature-Time Relations, *The SFPE Handbook of Fire Protection Engineering*, National Fire Protection Association, Quincy, Second Edition, Section 4, Chapter 8, 1995.

13) Lønvik, L.E., Opstad, K., *Software User's Guide for DCS - A Data Converting System, Version 1.20*, SINTEF - The Foundation for Scientific and Industrial Research at the Norwegian Institute of Technology, Report Number STF25 A90003, Norway, 1991.

14) New Zealand Fire Service, (1998) *New Zealand Fire Service Database Statistics, 1986-1997*, National Headquarters, Wellington, New Zealand.

15) Palisade, *Guide to Using @RISK: Risk Analysis and Simulation Add-In for Microsoft Excel or Lotus 1-2-3*, Palisade Corporation, New York, September 1996.

16) Palisade, *PRECISION TREE User's Guide: Decision Analysis Add-In for Microsoft Excel*, Palisade Corporation, New York, July 1997.

17) Quintiere, J.G., Surface Flame Spread, *The SFPE Handbook of Fire Protection Engineering*, National Fire Protection Association, Quincy, Second Edition, Section 2, Chapter 14, 1995.

18) Saito, K., Quintiere, J.G., Williams, F.A., *Upward Turbulent Flame Spread*, Proc. First International Symposium on Fire Safety Science, Hemisphere Publishing, New York, 1984.

19) Sundström, B, *A New Generation of Large Scale Fire Test Methods*, SP Swedish National Testing and Research Institute, SP Report 1990:12, Sweden, 1990.

20) Thureson, P., *EUREFIC - Cone Calorimeter Test Results, Project 4 of the EUREFIC Fire Research Programme*, SP Swedish National Testing and Research Institute, SP Report 1991:24, Sweden, 1991.

21) Tsantaridis, L., Östman, B., *Smoke, Gas and Heat Release Data for building Products in the Cone Calorimeter*, Trätek Report I 8903013, TräteknikCentrum, Stockholm, Sweden, 1991.

22) Walton, W.D., Thomas, P.H., Estimating Temperatures in Compartment Fires, *The SFPE Handbook of Fire Protection Engineering*, National Fire Protection Association, Quincy, Second Edition, Section 3, Chapter 6, 1995.

23) Williams, F.A., *Mechanisms of Fire Spread*, 16th International Symposium on Combustion, pp. 1281-1294, 1976.

9. APPENDIX LIST

Appendix A:	Parameters used in the Analytical Calculation
Appendix B:	@RISK Simulation Output Data
Appendix C:	Kokkala et al Modelled Materials
Appendix D:	Swedish Modelled Materials
Appendix E:	Eurefic Modelled Materials

10. APPENDIX A: PARAMETERS USED IN THE ANALYTICAL CALCULATION

Input Values used in the Analytical Flame Spread Model

Table 10-1: Swedish Input Values

Material No.	Material Name	Wall Height (m)	Burner Output	Burner Width (m)
S1	Insulating Fibre Board	27	100	0.34
S2	Medium Density Fibre Board	27	100	0.34
S3	Particle Board	27	100	0.34
S4	Gypsum Plasterboard	27	100	0.34
S5	PVC covering on S4	27	100	0.34
S6	Paper covering on S4	27	100	0.34
S7	Textile covering on S4	27	100	0.34
S8	Textile covering on Mineral Wool	27	100	0.34
S9	Melamine-faced Particle Board	27	100	0.34
S10	Expanded Polystyrene	27	100	0.34
S11	Rigid Polyurethane Foam	27	100	0.34
S12	Wood Panel (Spruce)	27	100	0.34
S13	Paper covering on S3	27	100	0.34

Table 10-2: Eurefic Input Values

Material No.	Material Name	Wall Height (m)	Burner Output	Burner Width (m)
E1	Painted Gypsum Paper Plaster Board	27	100	0.34
E2	Ordinary Plywood	27	100	0.34
E3	Textile Wall-covering on Gypsum Paper Plaster Board	27	100	0.34
E4	Melamine Faced High Density Non-combustible Board	27	100	0.34
E5	Plastic Faced Steel Sheet on Mineral Wool	27	100	0.34
E6	FR Particle Board - type B1	27	100	0.34
E7	Faced Rockwool	27	100	0.34
E8	FR Particle Board	27	100	0.34
E9	Polyurethane Foam Covered with Steel Sheet	27	100	0.34
E10	PVC-wall Carpet on Gypsum Paper Plaster Board	27	100	0.34
E11	FR Polystyrene	27	100	0.34

Table 10-3: Kokkala et al Input Values

Material No.	Material Name	Backing	Wall Height (m)	Density, ρ (kgm^{-3})	Burner Output	Burner Width (m)
T0412	Porous Fibre Board	Mineral Wool	27	80	100	1.2
T2312	Particle Board	Calcium Silicate Board	27	832	100	1.2
T2511	Particle Board	Mineral Wool	27	162	100	1.2
T1301	Textile Wall Covering on Calcium Silicate Board	Mineral Wool	27	258	100	1.2
T1002	Particle Board	Mineral Wool	27	162	70	1.2
T0203	Wood with Horizontal Grooves	Mineral Wool	27	540	100	1.2
T0903	Wood with Vertical Grooves	Mineral Wool	27	540	100	1.2

Material Parameters used in the Analytical Flame Spread Model

Table 10-1: Swedish Material Parameters

Material No.	Material Name	Density, ρ (kgm^{-3})	Q_{max} (kWm^{-2})	λ (s^{-1})
S1	Insulating Fibre Board	250	184	0.0090
S2	Medium Density Fibre Board	600	208	0.0027
S3	Particle Board	750	204	0.0030
S4	Gypsum Plasterboard	700	151	0.0390
S5	PVC covering on S4	682	210	0.0600
S6	Paper covering on S4	684	254	0.0600
S7	Textile covering on S4	691	408	0.0700
S8	Textile covering on Mineral Wool	184	466	0.0800
S9	Melamine-faced Particle Board	810	150	0.0016
S10	Expanded Polystyrene	20	325	0.0120
S11	Rigid Polyurethane Foam	30	247	0.0200
S12	Wood Panel (Spruce)	527	168	0.0075
S13	Paper covering on S3	726	197	0.0041

Table 10-2: Eurefic Material Parameters

Material No.	Material Name	Density, ρ (kgm^{-3})	Q_{max} (kWm^{-2})	λ (s^{-1})
E1	Painted Gypsum Paper Plaster Board	681	213	0.0850
E2	Ordinary Plywood	600	275	0.0060
E3	Textile Wall-covering on Gypsum Paper Plaster Board	724	312	0.0400
E4	Melamine Faced High Density Non-combustible Board	1055	106	0.0175
E5	Plastic Faced Steel Sheet on Mineral Wool	640	71	0.2000
E6	FR Particle Board - type B1	630	152	0.0250
E7	Faced Rockwool	87	126	0.0800
E8	FR Particle Board	755	69	0.0175
E9	Polyurethane Foam Covered with Steel Sheet	170	259	0.0125
E10	PVC-wall Carpet on Gypsum Paper Plaster Board	750	137	0.0095
E11	FR Polystyrene	37	667	0.0450

Table 10-3: Kokkala et al Material Parameters

Material No.	Material Name	Backing	Density, ρ (kgm^{-3})	Q_{max} (kWm^{-2})	λ (s^{-1})
T0412	Porous Fibre Board	Mineral Wool	80	190	0.0091
T2312	Particle Board	Calcium Silicate Board	832	245	0.0050
T2511	Particle Board	Mineral Wool	162	240	0.0040
T1301	Textile Wall Covering on Calcium Silicate Board	Mineral Wool	258	240	0.1535
T1002	Particle Board	Mineral Wool	162	240	0.0040
T0203	Wood with Horizontal Grooves	Mineral Wool	540	240	0.0124
T0903	Wood with Vertical Grooves	Mineral Wool	540	240	0.0124

11. APPENDIX B: @RISK SIMULATION OUTPUT DATA

Table 11-1: @RISK Output Data 1a – Swedish/Eurefic Materials

Name	Ave. R2 values				Swedish Data												
Description	All	Swedish	Eurefic		S1	S2	S3	S4	S5	S6	S7	S8	S9	S10	S11	S12	S13
Minimum =	363.73	367.27	122.96		37.1	31.2	36.2	13.6	10.5	9.9	19.4	46.6	52.2	149.4	678.7	55.2	27.8
Maximum =	4.37E+17	1.85E+09	9.53E+17		4350.2	2449.4	2235.7	283.9	349.1	490.4	1227.6	2.7E+5	1244.8	2E+10	3291.9	1501.5	2130.2
Mean =	1.55E+15	2.86E+07	3.37E+15		761.6	591.5	608.7	55.5	67.7	95.5	198.9	2447.3	513.0	3.7E+8	1983.4	482.6	518.8
Std Deviation =	1.81E+16	1.34E+08	3.95E+16		358.3	350.1	291.1	63.9	79.5	105.5	188.4	7511.7	218.1	1.7E+9	1152.3	192.2	264.1
Variance =	3.27E+32	1.81E+16	1.56E+33		1.3E+5	1.2E+5	8.5E+4	4.1E+3	6.3E+3	1.1E+4	3.5E+4	5.6E+7	4.8E+4	3E+18	1.3E+6	3.7E+4	7.0E+4
Skewness =	15.71	6.71	15.71		3.1	1.8	1.4	1.6	1.4	1.2	1.2	16.9	0.4	6.7	0.0	1.4	1.5
Kurtosis =	282.39	54.61	282.39		23.7	6.1	4.9	4.2	3.7	3.1	3.9	441.5	2.1	54.6	1.2	5.7	5.7
Mode =	416.88	632.20	161.54		800.1	501.9	546.4	15.3	11.4	24.4	64.8	988.6	418.6	665.6	682.5	462.7	470.8
5% Perc =	419.64	554.19	161.11		228.4	208.4	251.1	14.5	11.4	16.9	47.7	418.9	212.0	707.5	682.5	216.1	192.0
10% Perc =	479.15	617.88	161.65		410.5	290.0	330.8	14.7	11.4	18.7	53.8	688.3	272.9	1609.7	682.5	284.8	270.1
15% Perc =	521.14	637.58	263.73		520.3	341.6	389.4	15.0	11.4	20.6	57.5	808.1	309.0	1819.2	682.5	330.8	321.6
20% Perc =	558.26	669.92	356.84		594.5	388.0	432.8	15.3	12.0	22.8	60.0	878.9	340.0	2059.5	682.5	364.7	361.6
25% Perc =	602.27	699.15	420.40		648.6	423.4	468.2	15.3	13.3	24.4	62.3	927.8	365.5	2425.6	682.5	391.4	393.4
30% Perc =	664.84	722.79	497.39		692.0	452.7	494.7	15.3	15.0	24.4	64.8	962.3	384.6	2865.5	755.2	412.4	419.3
35% Perc =	746.45	758.61	594.58		722.2	473.1	514.9	16.1	17.3	24.4	64.8	988.6	399.3	3540.0	1064.0	429.7	439.4
40% Perc =	888.84	818.46	745.54		746.6	492.7	533.4	17.5	19.9	26.2	64.8	988.6	411.2	4613.4	1064.0	442.5	457.1
45% Perc =	1186.11	940.49	1030.06		767.2	501.9	546.4	19.5	23.7	29.7	66.7	988.6	418.6	6415.1	1356.7	454.6	470.8
50% Perc =	1670.93	1195.90	1723.42		782.3	501.9	546.4	22.5	27.7	34.8	74.2	988.6	418.6	9696.7	1628.4	462.7	470.8
55% Perc =	2896.78	1735.87	2998.83		800.1	501.9	546.4	26.4	33.4	41.3	88.7	988.6	418.6	1.7E+4	2422.7	462.7	470.8
60% Perc =	7215.44	3008.07	7257.40		800.1	501.9	546.4	31.5	40.1	51.5	129.7	988.6	508.7	3.3E+4	3006.8	462.7	470.8
65% Perc =	21873.36	6894.79	24381.37		800.1	501.9	546.4	37.9	48.9	66.8	248.1	988.6	607.0	8.3E+4	3133.7	462.7	470.8
70% Perc =	1.15E+05	1.95E+04	1.07E+05		800.1	501.9	546.4	46.9	61.2	93.6	307.4	1276.1	670.9	2.4E+5	3214.7	462.7	470.8
75% Perc =	6.74E+05	7.47E+04	6.16E+05		800.1	501.9	595.5	59.1	80.8	168.6	355.3	1612.7	722.0	9.6E+5	3266.2	462.7	470.8
80% Perc =	4.83E+06	4.10E+05	5.44E+06		800.1	780.2	793.4	85.8	131.2	214.7	388.5	2040.8	758.0	5.3E+6	3291.9	582.6	638.4
85% Perc =	5.90E+07	3.02E+06	7.76E+07		800.1	976.6	951.1	150.2	186.2	246.0	424.2	2738.8	788.8	3.9E+7	3291.9	684.2	794.4
90% Perc =	7.69E+08	2.06E+07	1.56E+09		979.7	1151.4	1085.3	178.6	209.9	278.0	467.1	4122.4	822.7	2.7E+8	3291.9	762.9	945.4
95% Perc =	6.80E+11	1.35E+08	1.53E+12		1301.1	1363.7	1240.3	201.7	243.6	312.0	540.7	7827.8	881.5	1.8E+9	3291.9	875.9	1098.4

Table 11-1: @RISK Output Data 1b – Swedish/Eurefic Materials

Name	Eurefic Data										
Description	E1	E2	E3	E4	E5	E6	E7	E8	E9	E10	E11
Minimum =	15.50	24.08	29.59	4.91	12.45	27.75	115.74	20.90	64.15	12.11	51.16
Maximum =	276.75	4031.88	836.34	262.11	23.18	359.61	1033.57	146.77	1.74E+4	514.62	1.0E+19
Mean =	47.49	682.59	230.30	47.43	13.56	96.67	353.32	38.00	1206.54	162.92	3.7E+16
Std Deviation =	52.47	642.04	136.06	61.30	1.39	90.75	39.29	21.35	1296.45	141.55	4.3E+17
Variance =	2.75E+3	4.12E+5	1.85E+4	3.76E+3	1.93	8.24E+3	1.54E+3	455.96	1.68E+6	2.00E+4	1.9E+35
Skewness =	1.94	1.38	1.15	1.79	1.98	1.13	5.44	3.08	4.18	0.67	15.71
Kurtosis =	5.64	4.21	3.44	5.01	7.51	2.64	67.66	12.14	31.55	1.71	282.39
Mode =	17.01	314.15	154.90	5.82	12.45	38.37	342.98	30.02	348.00	63.80	445.97
5% Perc =	16.26	143.72	96.94	5.82	12.45	32.02	331.80	27.67	225.43	28.44	445.97
10% Perc =	16.52	192.87	116.64	5.82	12.45	32.91	340.97	28.62	276.27	36.03	445.97
15% Perc =	16.74	229.61	128.10	5.82	12.50	33.71	343.31	28.77	313.54	43.31	1.63E+3
20% Perc =	17.01	261.64	135.28	6.01	12.55	34.44	344.33	28.87	338.91	50.03	2.73E+3
25% Perc =	17.01	286.85	141.82	7.31	12.60	35.10	344.91	28.99	348.00	54.52	3.18E+3
30% Perc =	17.01	314.15	146.76	9.18	12.66	35.92	345.32	29.10	348.00	59.05	3.89E+3
35% Perc =	17.42	314.15	150.69	11.33	12.72	36.74	345.69	29.27	686.85	62.71	4.88E+3
40% Perc =	18.42	314.15	154.00	13.70	12.80	37.99	345.95	29.46	853.27	63.80	6.54E+3
45% Perc =	19.77	314.15	154.90	16.87	12.89	38.37	346.18	29.71	939.04	63.80	9.65E+3
50% Perc =	21.68	314.15	154.90	20.25	12.99	38.37	346.41	30.02	993.44	64.58	1.70E+4
55% Perc =	24.48	314.15	155.73	24.95	13.14	42.28	346.61	30.02	1.04E+3	77.34	3.07E+4
60% Perc =	27.77	314.15	173.96	29.87	13.30	51.07	346.77	30.02	1.10E+3	116.60	7.75E+4
65% Perc =	32.73	483.30	227.80	36.18	13.47	65.13	346.93	30.88	1.18E+3	210.67	2.66E+5
70% Perc =	38.40	871.15	288.82	43.58	13.72	96.84	347.62	32.56	1.27E+3	295.42	1.17E+6
75% Perc =	46.01	1.17E+3	332.97	54.40	14.00	176.84	351.33	34.75	1.40E+3	322.90	6.78E+6
80% Perc =	61.00	1.35E+3	366.82	68.09	14.37	210.16	355.58	38.40	1.56E+3	343.61	5.98E+7
85% Perc =	96.03	1.49E+3	400.68	99.90	14.86	231.51	361.68	44.54	1.80E+3	358.31	8.54E+8
90% Perc =	149.61	1.65E+3	442.99	176.64	15.49	254.86	372.93	57.45	2.31E+3	374.91	1.7E+10
95% Perc =	173.61	1.92E+3	494.80	202.83	16.58	277.34	403.93	90.40	3.42E+3	399.18	1.7E+13

Table 11-1: @RISK Output Data 1c – Swedish/Eurefic Materials

Input Name	xpo value, xpo*	tig* HRR, q"*	tig** HRR, q"**	K
Description	Uniform(0.05,0.95)	Uniform(5,70)	Uniform(5,70)	Uniform(0.003,0.03)
Minimum =	0.050	5.00	5.01	0.0030
Maximum =	0.950	70.00	70.00	0.0300
Mean =	0.500	37.50	37.50	0.0165
Std Deviation =	0.260	18.76	18.76	0.0078
Variance =	0.068	352.08	352.08	0.0001
Skewness =	0	0	0	0
Kurtosis =	1.800	1.80	1.80	1.8000
Mode =	0.343	65.13	60.58	0.0058
5% Perc =	0.095	8.24	8.24	0.0043
10% Perc =	0.140	11.50	11.49	0.0057
15% Perc =	0.185	14.74	14.74	0.0070
20% Perc =	0.230	17.99	18.00	0.0084
25% Perc =	0.275	21.24	21.25	0.0097
30% Perc =	0.320	24.49	24.49	0.0111
35% Perc =	0.365	27.74	27.74	0.0124
40% Perc =	0.410	30.99	31.00	0.0138
45% Perc =	0.455	34.25	34.25	0.0151
50% Perc =	0.500	37.50	37.49	0.0165
55% Perc =	0.545	40.75	40.74	0.0178
60% Perc =	0.590	43.99	43.99	0.0192
65% Perc =	0.635	47.24	47.25	0.0205
70% Perc =	0.680	50.50	50.49	0.0219
75% Perc =	0.725	53.75	53.74	0.0232
80% Perc =	0.770	56.99	57.00	0.0246
85% Perc =	0.815	60.24	60.25	0.0259
90% Perc =	0.860	63.50	63.49	0.0273
95% Perc =	0.905	66.75	66.75	0.0286

Table 11-1: @RISK Output Data 2 – Kokkala et al Materials

Name	ave. R^2 value	Kokkala-Baroudi Data							Input Values			
Description	Kokkala Data	T0412	T2312	T2511	T1301	T1002	T0203	T0903	xpo value, xpo*	tig* HRR, q"*	tig** HRR, q"**	K
Equation	-	-	-	-	-	-	-	-	Uniform(0.05,0.95)	Uniform(5,70)	Uniform(5,70)	Uniform(0.003,0.03)
Minimum =	54.82	61.21	9.76	14.60	4.39	17.02	51.53	46.96	0.050	5.00	5.01	0.0030
Maximum =	33940.92	193210.1	6371.25	72937.20	2065.90	72981.81	5175.41	5177.93	0.950	70.00	70.00	0.0300
Mean =	2551.94	3576.39	1932.43	4852.35	153.31	4897.10	1226.39	1225.62	0.500	37.50	37.50	0.0165
Std Deviation =	2408.31	7208.64	1703.26	5075.28	261.63	5080.89	1125.00	1128.68	0.260	18.76	18.76	0.0078
Variance =	5.8E+6	51.7E+6	2.9E+6	25.8E+6	68450.27	25.8E+6	1.3E+6	1.3E+6	0.068	352.08	352.08	0.0001
Skewness =	3.25	10.46	0.02	4.86	2.22	4.84	0.25	0.25	0.000	0.00	0.00	0.0000
Kurtosis =	23.65	174.75	1.27	41.00	8.59	40.84	1.65	1.65	1.800	1.80	1.80	1.8000
Errors Calculated =	0	0	0	0	0	0	0	0	0	0	0	0
Mode =	2878.61	2472.47	67.05	94.47	4.70	34.27	78.31	70.74	0.370	24.83	8.58	0.0223
5% Perc =	62.48	124.46	39.44	63.64	4.86	34.27	65.97	59.38	0.095	8.25	8.25	0.0043
10% Perc =	83.28	131.33	51.69	94.47	5.78	111.83	68.89	61.79	0.140	11.50	11.50	0.0057
15% Perc =	263.58	138.11	67.05	375.38	6.94	435.62	71.67	64.38	0.185	14.74	14.74	0.0070
20% Perc =	956.04	301.12	67.05	2809.54	8.36	2868.67	75.09	68.17	0.230	18.00	18.00	0.0084
25% Perc =	1201.74	1633.44	67.05	3458.22	9.98	3521.03	78.31	70.74	0.275	21.25	21.25	0.0097
30% Perc =	1350.65	1858.10	77.33	3634.25	11.75	3693.13	78.31	70.74	0.320	24.50	24.49	0.0111
35% Perc =	1470.81	1939.27	149.21	3728.45	14.02	3784.71	92.70	90.80	0.365	27.74	27.75	0.0124
40% Perc =	1666.97	2008.59	333.54	3819.01	16.95	3871.48	151.32	152.60	0.410	30.99	31.00	0.0138
45% Perc =	1991.23	2085.88	1042.14	3916.96	20.50	3970.91	343.09	346.40	0.455	34.25	34.25	0.0151
50% Perc =	2332.06	2181.44	2598.55	4035.49	24.38	4088.38	1464.59	1465.27	0.500	37.50	37.49	0.0165
55% Perc =	2514.33	2291.57	3022.59	4195.23	29.73	4245.49	1845.58	1848.95	0.545	40.75	40.74	0.0178
60% Perc =	2663.64	2431.43	3208.47	4380.65	36.45	4430.97	1968.65	1972.87	0.590	43.99	44.00	0.0192
65% Perc =	2812.29	2633.23	3312.85	4602.35	47.78	4650.10	2048.30	2051.58	0.635	47.24	47.25	0.0205
70% Perc =	2976.83	2910.59	3391.37	4910.93	69.11	4957.90	2114.82	2118.77	0.680	50.50	50.50	0.0219
75% Perc =	3212.49	3281.87	3470.13	5295.84	120.07	5344.51	2184.54	2188.14	0.725	53.75	53.74	0.0232
80% Perc =	3545.49	3819.40	3561.17	5857.05	367.82	5908.05	2267.85	2269.67	0.770	56.99	57.00	0.0246
85% Perc =	4050.25	4747.66	3681.70	6758.18	473.67	6809.31	2377.99	2380.21	0.815	60.25	60.25	0.0259
90% Perc =	4946.88	6593.33	3860.30	8396.53	555.66	8451.09	2547.20	2549.13	0.860	63.50	63.49	0.0273
95% Perc =	6429.03	11676.55	4184.55	12369.99	699.12	12417.26	2890.74	2893.02	0.905	66.75	66.75	0.0286

12. Appendix C: Kokkala et al Modelled Materials

Global Variable Constants		
x_{po} value, x_{po*}	0.67	(-)
t_{ig*} HRR, q"*	11.9	(kWm^{-2})
t_{ig**} HRR, q"**	27.4	(kWm^{-2})
K	0.005	(m^2kW^{-1})

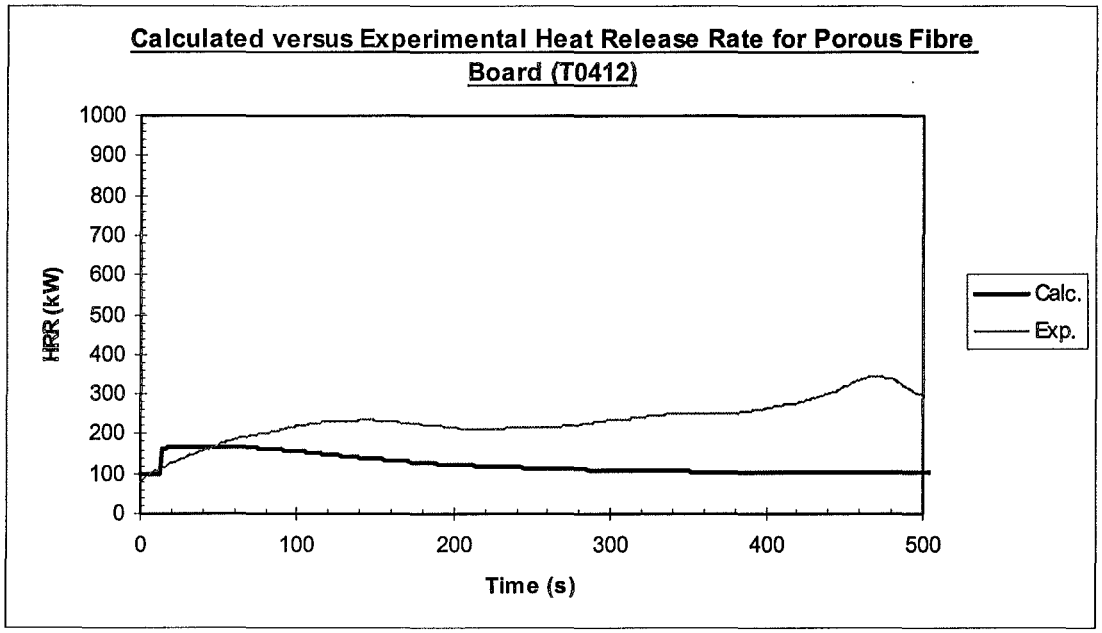

Figure 12.1: Material T0412 Flame Spread Comparison

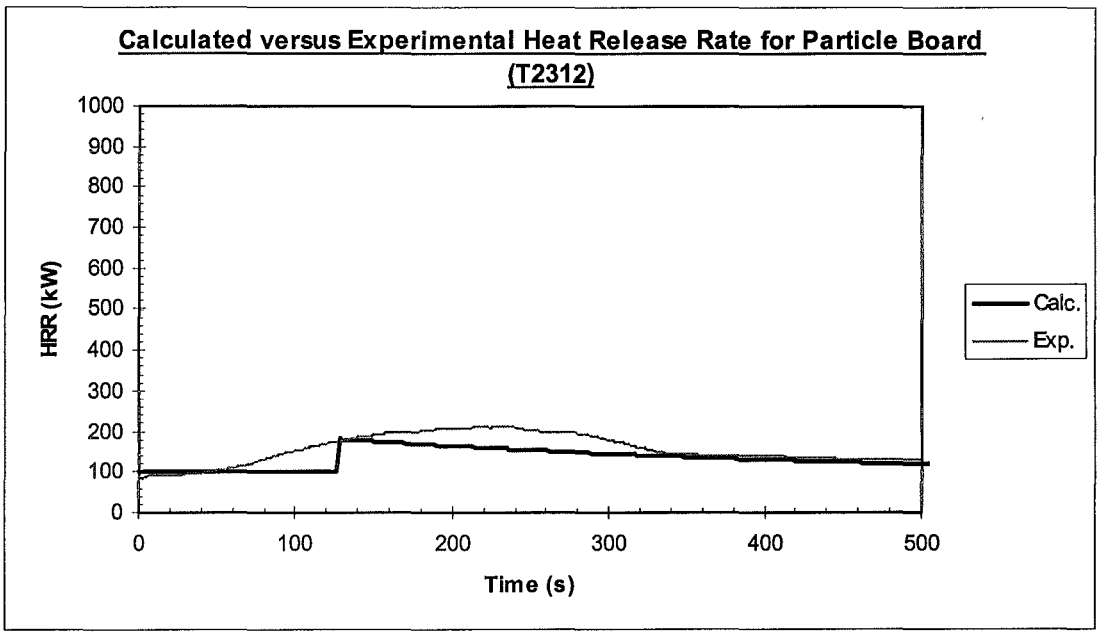

Figure 12.2: Material T2312 Flame Spread Comparison

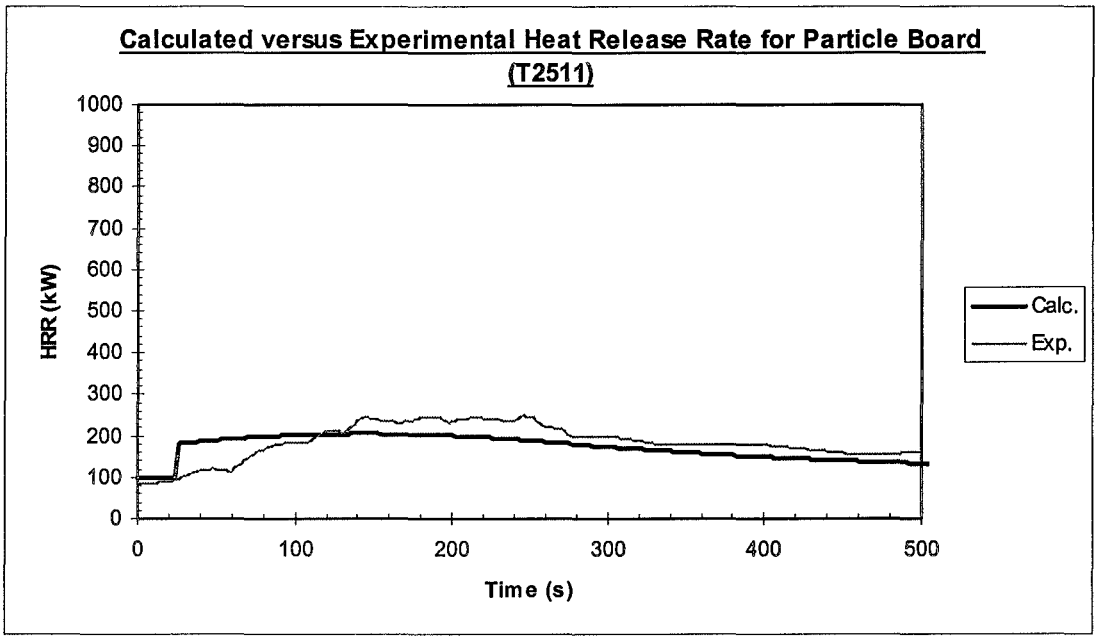

Figure 12.3: Material T2511 Flame Spread Comparison

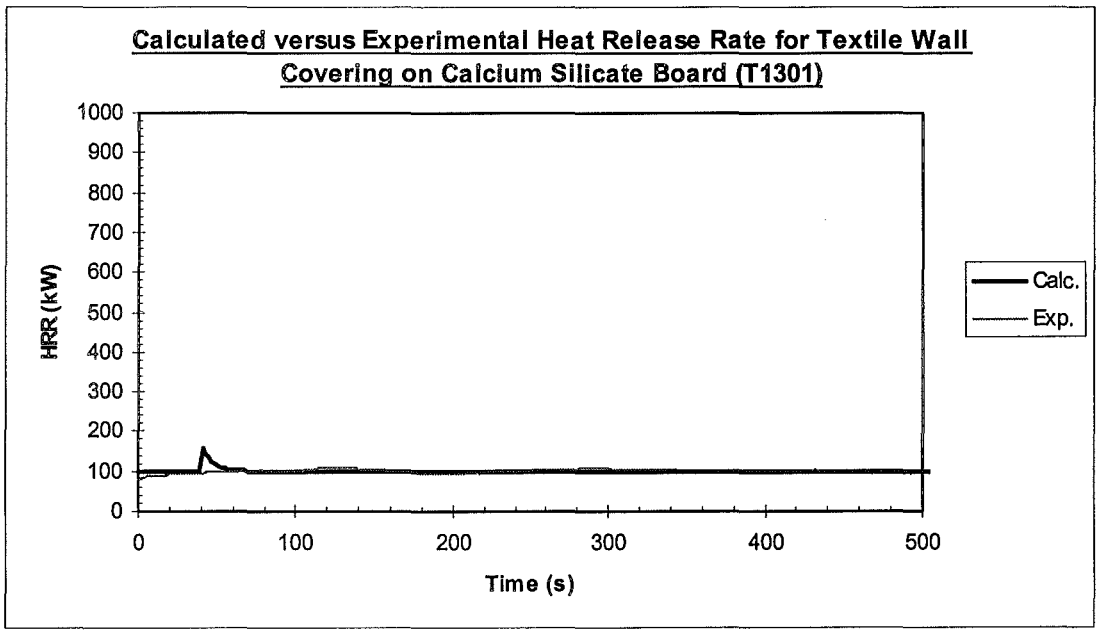

Figure 12.4: Material T1301 Flame Spread Comparison

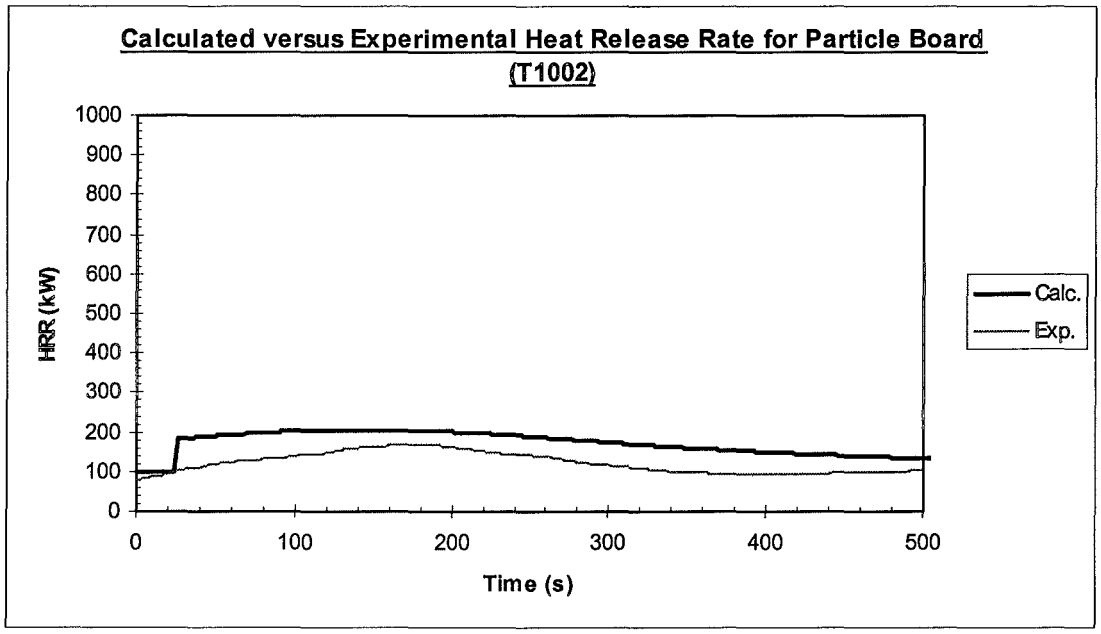

Figure 12.5: Material T1002 Flame Spread Comparison

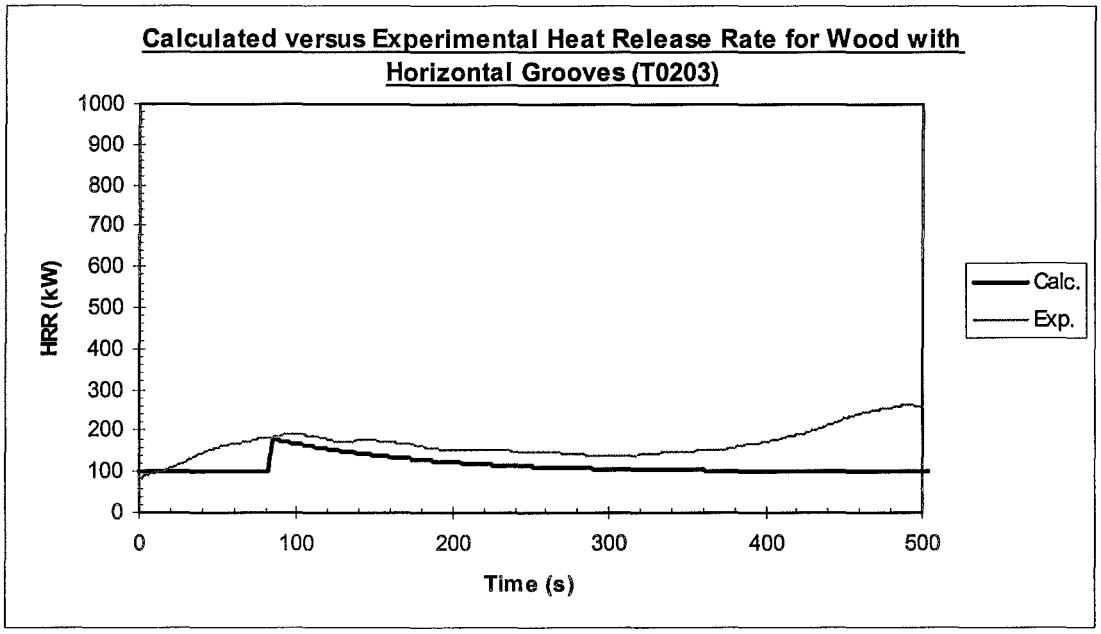

Figure 12.6: Material T0203 Flame Spread Comparison

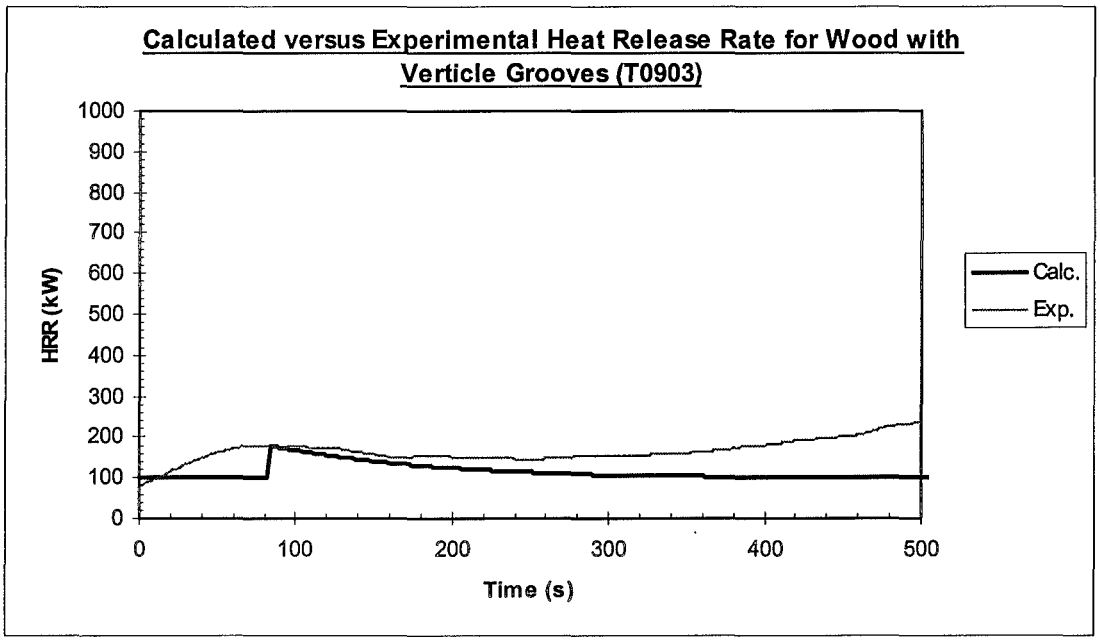

Figure 12.7: Material T0903 Flame Spread Comparison

13. APPENDIX D: SWEDISH MODELLED MATERIALS

Global Variable Constants		
x_{po} value, x_{po*}	0.18	(-)
t_{ig*} HRR, q"*	32.0	(kWm^{-2})
t_{ig**} HRR, q"**	45.7	(kWm^{-2})
K	0.018	(m^2kW^{-1})

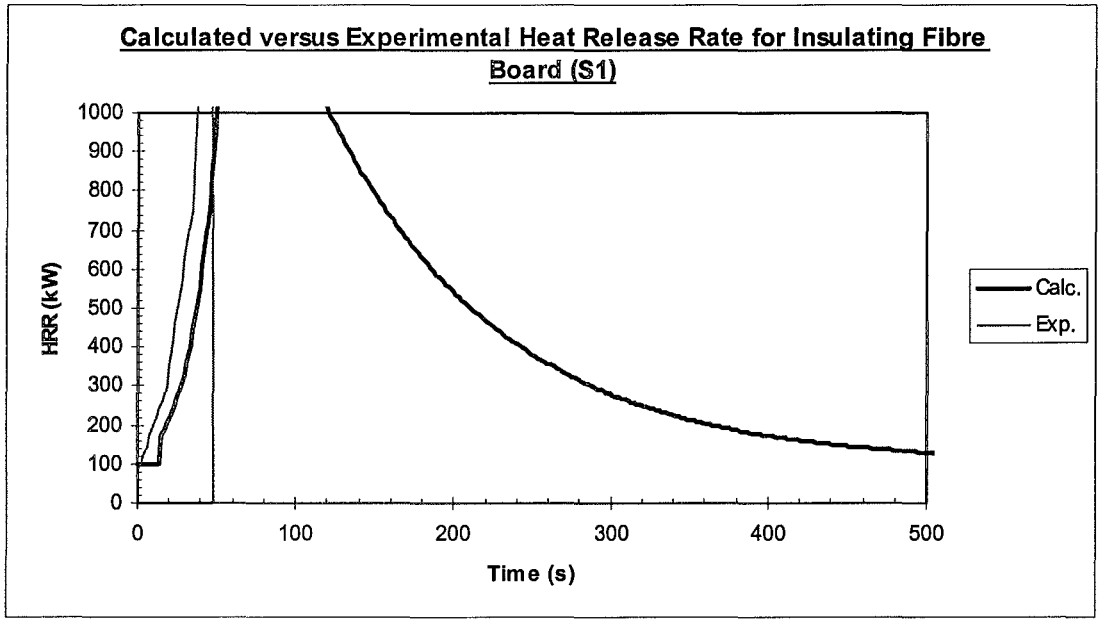

Figure 13.1: Material S1 Flame Spread Comparison

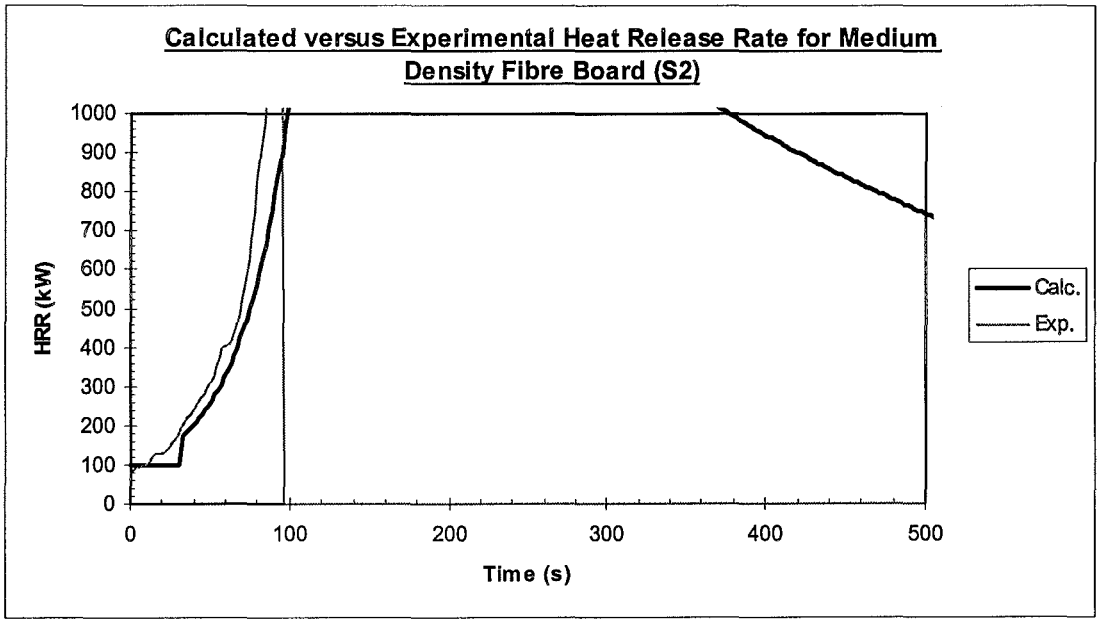

Figure 13.2: Material S2 Flame Spread Comparison

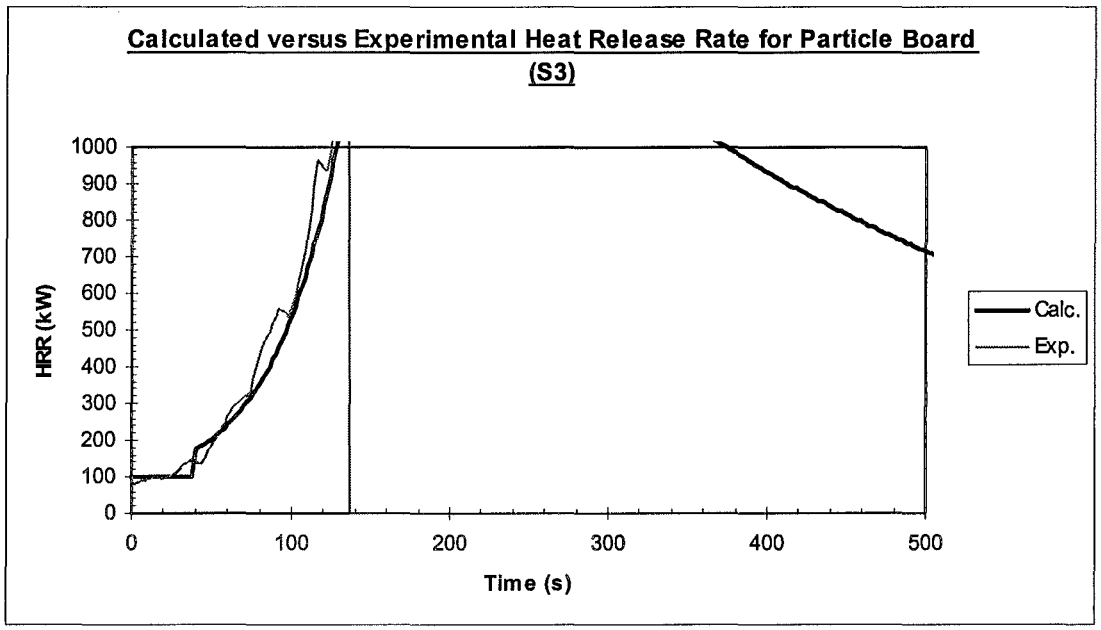

Figure 13.3: Material S3 Flame Spread Comparison

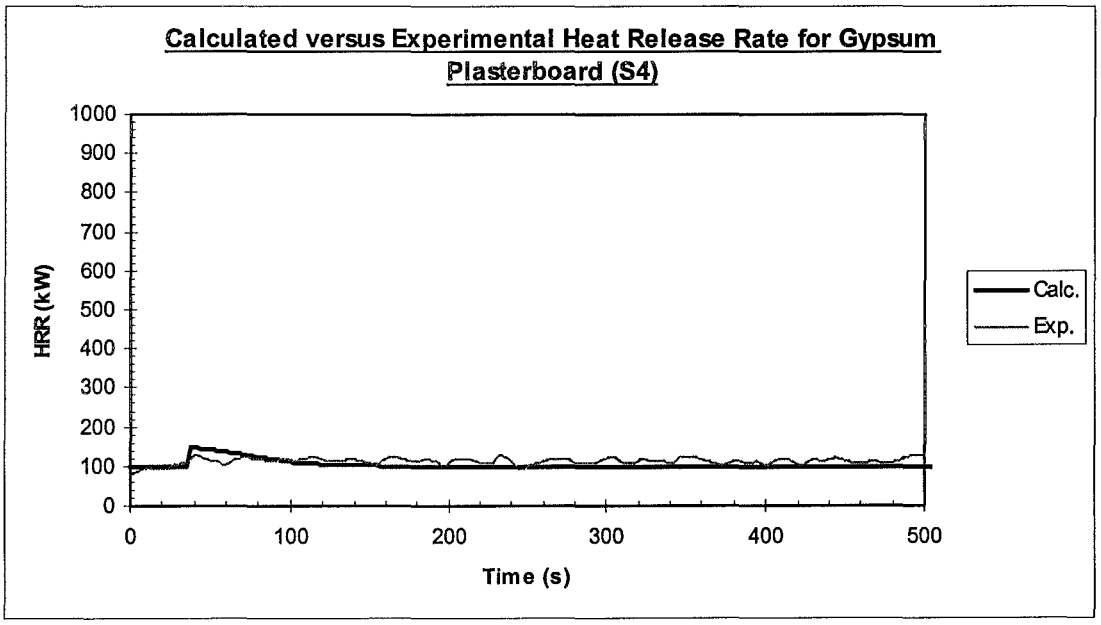

Figure 13.4: Material S4 Flame Spread Comparison

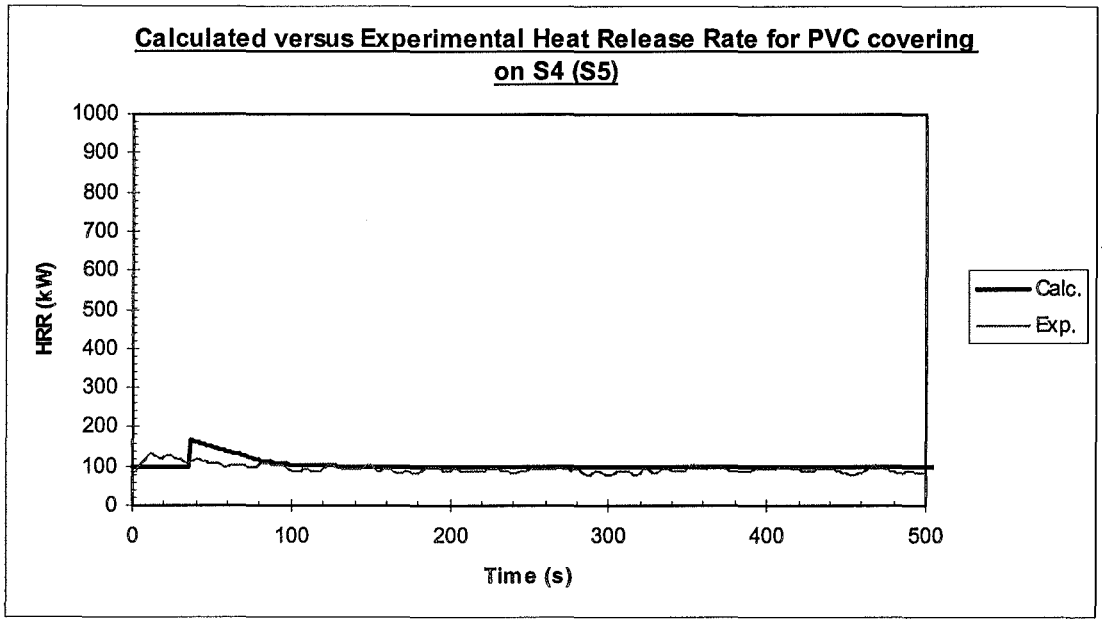

Figure 13.5: Material S5 Flame Spread Comparison

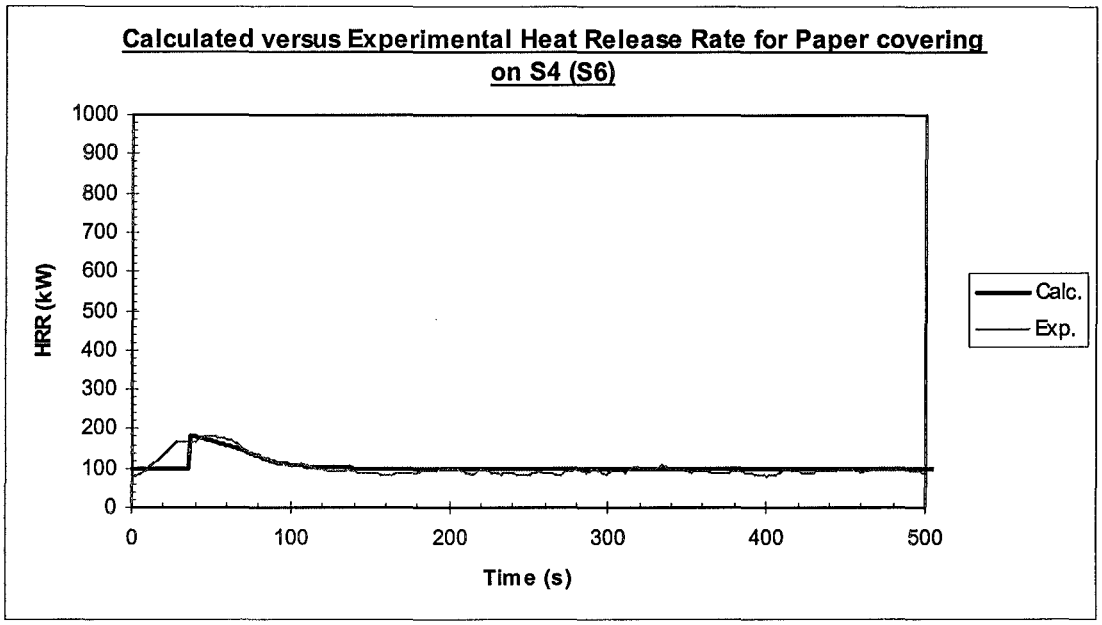

Figure 13.6: Material S6 Flame Spread Comparison

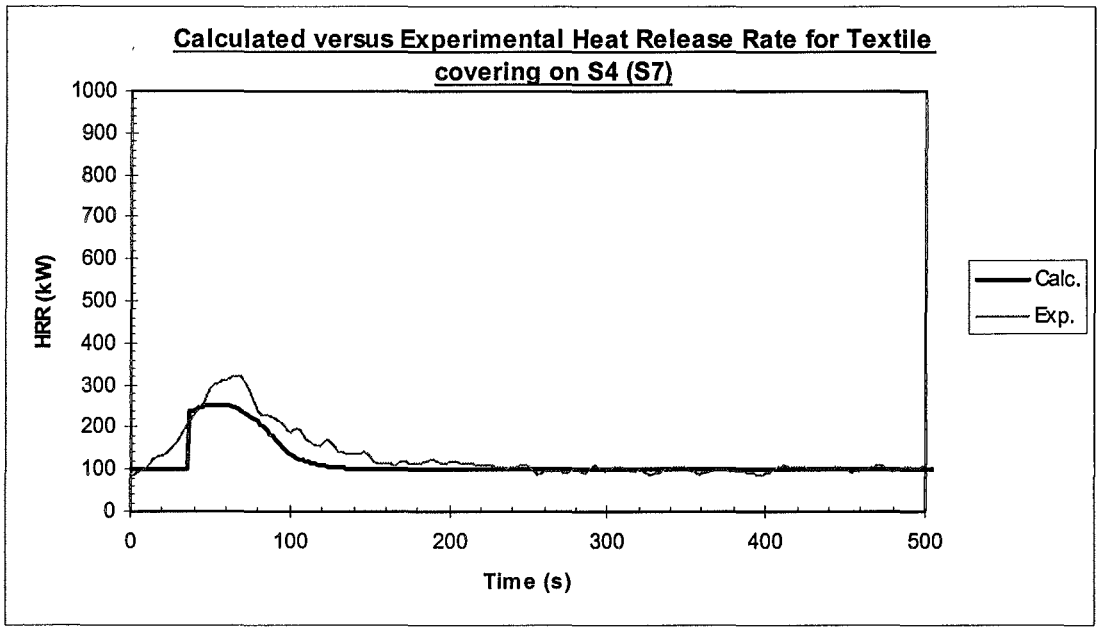

Figure 13.7: Material S7 Flame Spread Comparison

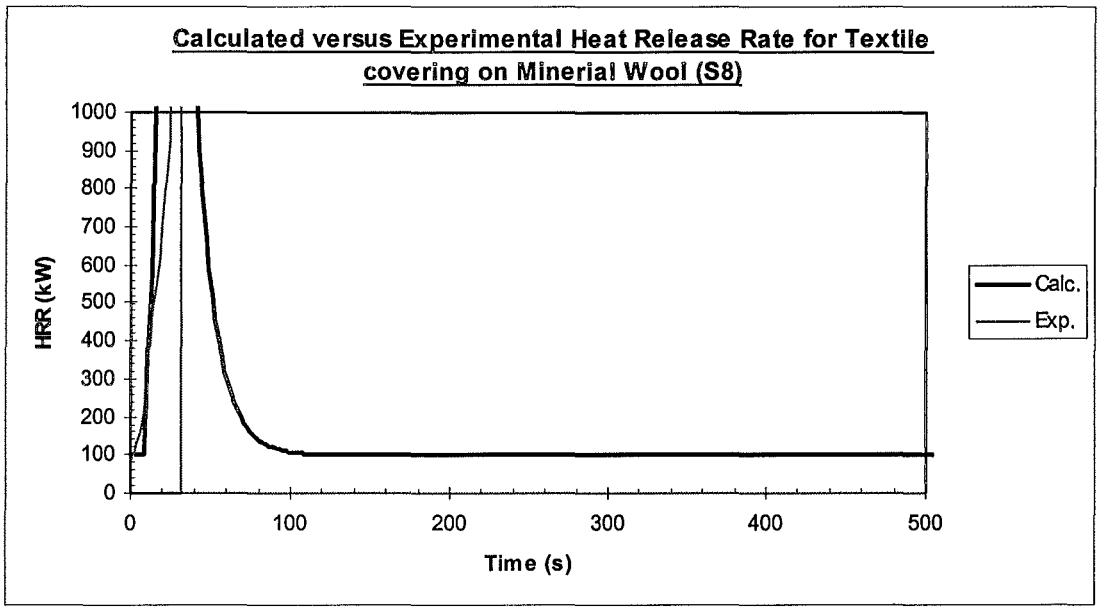

Figure 13.8: Material S8 Flame Spread Comparison

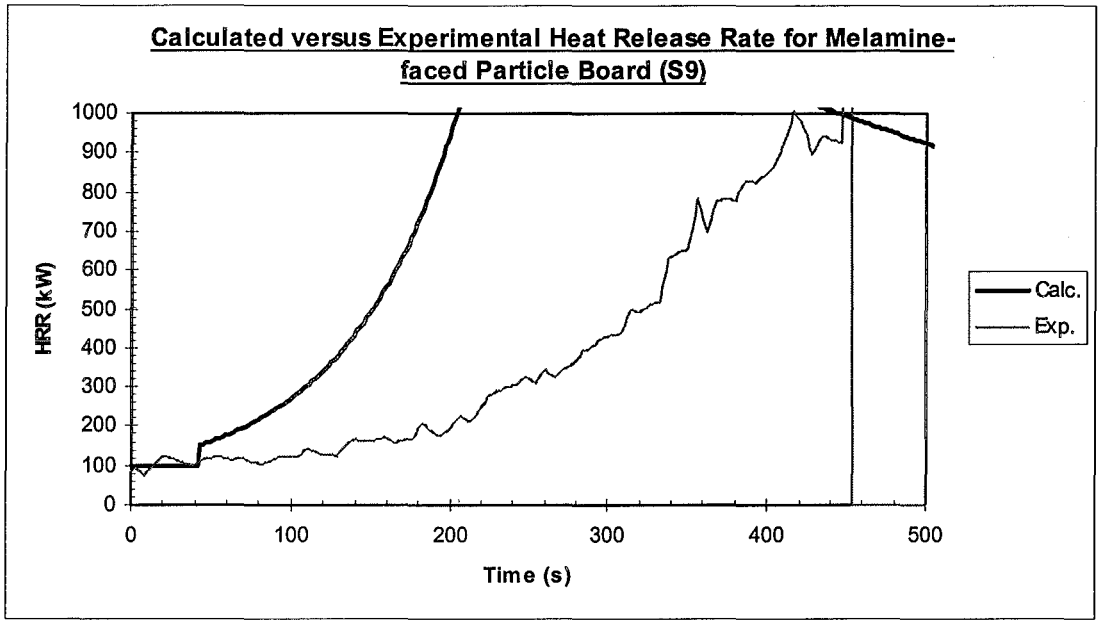

Figure 13.9: Material S9 Flame Spread Comparison

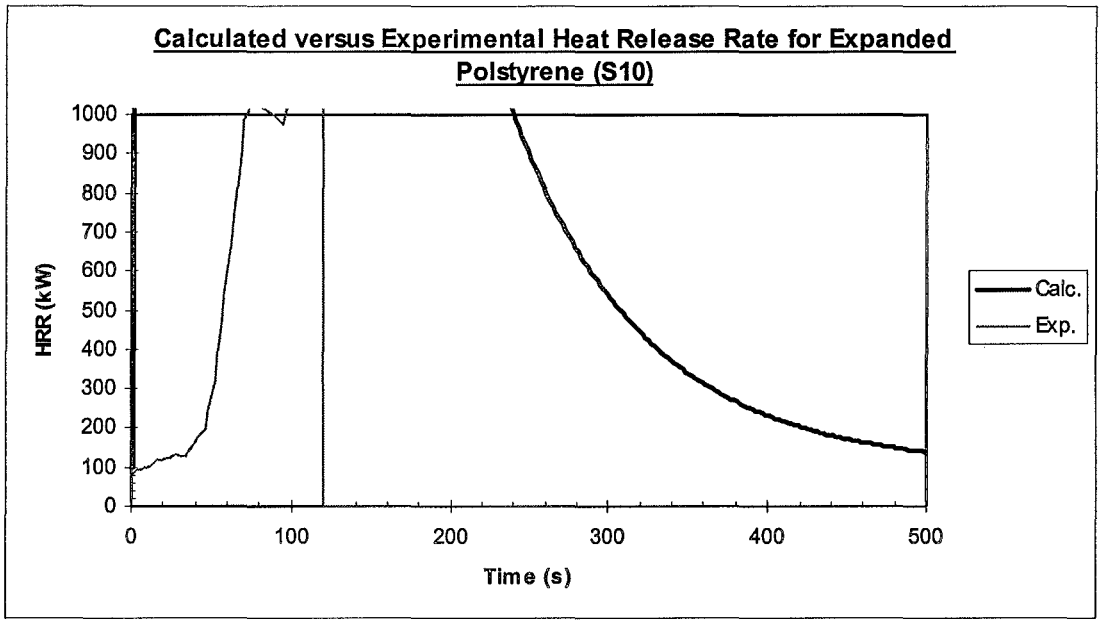

Figure 13.10: Material S10 Flame Spread Comparison

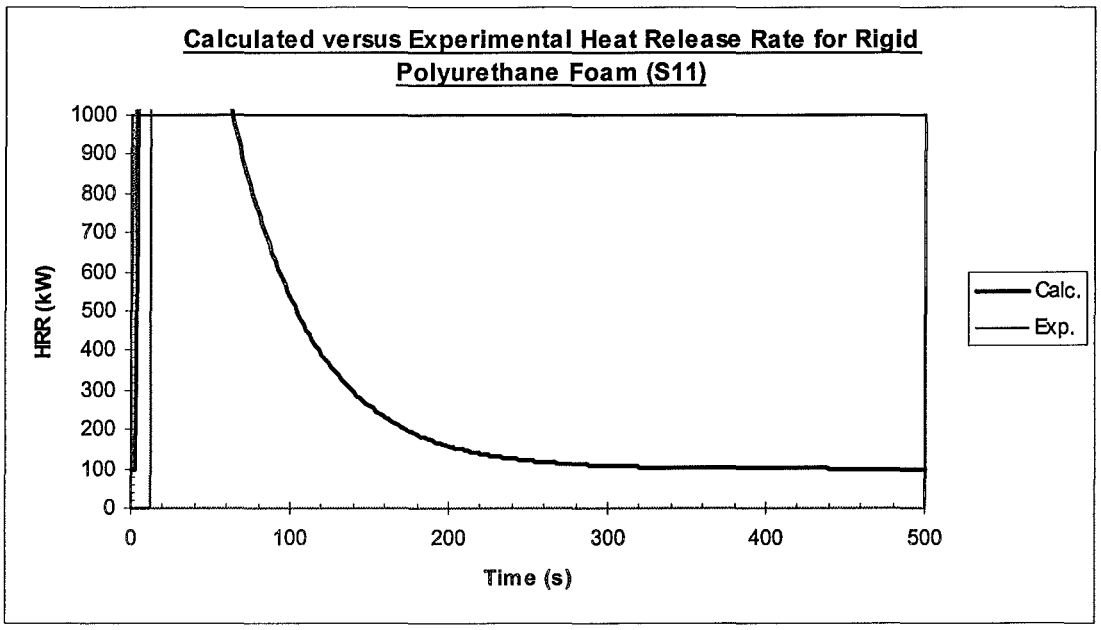

Figure 13.11: Material S11 Flame Spread Comparison

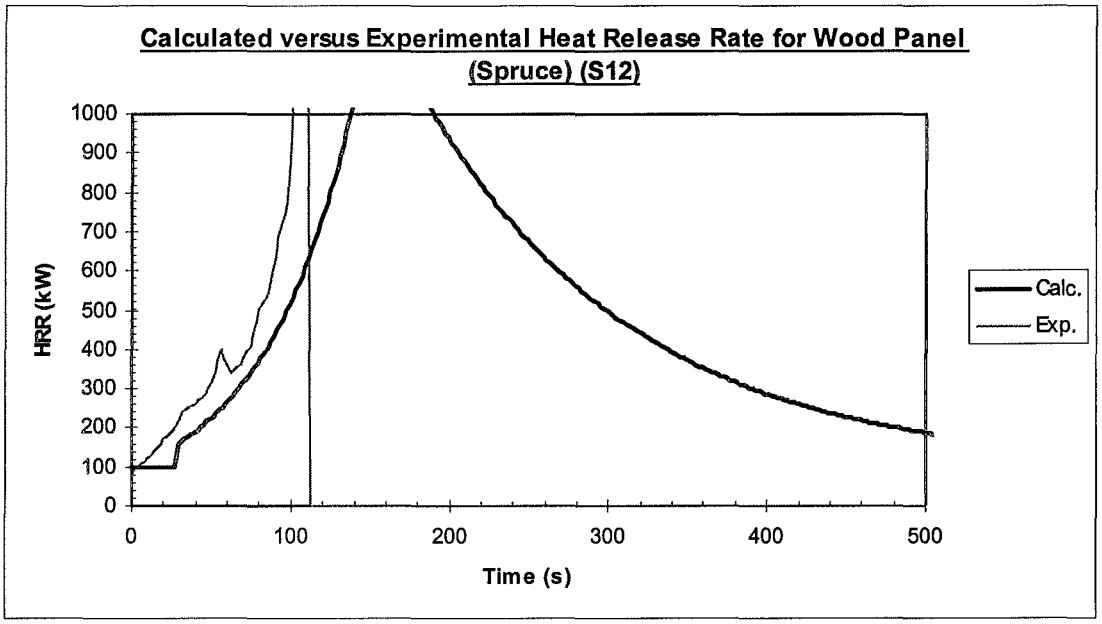

Figure 13.12: Material S12 Flame Spread Comparison

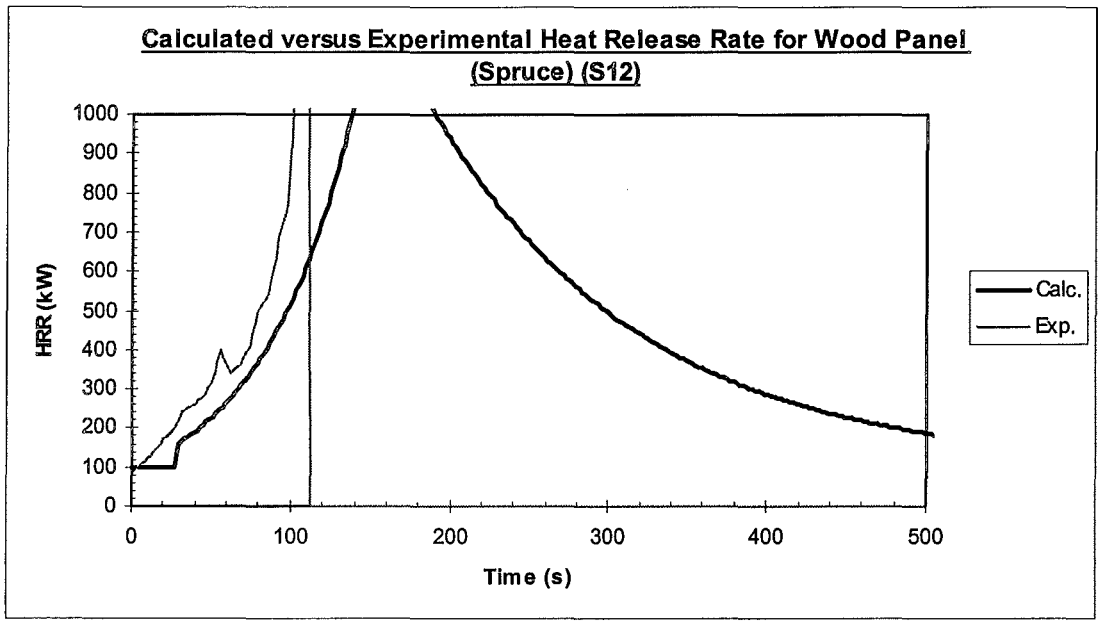

Figure 13.13: Material S13 Flame Spread Comparison

14. APPENDIX E: EUREFIC MODELLED MATERIALS

Global Variable Constants		
x_{po} value, x_{po*}	0.18	(-)
t_{ig*} HRR, q"*	32.0	(kWm^{-2})
t_{ig**} HRR, q"**	45.7	(kWm^{-2})
K	0.018	(m^2kW^{-1})

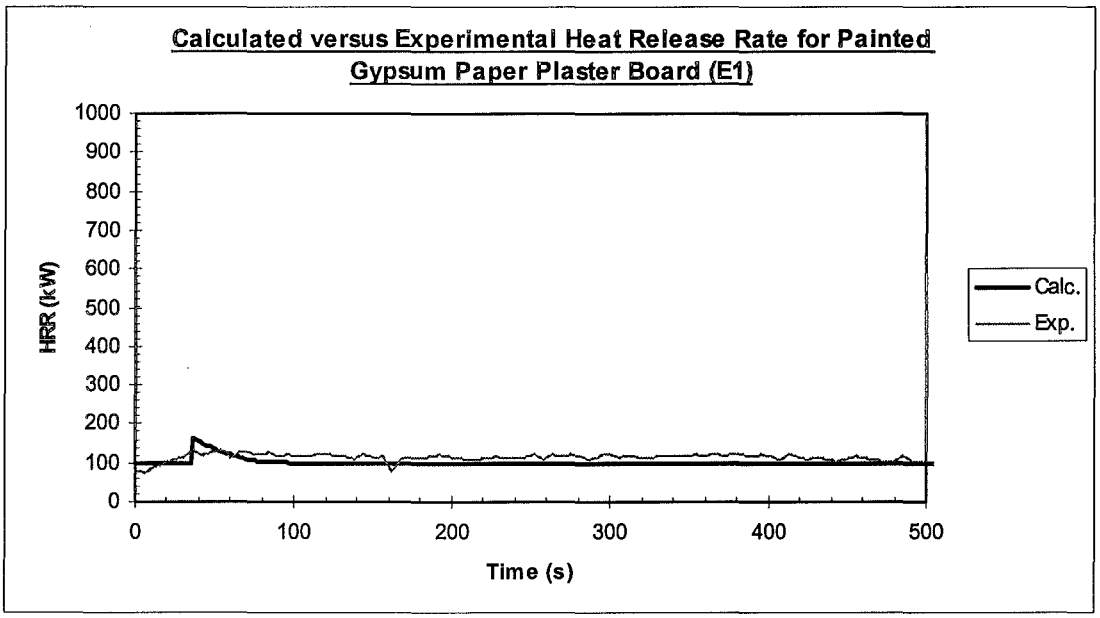

Figure 14.1: Material E1 Flame Spread Comparison

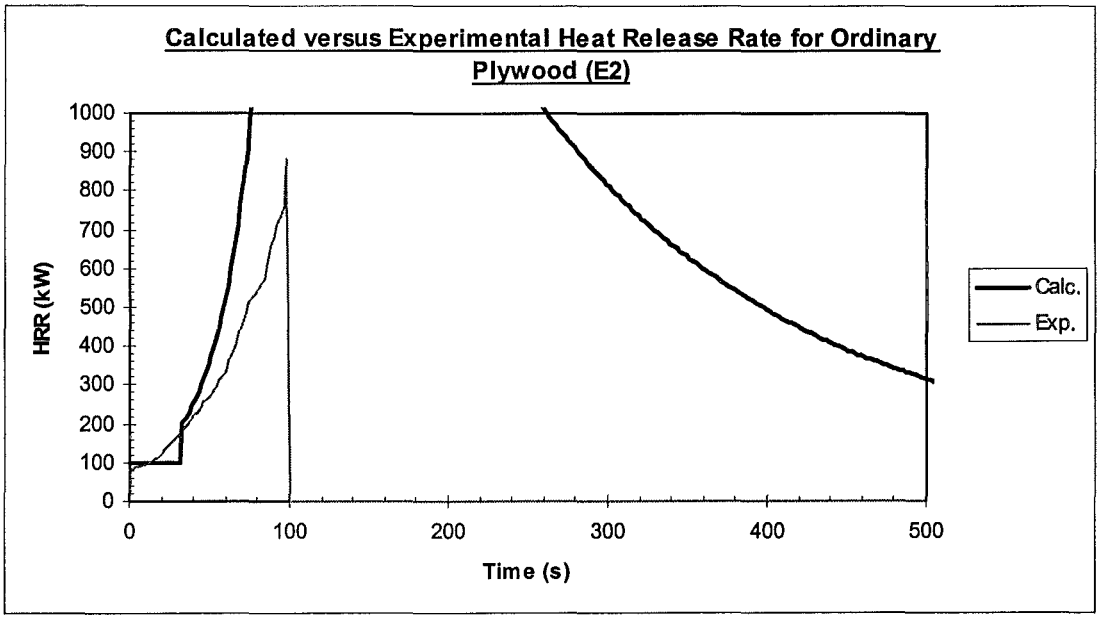

Figure 14.2: Material E2 Flame Spread Comparison

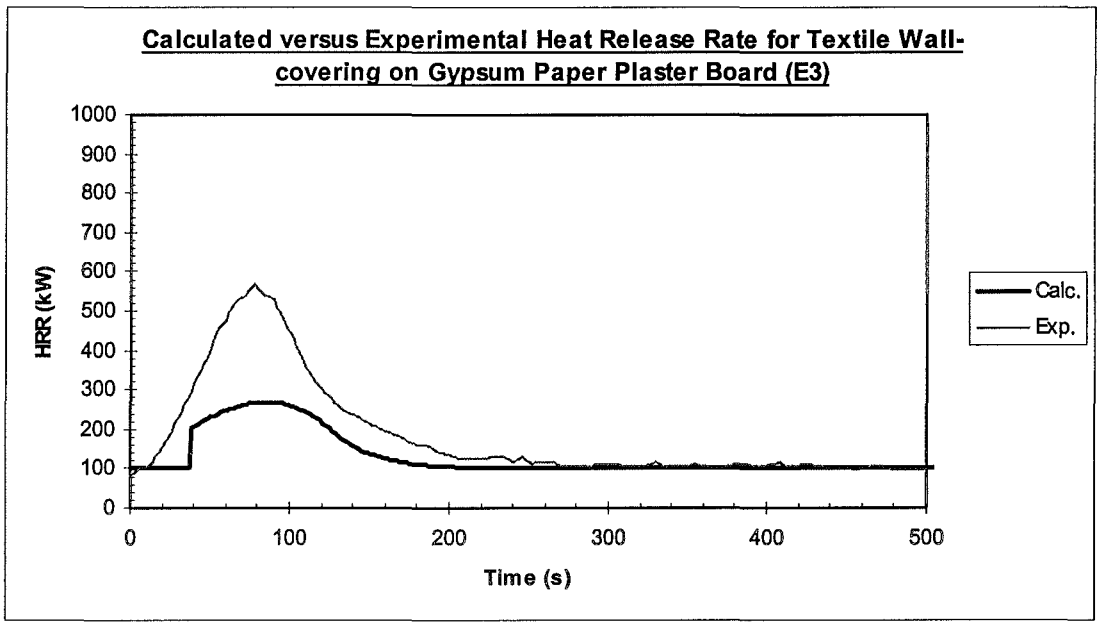

Figure 14.3: Material E3 Flame Spread Comparison

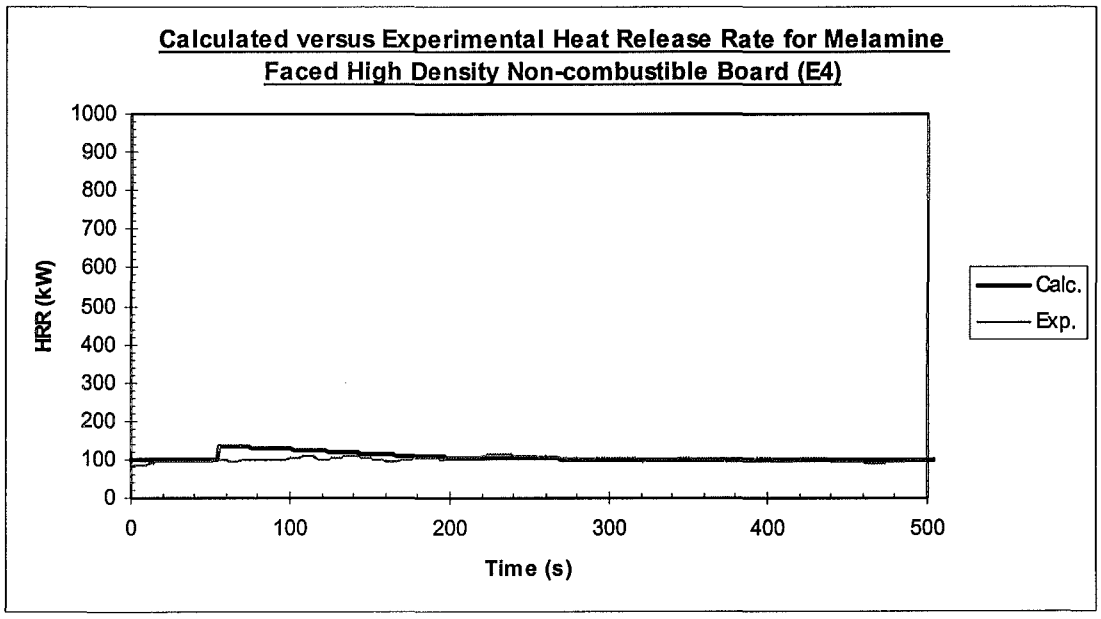

Figure 14.4: Material E4 Flame Spread Comparison

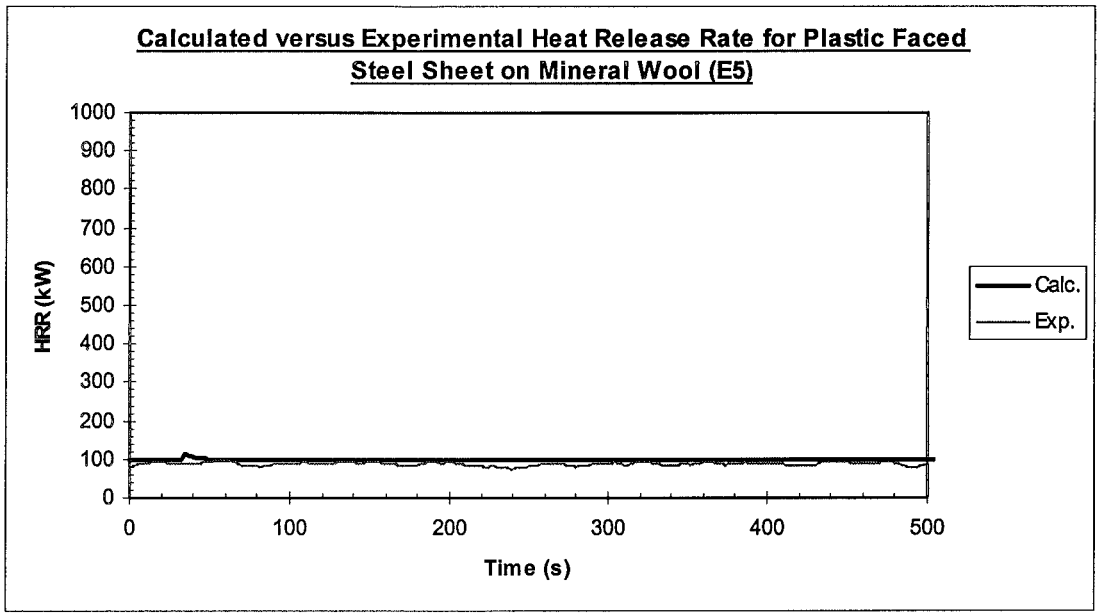

Figure 14.5: Material E5 Flame Spread Comparison

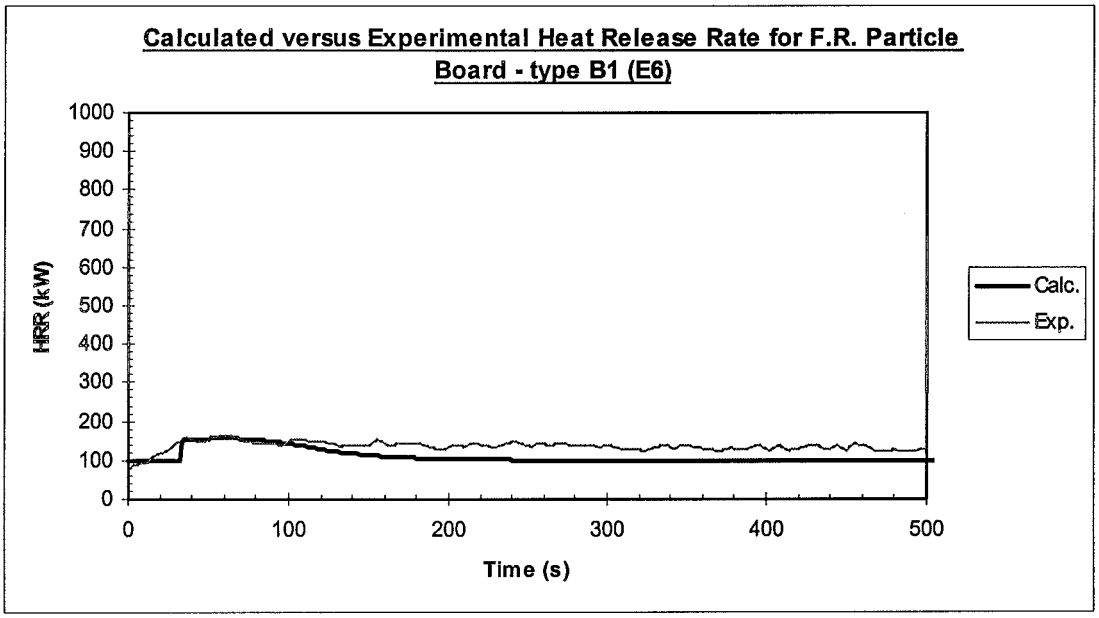

Figure 14.6: Material E6 Flame Spread Comparison

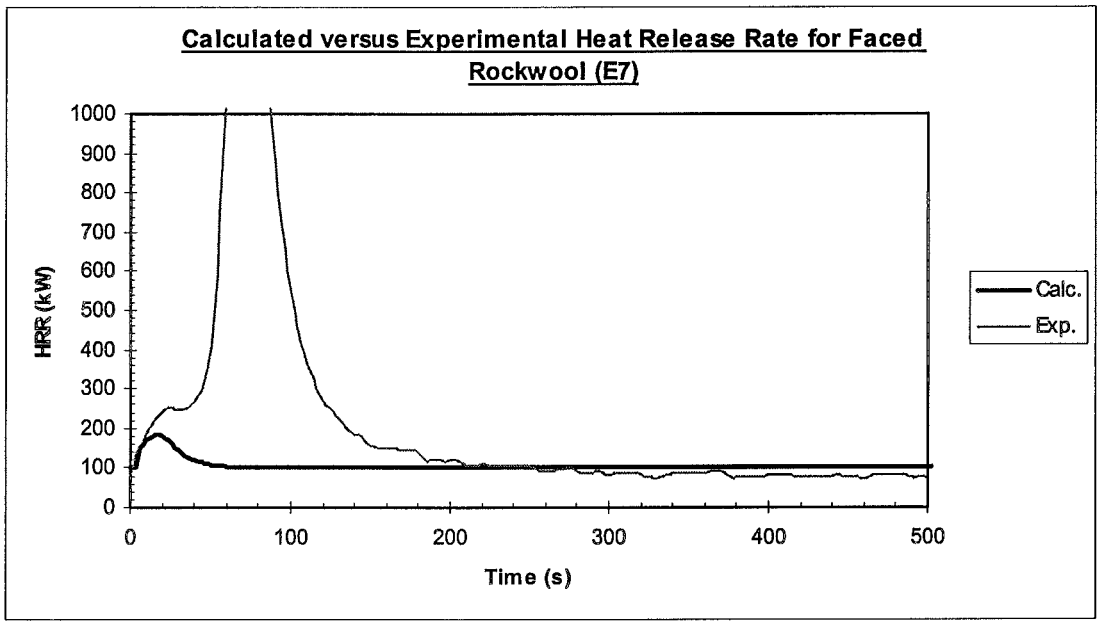

Figure 14.7: Material E7 Flame Spread Comparison

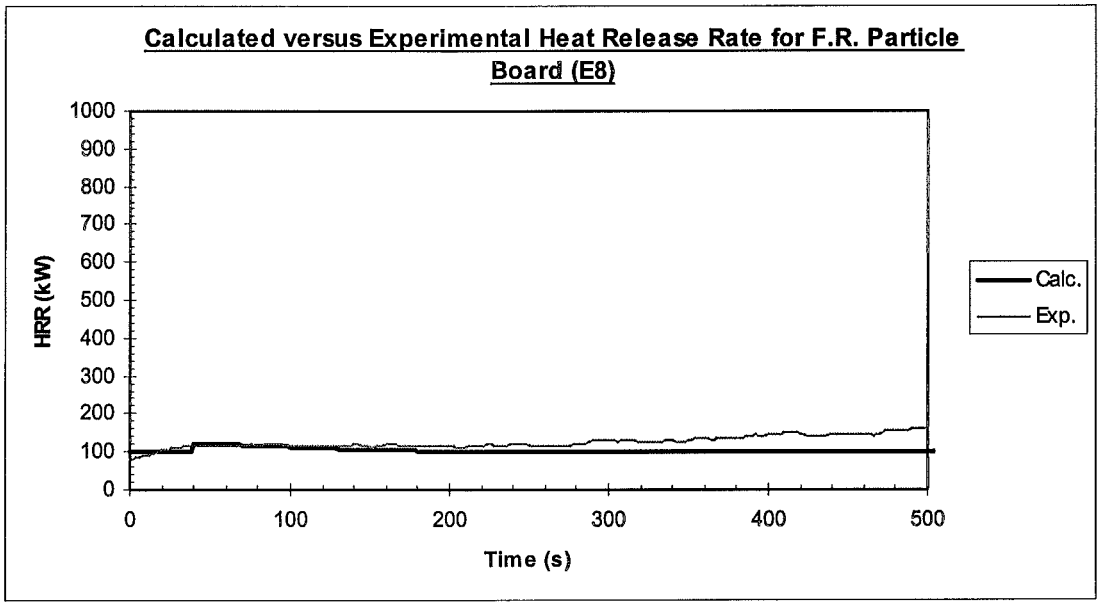

Figure 14.8: Material E8 Flame Spread Comparison

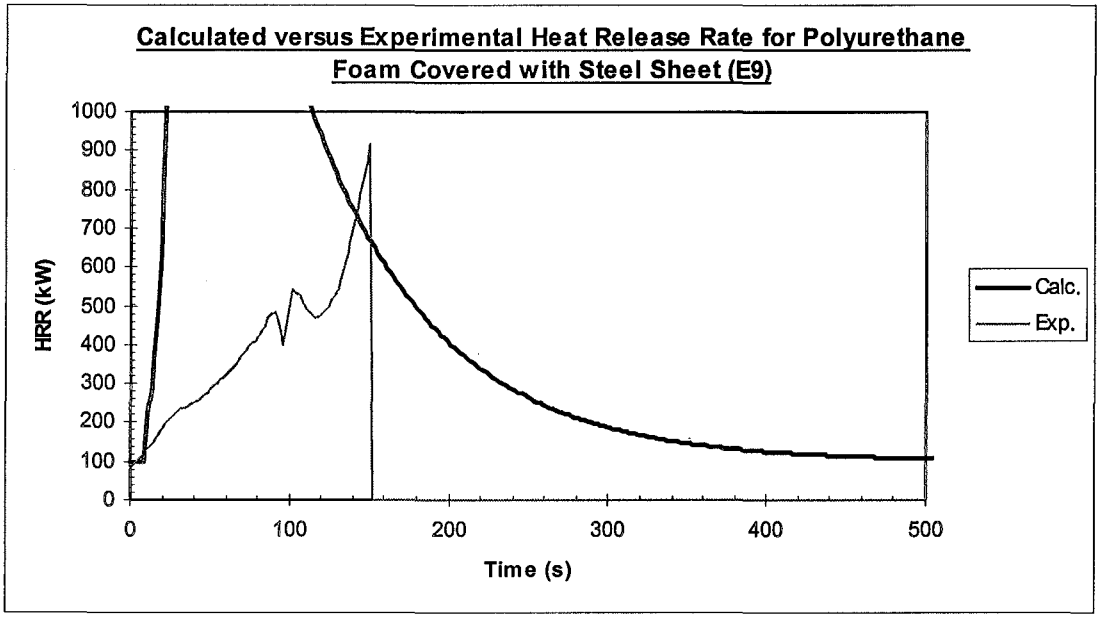

Figure 14.9: Material E9 Flame Spread Comparison

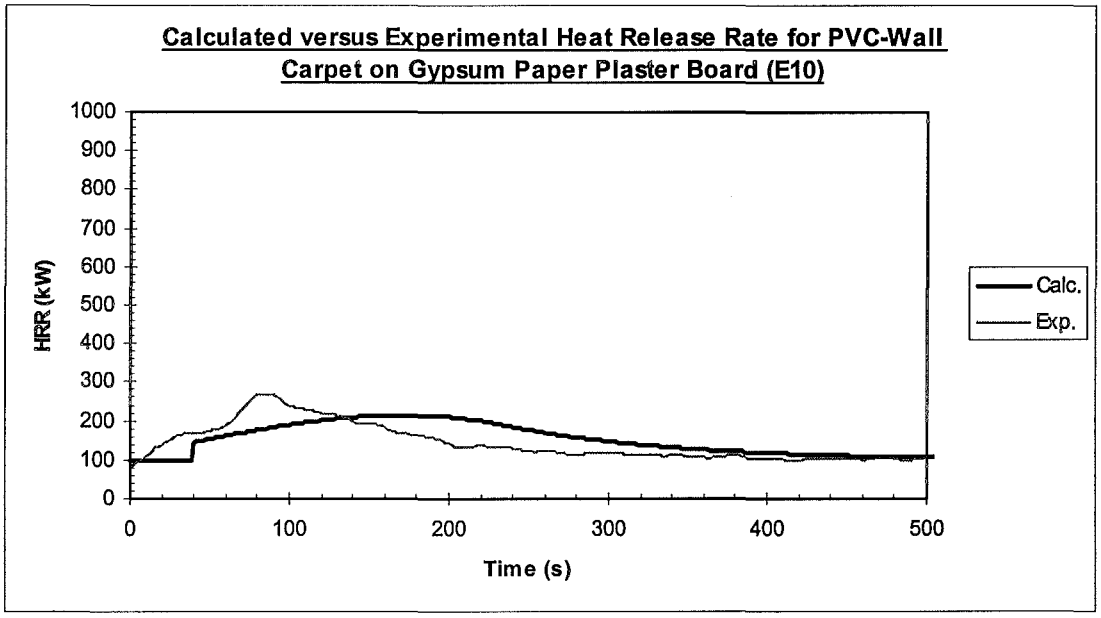

Figure 14.10: Material E10 Flame Spread Comparison

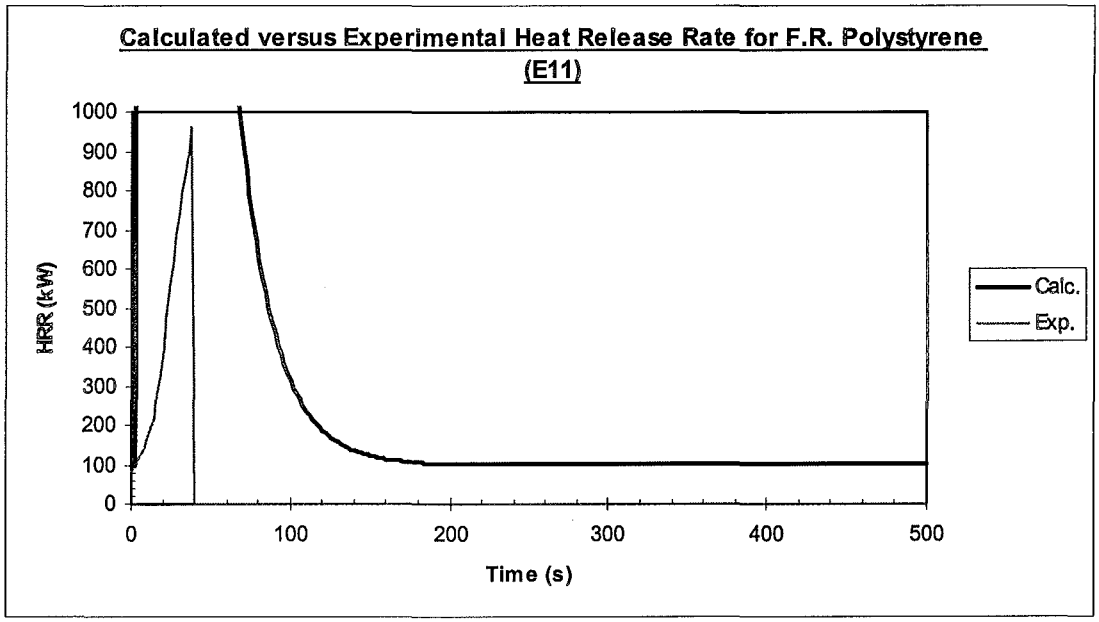

Figure 14.11: Material E11 Flame Spread Comparison

FIRE ENGINEERING RESEARCH REPORTS

95/1	Full Residential Scale Backdraft	I B Bolliger
95/2	A Study of Full Scale Room Fire Experiments	P A Enright
95/3	Design of Load-bearing Light Steel Frame Walls for Fire Resistance	J T Gerlich
95/4	Full Scale Limited Ventilation Fire Experiments	D J Millar
95/5	An Analysis of Domestic Sprinkler Systems for Use in New Zealand	F Rahmanian
96/1	The Influence of Non-Uniform Electric Fields on Combustion Processes	M A Belsham
96/2	Mixing in Fire Induced Doorway Flows	J M Clements
96/3	Fire Design of Single Storey Industrial Buildings	B W Cosgrove
96/4	Modelling Smoke Flow Using Computational Fluid Dynamics	T N Kardos
96/5	Under-Ventilated Compartment Fires - A Precursor to Smoke Explosions	A R Parkes
96/6	An Investigation of the Effects of Sprinklers on Compartment Fires	M W Radford
97/1	Sprinkler Trade Off Clauses in the Approved Documents	G J Barnes
97/2	Risk Ranking of Buildings for Life Safety	J W Boyes
97/3	Improving the Waking Effectiveness of Fire Alarms in Residential Areas	T Grace
97/4	Study of Evacuation Movement through Different Building Components	P Holmberg
97/5	Domestic Fire Hazard in New Zealand	KDJ Irwin
97/6	An Appraisal of Existing Room-Corner Fire Models	D C Robertson
97/7	Fire Resistance of Light Timber Framed Walls and Floors	G C Thomas
97/8	Uncertainty Analysis of Zone Fire Models	A M Walker
97/9	New Zealand Building Regulations Five Years Later	T M Pastore
98/1	The Impact of Post-Earthquake Fire on the Built Urban Environment	R Botting
98/2	Full Scale Testing of Fire Suppression Agents on Unshielded Fires	M J Dunn
98/3	Full Scale Testing of Fire Suppression Agents on Shielded Fires	N Gravestock
98/4	Predicting Ignition Time Under Transient Heat Flux Using Results from Constant Flux Experiments	A Henderson
98/5	Comparison Studies of Zone and CFD Fire Simulations	A Lovatt
98/6	Bench Scale Testing of Light Timber Frame Walls	P Olsson
98/7	Exploratory Salt Water Experiments of Balcony Spill Plume Using Laser Induced Fluorescence Technique	E Y Yii
99/1	Fire Safety and Security in Schools	R A Carter
99/2	A Review of the Building Separation Requirements of the New Zealand Building Code Acceptable Solutions	J M Clarke
99/3	Effect of Safety Factors in Timed Human Egress Simulations	K M Crawford
99/4	Fire Response of HVAC Systems in Multistorey Buildings: An Examination of the NZBC Acceptable Solutions	M Dixon
99/5	The Effectiveness of the Domestic Smoke Alarm Signal	C Duncan
99/6	Post-flashover Design Fires	R Feasey
99/7	An Analysis of Furniture Heat Release Rates by the Nordtest	J Firestone

99/8	**Design for Escape from Fire**	**I J Garrett**
99/9	**Class A Foam Water Sprinkler Systems**	**D B Hipkins**
99/10	**Review of the New Zealand Standard for Concrete Structures (NZS 3101) for High Strength and Lightweight Concrete Exposed to Fire**	**M J Inwood**
99/11	**Simple Empirical Method for Load-Bearing Light Timber Framed Walls at Elevated Temperatures**	**K H Liew**
99/12	**An Analytical Model for Vertical Flame Spread on Solids: An Initial Investigation**	**G A North**
99/13	**Should Bedroom Doors be Open or Closed While People are Sleeping? - A Probabilistic Risk Assessment**	**D L Palmer**
99/14	**Peoples Awareness of Fire**	**S J Rusbridge**
99/15	**Smoke Explosions**	**B J Sutherland**
99/16	**Reliability of Structural Fire Design**	**JKS Wong**

School of Engineering
University of Canterbury
Private Bag 4800, Christchurch, New Zealand

Phone 643 364-2250
Fax 643 364-2758